CONTROL OF INTRACELLULAR Ca^{2+} IN EPITHELIAL CELLS OF THE KIDNEY THICK ASCENDING LIMB

by

LONG-JUN DAI

M.Sc., The University of British Columbia, 1992

A THESIS SUBMITTED IN PARTIAL FULFILLMENT OF
DOCTOR OF PHILOSOPHY
in
THE FACULTY OF GRADUATE STUDIES

(Experimental Medicine, Department of Medicine)

We accept this thesis as conforming
to the required standard

THE UNIVERSITY OF BRITISH COLUMBIA

August 1995

In presenting this thesis in partial fulfillment of the requirements for an advanced degree at the University of British Columbia, I agree that the Library shall make it freely available for reference and study. I further agree that permission for extensive copying of this thesis for scholarly purposes may be granted by the head of my department or by his or her representatives. It is understood that copying or publication of this thesis for financial gain shall not be allowed without my written permission.

(Signature)

Department of Medicine

The University of British Columbia
Vancouver, Canada

Date Aug. 8, 1995

ABSTRACT

The cortical thick ascending limb of Henle's loop (cTAL) plays a fundamental role in salt reabsorption and concentration-dilution processes within the nephron. This study was performed to characterize the role of intracellular free Ca^{2+} ($[Ca^{2+}]_i$) in hormone-mediated signal transduction and to describe the function of Na^+/Ca^{2+} exchange in control of $[Ca^{2+}]_i$ in isolated cTAL cells from porcine kidney. Parathyroid hormone, arginine vasopressin, and atrial natriuretic peptide transiently increased $[Ca^{2+}]_i$ in a dose-dependent manner. The increment in $[Ca^{2+}]_i$ induced by these hormones was by intracellular release and entry through plasma membrane Ca^{2+} channels. These hormone-induced Ca^{2+} transients were modulated by cAMP, cGMP, and PKC activation. In order for intracellular Ca^{2+} to play a role in signal transduction mechanisms it is necessary to have regulated processes which maintain $[Ca^{2+}]_i$ at submicromolar levels. We evaluated the functional role of Na^+/Ca^{2+} exchange in cTAL cells. cTAL cells treated with ouabain had basal $[Ca^{2+}]_i$, 86 ± 2 nM. Removal of external Na^+ or voltage depolarization with KCl resulted in rapid and reversible maximal elevation of $[Ca^{2+}]_i$, 1023 ± 72 nM ($n=28$), which was dependent on the presence of external Ca^{2+} and elevated $[Na^+]_i$. The activity of Na^+/Ca^{2+} exchange was modulated by protein phosphorylation as calmodulin inhibition decreased and phosphatase inhibition increased the apparent exchange activity. The presence of a Na^+/Ca^{2+} exchanger was confirmed with northern hybridization techniques. A gene transcript which encodes a portion of the intracellular loop of the renal Na^+/Ca^{2+} exchanger was amplified from cortical tissue and cTAL cells by polymerase chain reaction (PCR) using primers flanking the alternative splicing site. Southern hybridization and DNA sequencing demonstrated the isoform contained exons B and D characteristic of one isoform (NACA3) of the renal

Na^+/Ca^{2+} exchanger. The results provide both functional and molecular evidence for a Na^+/Ca^{2+} exchanger in cTAL cells of the porcine kidney. It is likely that Na^+/Ca^{2+} exchange plays an important role in $[Ca^{2+}]_i$ control and thus hormonal regulation of electrolyte reabsorption within the cTAL cells.

TABLE OF CONTENTS

LIST OF FIGURES

ABBREVIATION

TAL: Thick ascending limb of Henle's loop

cTAL: Cortical thick ascending limb of Henle's loop

$[Ca^{2+}]_i$: Intracellular free Ca^{2+} concentration

$[Na^+]_i$: Intracellular free Na^+ concentration

PTH: Parathyroid hormone

AVP: Arginine vasopressin

ANP: Atrial natriuretic peptide

cAMP: Adenosine 3',5'-cyclicmonophosphate

cGMP: Guanosine 3',5'-cyclicmonophosphate

IP_3: Inositol triphosphate

PIP_2: Phosphoinositide 4',5'-bisphosphate

DAG: Diacylglycerol

TPA: 12-O-tetradecanoyl-phorbol 13-acetate

PLC: Phosphoinositide-specific phospholipase C

PKA: Protein kinase A

PKC: Protein kinase C

PKG: cGMP-dependent protein kinase

TG: Thapsigargin

EGTA: Ethylene glycol-bis(ß-aminoethyl ether) N,N,N',N'-tetraacetic acid

ACKNOWLEDGEMENT

I would like to thank Dr. Gary A. Quamme for his guidance and support throughout this work. I am grateful to Don Huysmans, Gordon Ritchie, and Brian Bapty for their technical assistance.

A special thanks to my wife, Hong-ying Li, and my son, James J. Dai, I could not complete my degree study without their understanding and support.

GENERAL INTRODUCTION

Calcium is an important cation in the body, representing about 2% of total body weight. It is also the most important structural element, occurring not only in combination with phosphate in bone and teeth but also with phospholipids and proteins in cell membranes where it plays a vital role in the maintenance of membrane integrity and in controlling the permeability of the membrane to many ions including calcium itself. It is widely involved in many physiological and biochemical processes throughout the body including the coagulation of blood, the coupling of muscle excitation and contraction, the regulation of nerve excitability, cell reproduction, the control of many enzyme reactions. More recently, intracellular calcium has been determined to be an important second messenger involved in hormonally-mediated signal transduction processes.

I. Calcium Distribution and Metabolism

An average adult human contains 1,300 gm of calcium. Most of the body calcium (99%) is located in the bone; the remainder is in the cell of which only a small fraction is in the ionized form, Ca^{2+}. Total calcium concentration in extracellular fluid of adult humans is 2.5 mM, or 10 mg/dl. In plasma, 60% is ultrafilterable across the glomerular capillaries. The rest (40%) is bound to plasma proteins, primarily albumin. Of the ultrafilterable component, 10% of the total calcium is complexed to polyvalent anions such as phosphate, citrate, bicarbonate, and sulfate. The remaining unbound fraction is free, ionized Ca^{2+}, which has a concentration of about 1.25 mM or 5 mg/dl in the ultrafiltrate (1). Precise homeostatic control of Ca^{2+} level in plasma and extracellular fluid is dependent on sensitive

negative feedback control of the secretion of PTH and calcitonin which in turn acts upon bone, kidney and gut to restore normal calcium levels.

II. Renal Handling of Calcium

The kidney is a major regulator of calcium homeostasis. Renal handling of calcium is normally a filtration-reabsorption process. Following its ultrafiltration across the glomerular capillaries, calcium is reabsorbed throughout the length of the nephron. Segmental calcium transport has been described with the aid of micropuncture techniques in a large number of animal species (2,3,4). In all mammals studied to date, calcium is handled in different ways along the nephron segments.

II.1. Proximal tubule. The majority of the filtered calcium (65%) is reabsorbed in the proximal convoluted tubule. The ratio of the calcium concentration in tubule fluid relative to that in plasma ultrafiltrate, TF_{Ca}/UF_{Ca}, is reportedly between 1.0 and 1.2 in all species studied to date (2,3,4). The consistent observation that TF_{Ca}/UF_{Ca} remains close to unity along the proximal tubule suggests that calcium reabsorption parallels sodium and fluid reabsorption in this segment. Calcium reabsorption in the proximal tubule is predominantly passive through the paracellular pathway. A small amount of calcium reabsorption may be transcellular (2,3,4).

II.2. Thick ascending limb of Henle's loop. The thick ascending limb of the loop (TAL) corresponds to the last segment of the loop of Henle. It extends from the boundary between inner and outer medulla up to or just beyond the *macula densa* in the cortex. The thick ascending limb, therefore, includes a medullary portion (mTAL) and a cortical portion (cTAL). The general cell organization and ultrastructure as well as the main transport

properties are similar in TAL from all species studied to present. There is a single type of cell in each TAL portion. These cells are of a relatively small size but contain, on the peritubular cell border, many deep membrane infoldings, surrounded by a large number of adjacent mitochondria. Junctional complexes are highly permeable to salt but relatively impermeable to water. Apical membranes form only few and short microvilli; they contain a particular protein, the Tamm-Horsfall protein, which is characteristic of mTAL and cTAL cells (5). This protein was employed as a specific marker to isolate cTAL cells in the present study.

The TAL has been called the "diluting segment" in view of its ability to reabsorb solutes in excess of water. The fluid delivered by this segment to the distal convolution is hypotonic and contains concentrations of NaCl that usually range between 30% and 40% of that present in plasma ultrafiltrate. Other ion species have also been observed to be preferentially reabsorbed in TAL. This is the case for potassium and for the divalent cations Ca^{2+} and Mg^{2+}. Actually, TAL is the major site for Mg^{2+} reabsorption in the kidney (6,7). TAL may also constitute an important site of fluid acidification and ammonia transport (8).

Approximately 25% of the filtered calcium is reabsorbed in TAL. Significant quantities of calcium are reabsorbed in cTAL but not in mTAL (6). The lumen-positive voltage that normally exists across the epithelial cells of the TAL is an important driving force for passive calcium reabsorption in this segment.

TAL is one of the nephron segments where some hormones, such as PTH, glucagon, ADH, calcitonin, and isoproterenol, regulate NaCl and divalent cation reabsorption (9,10,11). The increase in basolateral Cl^- conductance and the activity of the apical Na^+-$2Cl^-$-K^+

cotransporter is thought to be the cellular mechanism accounting for the hormone-mediated increase in NaCl and divalent cation transport (12).

II.3. Distal tubule and collecting duct. About 8% of the filtered calcium is reabsorbed in distal convoluted tubule and less than 2% in collecting duct. TF_{Ca}/UF_{Ca} falls along the length of the distal tubule, to about 0.3. This concentration profile, taken together with the lumen-negative transepithelial potential difference, provides direct evidence for an active Ca^{2+} reabsorptive mechanism that proceeds against both chemical and electrical gradients. Both Ca^{2+}-ATPase and Na^+/Ca^{2+} exchange transport processes are involved in the active Ca^{2+} reabsorption in these nephron segments (13,14).

III. Ca^{2+} as an Intracellular Messenger

$[Ca^{2+}]_i$ of any cell is extremely low ($\sim 10^{-7}$ M), whereas its concentration in the extracellular fluid is high ($> 10^{-3}$M). Thus there is a large chemical gradient tending to drive Ca^{2+} into the cytosol across the plasma membrane. Intracellular Ca^{2+} is sequestered in endoplasmic reticulum (ER) and other compartments. When a signal transiently opens Ca^{2+} channels in either the plasma membrane or ER membrane, Ca^{2+} rushes into the cytosol, dramatically increasing the local Ca^{2+} concentration and activating Ca^{2+}-sensitive response mechanisms in the cell. For this signaling mechanism to work, the intracellular free Ca^{2+} concentration ($[Ca^{2+}]_i$) must be kept at a low concentration. This is achieved by the calcium pump, Ca^{2+}-ATPase, and by Na^+/Ca^{2+} exchangers in their plasma membrane (15,16). A Ca^{2+} pump in the membrane of the specialized intracellular compartment also plays an important role in maintaining low $[Ca^{2+}]_i$ (17).

In recent years it has become clear that Ca^{2+} acts as an intracellular messenger in a wide variety of cellular responses. Two pathways of Ca^{2+} signaling have been defined, one used mainly by electrically active cells and the other used by almost all eucaryotic cells. The first of these pathways has been particularly well studied in nerve cells, in which depolarization of the plasma membrane causes an influx of Ca^{2+} into the cell through voltage-gated Ca^{2+} channels. In the second, ubiquitous pathway the binding of extracellular signaling molecules to cell surface receptors cause the release of Ca^{2+} from the calcium-sequestering compartment; the events at the cell surface are coupled to the opening of Ca^{2+} channels in the internal membrane through yet another intracellular messenger molecule, inositol triphosphate (IP_3). Production of this messenger results from the breakdown and subsequent resynthesis of inositol phospholipids triggered by a receptor protein that activates an enzyme called phosphoinositide-specific phospholipase C (PLC) in the plasma membrane. PLC cleaves phosphoinositide 4,5-bisphosphate (PIP_2) to generate two products: IP_3 and diacylglycerol (DAG). IP_3 releases Ca^{2+} from the calcium-sequestering compartment through IP_3 receptors. DAG has two potential signaling roles. It can be further cleaved to release arachidonic acid, which can be used in the synthesis of prostaglandins and related lipid signaling molecules; or , more important, it can activate a specific protein kinase, protein kinase C (PKC), which can then phosphorylate a number of proteins with different functions in the target cell.

Fig. 1 summarizes the induction and function of Ca^{2+} transients within a polarized cell. A Ca^{2+} transient is a short burst of elevated $[Ca^{2+}]_i$ induced by an extracellular signal. Two mechanisms operate to attenuate the Ca^{2+} transient: 1) some of the IP_3 is rapidly dephospho-

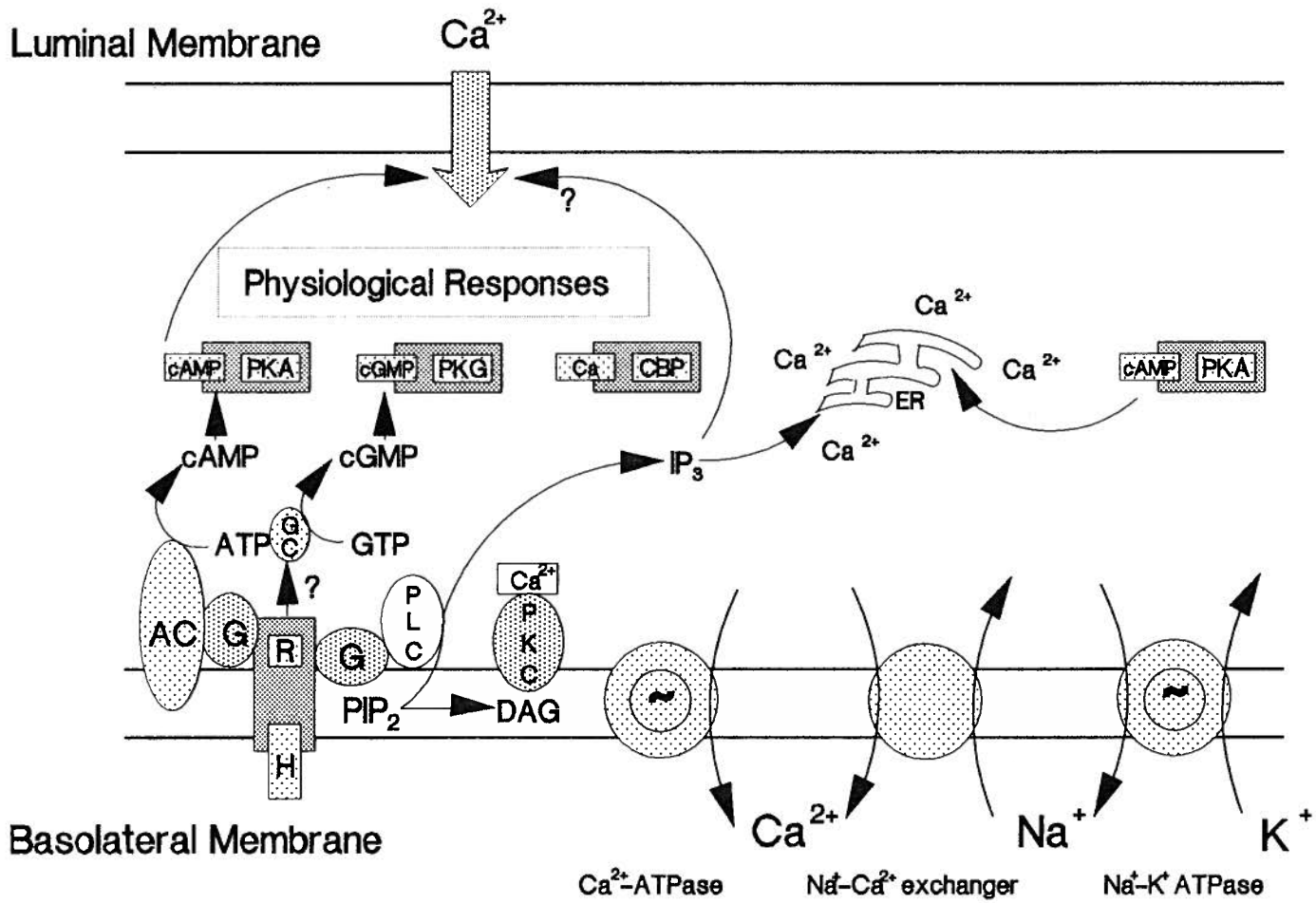

Fig.1. Agonist-induced intracellular Ca^{2+} elevation in a polarized cell. Agonist-receptor interaction induces generation of the second messengers, cAMP, cGMP, DAG and IP_3, through G-protein-mediated processes. IP_3 is known to release intracellular Ca^{2+} through IP_3 receptors located in the membrane of intracellular Ca^{2+} stores. It also indirectly activates Ca^{2+} influx through Ca^{2+} channels by some unknown mechanisms. cAMP stimulates both Ca^{2+} entry and Ca^{2+} release through cAMP-dependent protein kinase (PKA) (18). Agonist-mediated physiological responses can be elicited by Ca^{2+}-binding protein (CBP), PKA, protein kinase C (PKC), cGMP-dependent protein kinase (PKG), and other calcium-activated enzymes. Low $[Ca^{2+}]_i$ is achieved by Ca^{2+}-ATPase and Na/Ca^{2+} exchanger in the plasma membrane. AC: adenylate cyclase; GC: guanylate cyclase; DAG: diacylglycerol; H: hormone; R: receptor.

rylated (and thereby inactivated) by a specific phosphatase, or further phosphorylated to form IP_4; and 2) the Ca^{2+} that enters the cytosol is rapidly removed out of the cell, by both Ca^{2+}-ATPase and Na^+/Ca^{2+} exchange.

IV. Objectives of the Present Studies

The hypotheses of the present study are as follows: Intracellular Ca^{2+} is a part of PTH-, AVP-, and ANP-induced signal transduction; and Na^+/Ca^{2+} exchanger is present and plays an important role in maintaining basal intracellular Ca^{2+} level in cortical thick ascending limb (cTAL) cells. It was decided to concentrate on the cTAL segment in this study because of its important role in NaCl and divalent cation conservation.

A number of hormones through their respective receptors control cellular function within cTAL (11,19,20). These receptors generate cAMP (11,19), but to date no evidence has been given to indicate that other signaling pathways, including PKC, IP_3, and $[Ca^{2+}]_i$, play a role in the hormone-mediated signal transduction mechanisms in cTAL cells. The first objective of this study was to determine the presence of Ca^{2+} transients or signals in cTAL cells. Second, we wanted to explore some of the interactions of the various hormone processes to find out how the various hormones interact to orchestrate regulatory controls in these cells. Finally, if $[Ca^{2+}]_i$ is significant in regulating function it was thought important to determine how cTAL cells control $[Ca^{2+}]_i$. The evidence to date suggested that Na^+/Ca^{2+} exchange is not present in cTAL cells. Accordingly, we determined that cTAL cells contain a Na^+/Ca^{2+} exchange and that this exchange could be regulated by phosphorylation events. These studies indicated that Ca^{2+} plays an important role in hormone signals.

CHAPTER 1. HORMONE-MEDIATED Ca^{2+} SIGNALING IN cTAL CELLS

I. Background

To serve as intracellular messenger, a compound must meet several requirements. Most important, its intracellular concentration must be very low and precisely controlled, so that short-lived transmembrane fluxes of the messenger would be able to change significantly its intracellular level and thus modulate the messenger-sensitive cellular processes. In addition, it must bind its substrates selectively. Ca^{2+} meets these requirements because of the high coordination number and irregular coordination geometry that considerably enhance the specifity of its binding to biological molecules. It is now established that Ca^{2+} plays an important role as a messenger and modulator of intracellular processes. It is worth noting that, when Ca^{2+} is the intracellular messenger of an external stimulus, the actual signal that initiates the response is not Ca^{2+} itself, but a member of Ca^{2+}-binding proteins. These proteins, functionally inert in the absence of bound Ca^{2+}, become active upon binding Ca^{2+}. An increase in intracellular free Ca^{2+} ($[Ca^{2+}]_i$) caused by hormonal or electrical signals can trigger responses such as contraction, secretion, cellular proliferation, metabolic adjustments, and changes in gene expression in addition to the control of electrolyte transport (21,22).

The induction, propagation, and termination of the Ca^{2+} signal is highly controlled by various mechanisms. The major entry of cytosolic Ca^{2+} seems to be via calcium channels located in both plasma and intracellular organelle membranes. Mechanisms must also exist for the extrusion of Ca^{2+} from cell interior, to avoid the accumulation of cytosolic calcium. The two main mechanisms are efflux of Ca^{2+} through Na^+/Ca^{2+} exchange and ATP-dependent calcium pump in the membrane. In addition, intracellular release, buffering, and

sequestration of intracellular calcium stores are also involved in the dynamic processes of $[Ca^{2+}]_i$ balance. To understand completely the extent of Ca^{2+}'s role as a second messenger, we need to elucidate how cytosolic Ca^{2+} levels are regulated. This requires an understanding of how influxes from and effluxes to the extracellular space cross the plasma membrane. It also entails knowledge of how Ca^{2+} is sequestered and released from both membrane-bound and nonmembranous intracellular organelles.

The cortical thick ascending limb (cTAL) of Henle's loop plays a fundamental role in salt reabsorption within the nephron (23,24). Electrolyte transport within the cTAL cells is sensitively controlled by many regulatory hormones including parathyroid hormone (PTH), arginine vasopressin (AVP), atrial natriuretic peptide (ANP), calcitonin, and glucagon, among others (12,25-27). The physiological concentration of these peptide hormones is less than 10^{-8} M. Morel *et al* (19) have shown that PTH, calcitonin, and glucagon stimulate cyclic adenosine monophosphate (cAMP) release in rabbit cTAL cells; accordingly, appropriate receptors are present for these peptide hormones. In turn, these peptides acting through cAMP and protein kinase A activation are responsible for control of electrolyte transport in the cTAL (12,23,24). In addition, these hormones may act through alternative pathways. In many cells, hormone binding to receptors activate phospholipase C with the generation of diacylglycerol (DAG) and IP_3 (28). DAG activates protein kinase C leading to specific effects on receptor and transport function. IP_3 is a second messenger that controls many cellular processes by generating internal Ca^{2+} signals (28). In turn, intracellular Ca^{2+} transients often activate various kinases, modify enzyme responses, and alter channel activity (29,30,31). These responses may be involved in control of epithelial NaCl transport (23,24).

The objective of the initial studies was to establish and characterize hormone-mediated responses of intracellular Ca^{2+} signals in isolated cTAL cells. In addition, the possible interactions between Ca^{2+} and other second messengers were also explored.

II. Materials and Methods

II.1. Materials

Dulbecco's modified Eagles' medium (DMEM) and Ham's medium containing D-glucose (5.0 g/L), L-glutamine (5 mM), 10% FCS was from GIBCO (Grand Island, NY). Goat anti-human uromucoid (Tamm-Horsfall glycoprotein) serum was purchased from Organon Teknika (Rockville, MD), and affinity-purified rabbit anti-goat immunoglobulin G (IgG) were obtained from Sigma (St. Louis, MO); and fura-2/AM was obtained from Molecular Probes (Eugene, OR). Parathyroid hormone, arginine vasopressin, calcitonin, glucagon, bradykinin, angiotensin II, atrial natriuretic peptide, and 8-bromo-adenosine-3',5'-cyclic monophosphate (8-BrcAMP) were from Sigma. Collagenase Type V-S and 12-O-tetradecanoylphorbol 13-acetate (TPA) were also from Sigma. All other chemicals were acquired from Sigma or Fisher Scientific (Mississauga, Ont.).

II.2. Methods

II.2.1. Isolation of cTAL cells from porcine kidneys

Cortical thick ascending limb cells were isolated by a double antibody technique according to previously published methods (7). This method is based on the unique distribution of Tamm-Horsfall protein along the surface membrane of thick ascending limb of Henle's loop (5).

II.2.1.1. Culture dishes coated with rabbit anti-goat IgG antibody. All procedures were performed under sterile conditions. 5 ml of phosphate-buffered saline (PBS; composition in mM: 137 NaCl, 2.7 KCl, 8.1 Na_2HPO_4, pH 7.4) containing 80 μg of affinity-purified rabbit anti-goat IgG antibody was added to each of four culture dishes (Corning, 80 mm), and the dishes were incubated overnight at 4°C. Immediately before the antibody-coated dishes were to be used for immunoadsorption, the antibody solution was aspirated and the dishes were washed four times with 3 ml of 1% bovine serum albumin in PBS. Finally, the dishes were tilted near upright for three minutes and excess liquid was removed by aspiration.

II.2.1.2. Dispersion of inner cortex tissue. Young pigs (30 ~ 50 days old) were killed with a lethal dose pentobarbital sodium administered through cardiac puncture. The kidneys were removed and placed in the ice cold Hepes-buffered Krebs solution (HBK; composition in mM: 5 KCl, 145 NaCl, 1 Na_2HPO_4, 5 glucose, 1 $CaCl_2$, 0.5 $MgCl_2$, and 10 Hepes; pH 7.4). Tissue from the innermost third stripe of the cortex was dissected and washed three times with ice cold HBK. Approximately 40 ml of 0.1% collagenase in HBK with 1% BSA was added to the cortical tissue (about 6 gm from two kidneys). The tissue was incubated at 37°C for about 10 min in a shaker. An appropriate degree of cell dispersion was evidenced by the appearance of numerous large tubule fragments. The digestion was stopped by adding appropriate amount of ice cold HBK. Cell suspension was collected through a tea strainer and centrifuged at 700 rpm for 2 min.

II.2.1.3. Isolation of cTAL cells. The cell pellet was washed three times with HBK, then, resuspended in 10 ml of DMEM/NF12 medium containing 100 μl of primary antibody,

goat anti-human uromucoid serum (50 mg protein/ml). The incubation was continued for 30 min on ice with occasional swirling. The cells were then collected by centrifugation, washed twice with PBS, and resuspended in 4 ml of PBS. One ml of cell suspension was applied to each of four antibody-coated dishes in four successive equal aliquots. Each aliquot was allowed to stand on the plates for 5 min; nonadherent cells were removed with one wash with 5 ml of PBS. The dishes were washed six times with 5 ml of PBS following the fourth incubation. To dislodge freshly isolated cTAL cells from the dishes, 5 ml of PBS was added to each dish and the dish was tapped sharply on the side several times with a scalpel handle. The suspended cells were then pipetted into a sterile tube and collected by centrifugation. The cell pellet was resuspended in 3 ml of DMEM/NF12 containing 10% fetal calf serum, 5 mM L-glutamine, 50 units/ml penicillin, and 50 μg/ml streptomycin. The cTAL cell suspension was plated on glass coverslips or plastic multiwell dishes. The cTAL cells grew on the appropriate support in 95-5%, air-CO_2. About one week after seeding, the subconfluent cTAL cells were used for the experiments.

II.2.2. Determination of cytosolic free Ca^{2+}

The fluorescent Ca^{2+} indicator, fura-2, is widely used for direct measurement of intracellular free Ca^{2+} concentration ($[Ca^{2+}]_i$) based on its fluorescent property (32,33). When fura-2 is loaded into the cell, the dye has only two molecular forms, free and Ca^{2+}-bound. Both fura-2 and its Ca^{2+} complex fluorescence strongly, but their excitation peaks differ in wavelength. Fura-2 shifts its excitation peak from about 385 nm to 335 nm upon binding Ca^{2+}. The extent of the shift between the two wavelengths depends on the amount of intracellular Ca^{2+} concentration. Measurements at two wavelengths suffice in principle

to indicate the ratio of bound to free dye and hence the $[Ca^{2+}]_i$.

II.2.2.1. Cell loading with fura-2. Isolated cTAL cells were loaded with 10 μM fura-2/AM according to previously described techniques (34). The fluorescent dye, dissolved in dimethylsulfoxide (DMSO), was added directly to the medium with the aid of Pluronic F-127 (0.05%) and incubated for 30 min at 23°C. The final concentration of DMSO in the medium did not exceed 0.2%.

II.2.2.2. De-esterification. Fura-2/AM is hydrophobic and thus it passes easily into cells across the plasma membrane. Once inside cells, cytosolic esterases cleave the acetoxymethyl groups from fura-2 molecule rendering a compound which is highly charged and which cannot cross cellular membranes. Thus, it is theoretically trapped in the cytosol. Since the incomplete de-esterification of the dye in cytoplasm will interfere with the $[Ca^{2+}]_i$ measurement cells loaded with fura-2 should be de-esterified completely. Loaded cells were washed 2X with a buffered salt solution (in mM): 145 NaCl, 4 KCl, 1 $CaCl_2$, 1 KH_2PO_4, 18 glucose, and 20 HEPES/Tris (pH 7.4) with or without Ca^{2+} depending on the different purpose of the experiments. The cells were incubated a further 20 min to ensure complete de-esterification and finally washed with fresh buffer solution.

II.2.2.3. Determination of $[Ca^{2+}]_i$. Glass coverslips, with cTAL cells loaded with fura-2, were mounted in a plexiglass chamber containing 250 μl buffer and placed on the mechanical stage of a Nikon inverted microscope with a Fluor x100 objective, and fluorescence was monitored under oil immersion within a single cell over the course of study. The fluorescence signal was recorded at 505 nm with excitation wavelengths alternating between 335 and 385 nm using a spectrofluorometer (Deltascan; Photon Technologies,

Santa Clara, CA). Averaged light intensities over excitation periods at each of the two wavelengths were used to calculate 338/385 ratios after background substraction. At the end, $[Ca^{2+}]_i$ was calculated as described by Grynkyewicz *et al* (35) and Malgaroli *et al* (36) based on the equation:

$$[Ca^{2+}]_i = K_D(R\text{-}R_{min}/R_{max}\text{-}R)S_{f2}/S_{b2}$$

Where K_D is the association constant; R_{min} is the fluorescence ratio at the excitation wavelengths 335/385 nm for uncomplexed fura-2 (zero calcium); R_{max} is the ratio of fluorescence at the wavelengths 335/385 nm for fura-2 saturated with Ca^{2+}; S_{f2} and S_{b2} are the fluorescence intensities at 385 nm with zero Ca^{2+} and excess Ca^{2+}, respectively; R is the ratio of fluorescence at wavelength ratio 335/385 nm of the sample to be measured. Using ratios, dye content and instrumental sensitivity are free to change between one ratio and another since they cancel out in each ratio. Of course, stability is required within each individual ratio measurement; also R, R_{min} and R_{max} should all be measured on the same instrumentation so that any wavelength biases influence all of them equally.

The bothing solution was changed by a superfusion-suction system. The given hormone concentrations were added to the bathing solution without changing buffer.

All results are expressed as mean $\pm$ S.E. where indicated. Significance was determined by one-way analysis of variance. A probability of $p < 0.05$ was taken to be statistically significant.

III. Results

The isolated cTAL cells when grown to confluence have a morphological appearance

of epithelial cells. They had cuboidal structure when grown on filters and developed small domes, five to six cells in diameter, when cultured on solid supports for an extended period of time. The morphological appearance is consistent with the observations of Allen *et al* (37). The cTAL cells possessed Na/K/Cl cotransport as indicated by bumetamide sensitive ^{86}Rb uptake, amounting to 40% of control uptake pmol.mg protein^{-1}.min^{-1} (n = 3). These cells also possessed sodium-dependent phosphate transport function demonstrated by ^{32}P uptake. ^{32}P uptake in the presence of Na^+ was significantly greater than that in the absence of Na^+, 73.7 $\pm$ 2.0 and 38.52 $\pm$ 3.5 pmol.mg protein^{-1}.min^{-1} respectively (n = 6, $p < 0.01$). The above assayed characteristics indicate that the cultured cells have retained many of the functions typical of thick ascending limb cells.

Porcine cTAL cells possess a large number of receptors as illustrated by hormone-induced Ca^{2+} transients (Fig.2). Parathyroid hormone (PTH, basal $[Ca^{2+}]_i$, 86$\pm$5 nM, to stimulated peak concentrations of 608$\pm$99 nM, n=7), glucagon (74$\pm$8 to 690$\pm$257 nM, n=4), arginine vasopressin (AVP, 78$\pm$3 to 766$\pm$162 nM, n=6), calcitonin (97$\pm$3 to 973$\pm$79 nM, n=3), bradykinin (83$\pm$8 to 843$\pm$89 nM, n=3), angiotensin II (Ang.II, 80$\pm$6 to 923$\pm$187 nM, n=3), atrial natriuretic peptide (ANP, 104$\pm$6 to 653$\pm$112 nM, n=4), the truncated analogue of ANP, C-ANP-(4-23) (82$\pm$1 to 427$\pm$41 nM, n=5), and its analogue, C-type natriuretic peptide (CNP, 84$\pm$4 to 209$\pm$18 nM, n=5) elicited Ca^{2+} transients when applied at maximal hormone concentrations (10^{-7} M). The hormones were added where indicated (Fig.2) and not removed throughout the study. These studies confirm that numerous hormonal receptors are present in porcine cTAL cells and show for the first time that activation of the receptors are associated with an increase in $[Ca^{2+}]_i$. It is likely that these transient increases

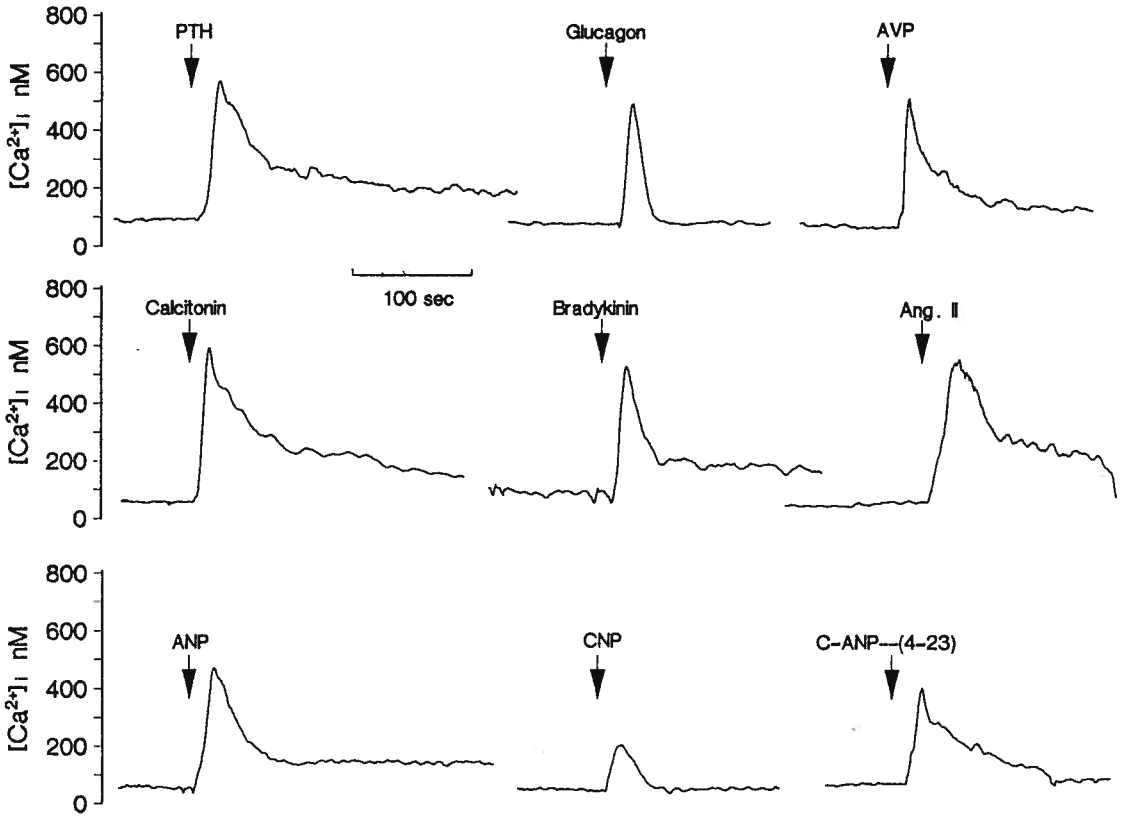

Fig.2. Hormone-mediated Ca^{2+} signals in isolated porcine cortical thick ascending limb (cTAL) cells of Henle's loop. Parathyroid hormone (PTH), glucagon, arginine vasopressin (AVP), calcitonin, bradykinin, angiotensin II (Ang.II), atrial natriuretic peptide (ANP), C-type natriuretic peptide (CNP) and the truncated analogue of ANP (C-ANP-(4-23)) were added, where indicated, at concentrations of 10^{-7} M. Intracellular free Ca^{2+} concentration ($[Ca^{2+}]_i$) was determined by microfluorescence on single subconfluent cTAL cells using fura-2. Illustrations are representative of 3-7 cells for each hormone.

in $[Ca^{2+}]_i$ are part of the intracellular signaling processes which may play an important role in cell function. It would seem important to characterize these Ca^{2+} transients to better understand hormonal controls and interactions among the hormone-mediated signal transduction processes. In the present study, PTH-, AVP- and ANP-induced Ca^{2+} transients were further characterized with fluorescent techniques.

III.1. PTH-induced Ca^{2+} transients

PTH resulted in a dose-dependent increase in $[Ca^{2+}]_i$ with a half-maximal Ca^{2+} response using about 10^{-9} M hormone concentration (Fig.3). As shown in Fig.2, PTH-induced Ca^{2+} transient was composed of two phases. The first phase was very fast and maintained only about 50 sec.; the second phase was slow and sustained for more than 200 sec. These two phases might derive from different sources and controlled by different mechanisms.

To verify the contribution of Ca^{2+} entry across the plasma membrane to the PTH-mediated Ca^{2+} transient, nifedipine (a Ca^{2+} channel blocker), nominal Ca^{2+}-free solution, and calcium analogue, Mn^{2+}, were applied to cTAL cells before or during PTH administration. In normal cTAL cells, 10^{-7} M PTH induced elevation of $[Ca^{2+}]_i$, from basal 86 ± 6 nM to 607 ± 99 nM, n=7. Pretreatment of the cells with nifedipine diminished the increment in $[Ca^{2+}]_i$ (Fig.4). Basal $[Ca^{2+}]_i$ was 86 ± 4 nM which rose to 218 ± 111 nM following 10^{-7} M PTH and rapidly returned to basal levels of 95 ± 9 nM, n=4, within 95 sec. In the absence of external Ca^{2+} (Ca^{2+}_o) and with the addition of 0.5 mM EGTA to the bathing solution, Ca^{2+} transient was mitigated (Fig.4, basal 85 ± 5 to 472 ± 121 nM, n=3, $P<0.05$). Next, we used Mn^{2+} to define the component of calcium entry versus intracellular Ca^{2+} release. Mn^{2+} is

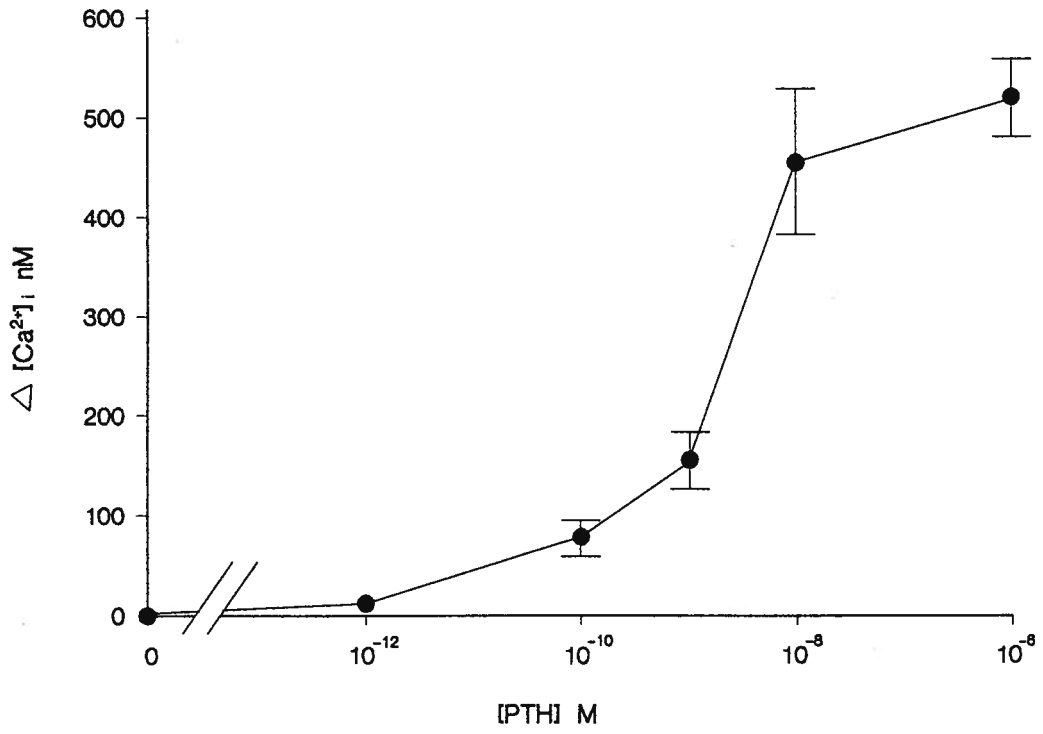

Fig.3. Dose-dependent increases in $[Ca^{2+}]_i$ with PTH. PTH was added to the perfusion solution bathing the porcine cTAL cells at the concentrations indicated. $\Delta[Ca^{2+}]_i$ is the difference between maximal $[Ca^{2+}]_i$ concentration and the basal levels of $[Ca^{2+}]_i$ measured in resting cells. Values are mean $\pm$ SE and represent responses in 3-7 individual cells.

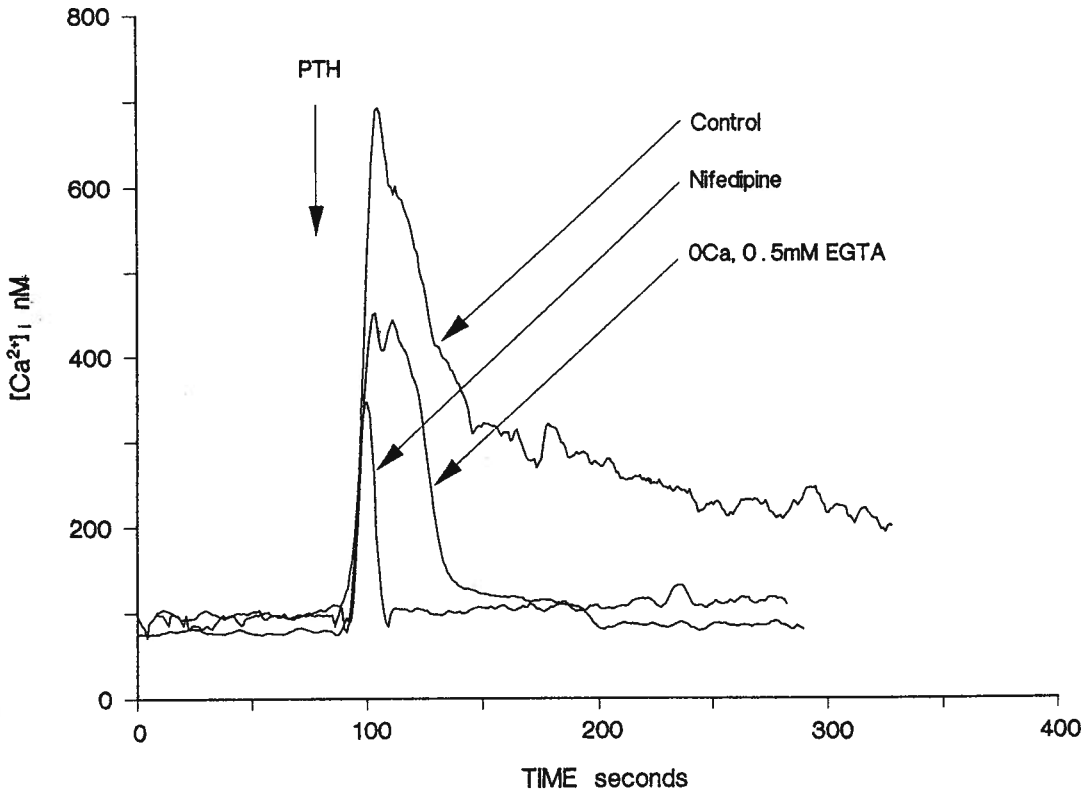

Fig.4. Characterization of PTH-induced Ca^{2+} transients in porcine cTAL cells. Nifedipine, 10 μM, was added with 10^{-7} M PTH where indicated. Also shown is the effect of removal of external Ca^{2+} from bath buffer solution with the addition of 0.5 mM EGTA 5 min before treatment with PHT. Fluorescence tracings are representative of 3-4 cells for each manipulation from different cell preparations.

able to enter the cell through Ca^{2+} channels and quenches fura-2 fluorescence. As shown in Fig.5, Mn^{2+} quenched the dye during the stimulation with PTH, indicating that Ca^{2+} channels in the plasma membranes are involved in the PTH-induced Ca^{2+} transients.

The above results suggest that PTH releases intracellular Ca^{2+} and initiates Ca^{2+} entry across the plasma membrane of the cTAL cell. To assess the source of PTH-induced Ca^{2+} release, we used thapsigargin, a specific inhibitor of microsomal Ca^{2+} adenosine-triphosphatase (ATPase) which depletes endoplasmic reticulum Ca^{2+} stores (38,39). Thapsigargin (1.5 μM) did not by itself alter resting $[Ca^{2+}]_i$ levels in the cTAL cells. Thapsigargin added to the buffer solution 30 min, prior to the addition of 10^{-7} M PTH, diminished the hormone-mediated increment in $[Ca^{2+}]_i$ (basal 86 ± 3 to 220 ± 44 nM, n=7, $P<0.05$)(Fig.6). These data suggest that endoplasmic reticulum Ca^{2+} stores are important in PTH-mediated Ca^{2+} signaling.

In summary, PTH administration leads to concentration-dependent transient increments in $[Ca^{2+}]_i$ which results, in part, from intracellular release from endoplasmic reticulum and, in part, from entry of Ca^{2+} across the plasma membrane.

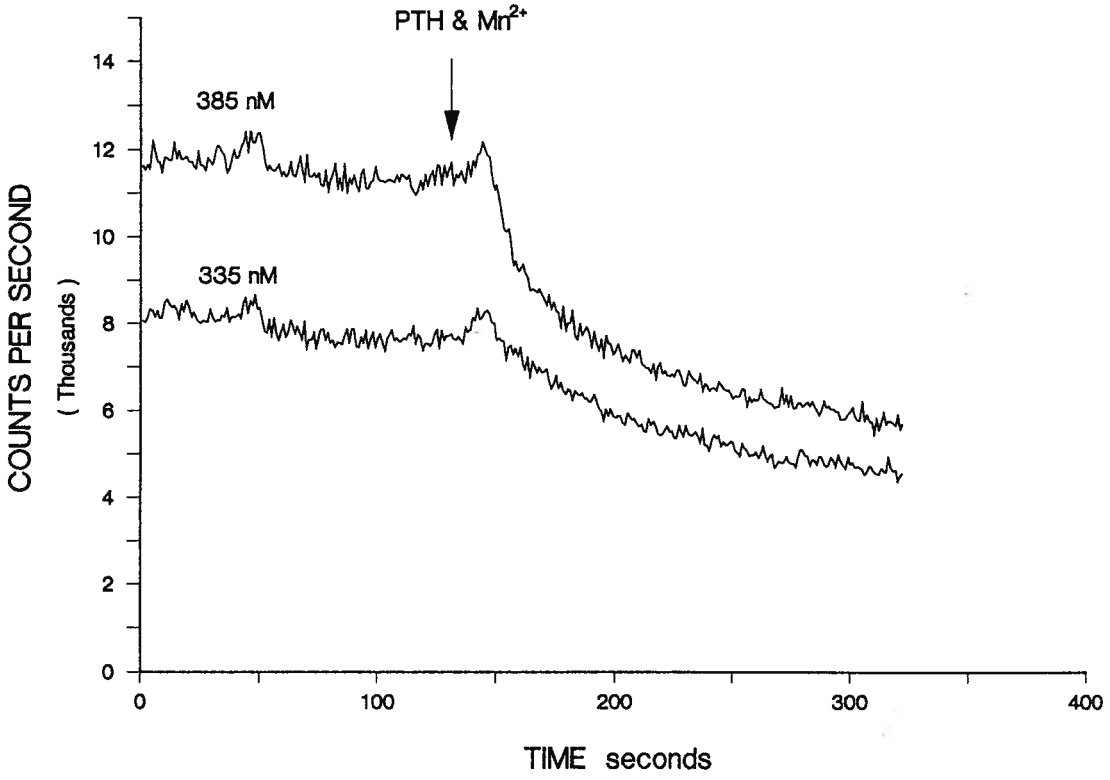

Fig.5. Changes in fluorescence emission at 335 and 385 nm excitation wavelengths with $MnCl_2$. 0.5 mM $MnCl_2$ was added into bath solution with 10^{-7} M PTH where indicated. Fluorescence tracings are representative of 3 cells.

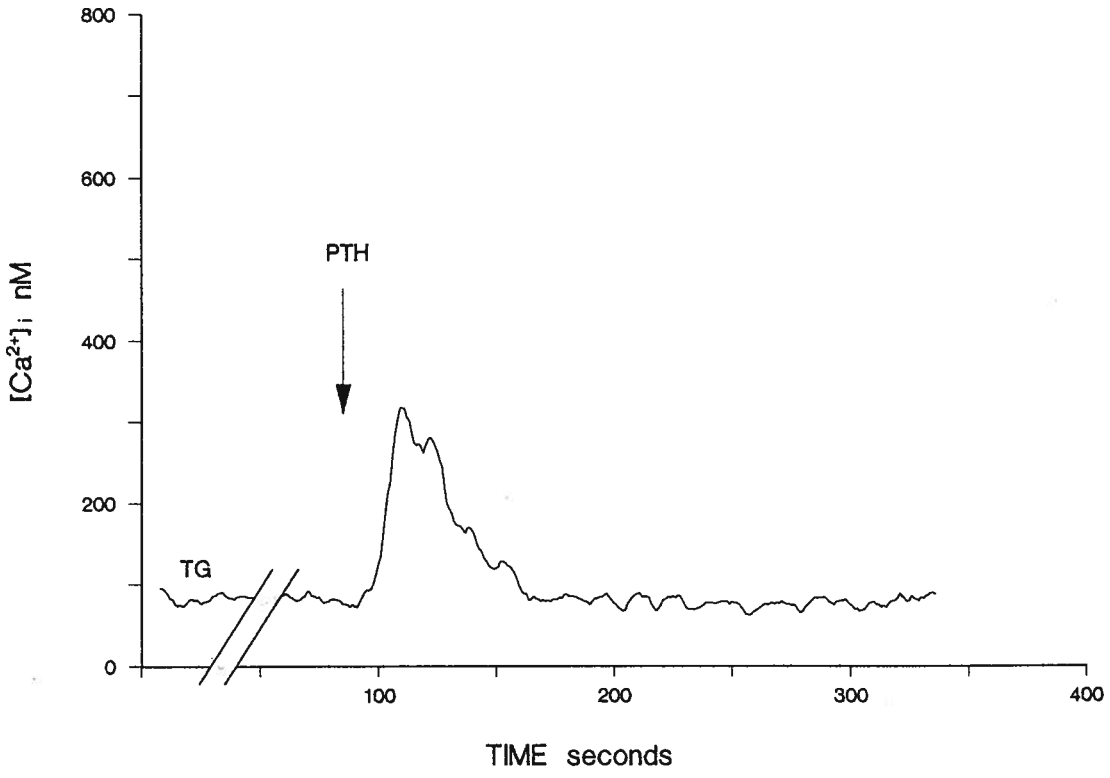

Fig.6. The effect of thapsigargin on PTH-induced Ca^{2+} transients. 1.5 mM thapsigargin (TG) was added 30 min prior to the addition of 10^{-7} M PTH. Fluorescence tracing is representative of 3 cells.

III.2. AVP-induced Ca^{2+} transients

AVP induces an increase in $[Ca^{2+}]_i$ in a dose-dependent fashion (Fig.7). The hormone concentration necessary for half-maximal response is in order of $5.0x10^{-9}$M. Next, we used various approaches given above to determine the source of Ca^{2+} in the signaling process. Nifedipine, Ca^{2+}-free bath buffer solutions (Fig.8), Mn^{2+} (Fig.9), and thapsigargin (Fig.10) were used to determine the source of Ca^{2+} transients mediated by AVP. The AVP-mediated Ca^{2+} signal appears to be mainly composed of intracellular Ca^{2+} release followed by Ca^{2+} entry into the cytosol. This conclusion is based on the observation that the removal of Ca^{2+}_o from the bath buffer solution and the addition of 0.5 mM EGTA inhibited AVP-induced Ca^{2+} increase by a small amount (395 ± 62 nM, $n=3, P<0.05$,compared to stimulated control values) (Fig.8). Nifedipine did not significantly diminish the maximal $[Ca^{2+}]_i$ increase (basal, 89 ± 4 to stimulated, 538 ± 203 nM, $n=4, P>0.05$)(Fig.8). Thapsigargin completely abolished the Ca^{2+} signal ($[Ca^{2+}]_i$ changes: 83 ± 7 to 83 ± 7 nM, $n=3$) (Fig.10).

In summary, AVP-mediated Ca^{2+} transients are dose-dependent and result from both intracellular Ca^{2+} release and Ca^{2+} entry across the plasma membrane. Compared with PTH-mediated Ca^{2+} transients, intracellular Ca^{2+} release contributes a major part to the AVP-mediated Ca^{2+} signal.

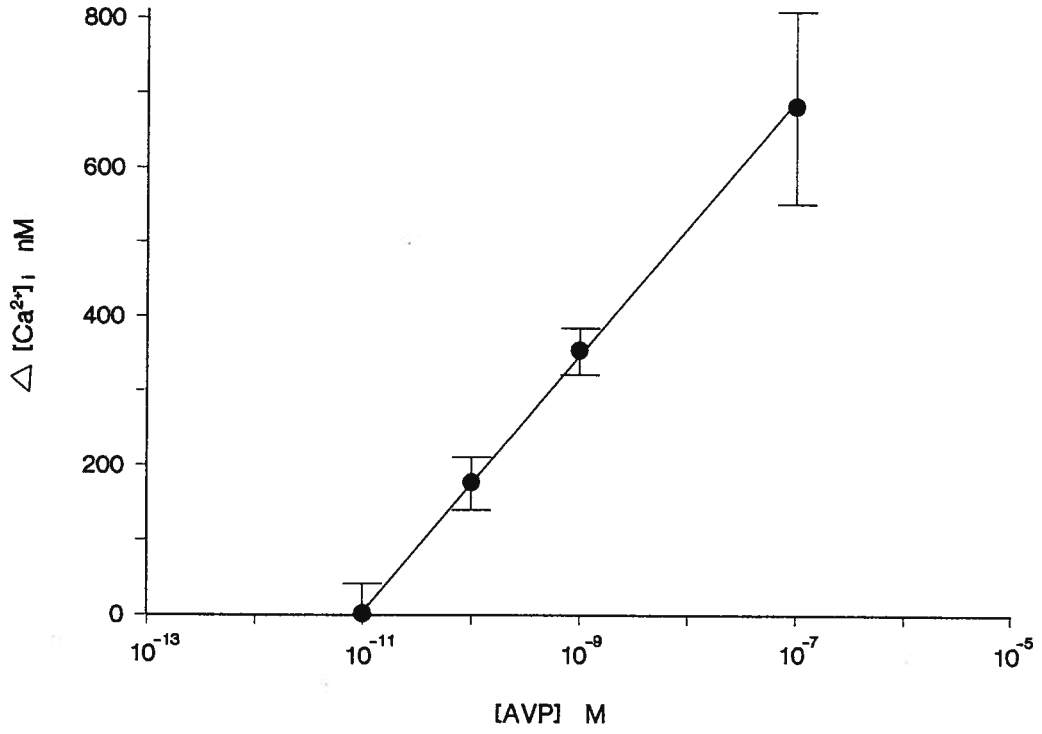

Fig.7. Dose-dependent initiation of Ca^{2+} transients with AVP in cTAL cells. AVP was added at the concentrations indicated and $\Delta([Ca^{2+}]_i)$ represents the change from basal to peak $[Ca^{2+}]_i$ concentrations. Values are mean $\pm$ SE for 4-7 cells per concentration.

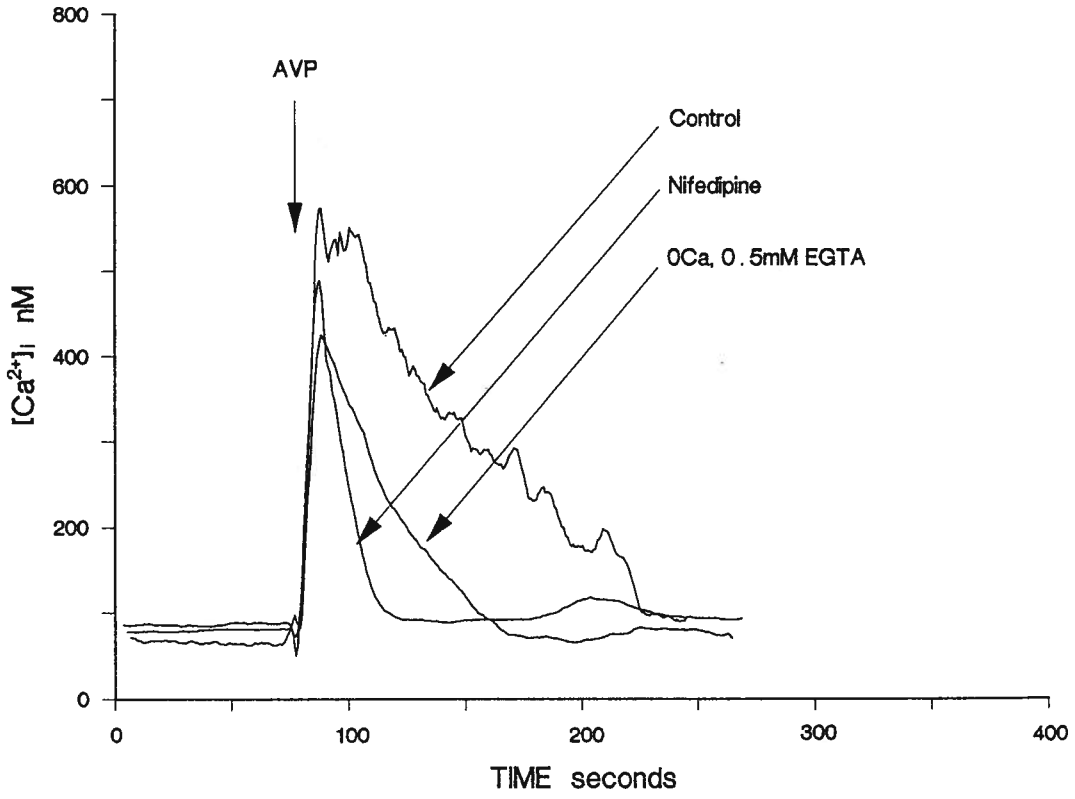

Fig.8. Characterization of AVP-induced Ca^{2+} transients in cTAL cells. 10 μM nifedipine was applied to the cell prior to application of 10^{-7} M AVP (representative of 4 cells from different preparations). Also shown is a representative experiment, one of three, in which external Ca^{2+} was removed from the bath and 0.5 mM EGTA added 5 min before treatment with 10^{-7} M AVP.

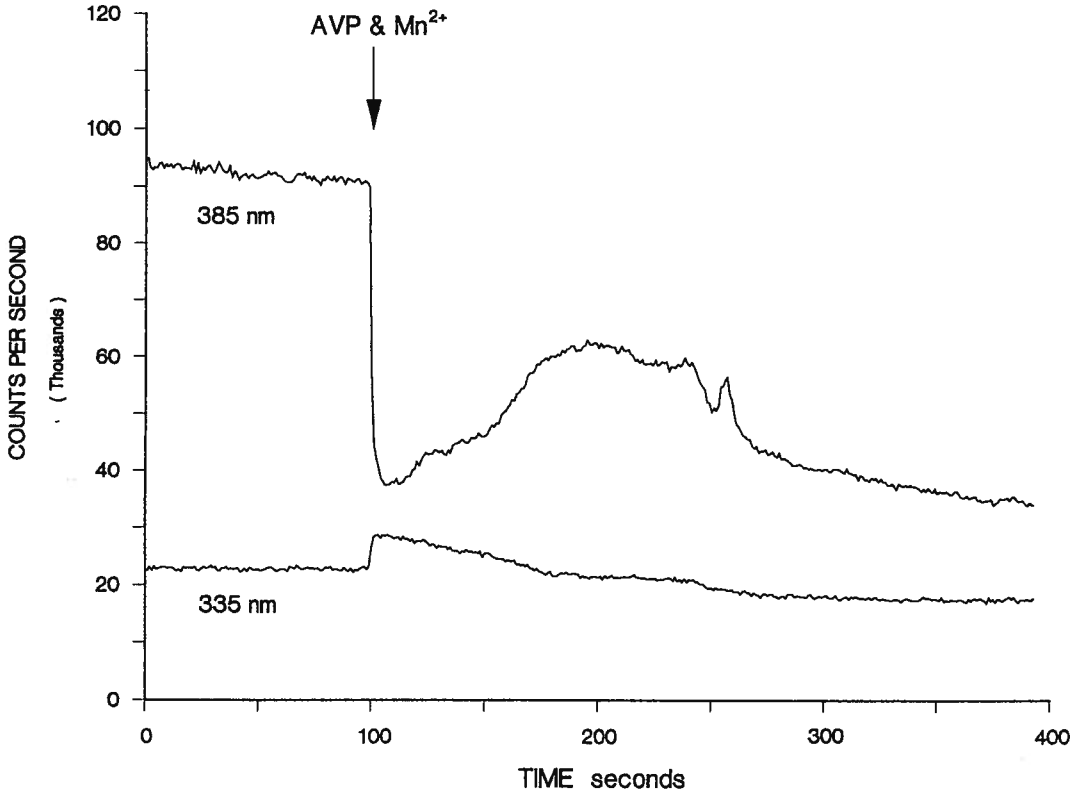

Fig.9. The effect of Mn^{2+} on fluorescence emission. 0.5 mM $MnCl_2$ was added to external buffer solution with 10^{-7} M AVP. The fluorescence emission was recorded at 335 and 385 nm excitation wavelengths (representative of 3 separate experiments).

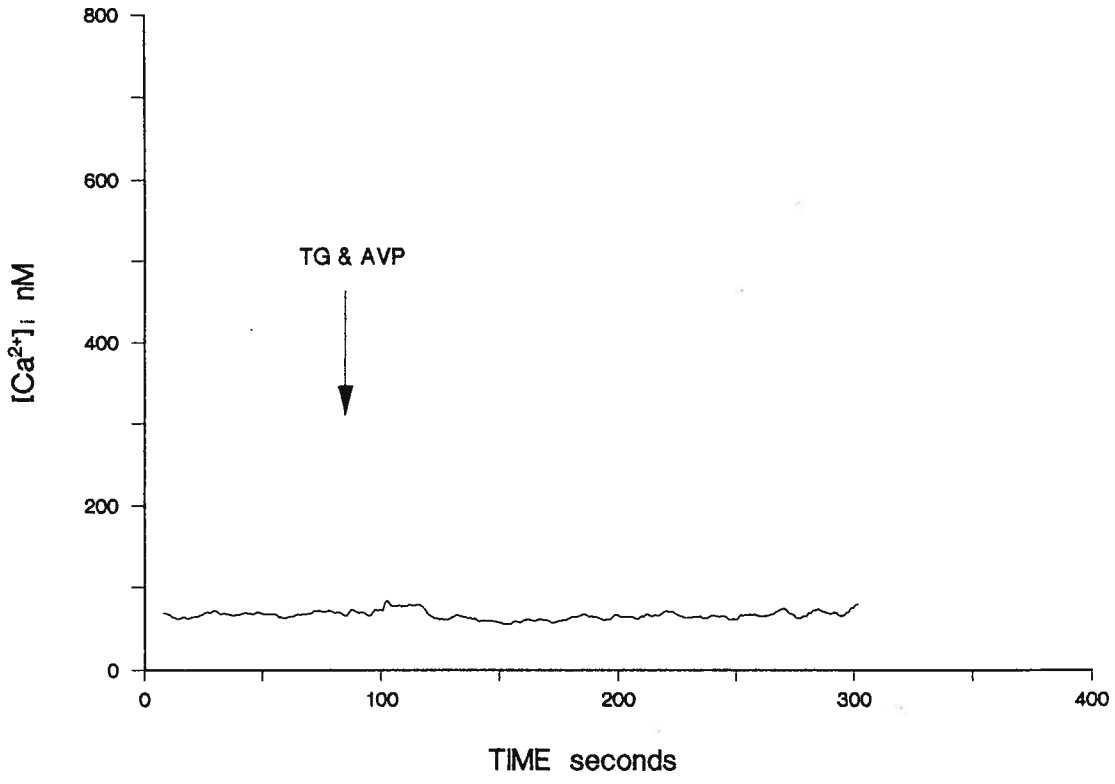

Fig.10. Effect of thapsigargin on AVP-induced Ca^{2+} transients. Thapsigargin (TG, 1.5 μM) was added 30 min prior to the application of 10^{-7} M AVP. This tracing is representative of 3 individual cells.

III.3. cAMP-mediated Ca^{2+} transients

We have previously reported that many of the peptide hormones used here stimulated cAMP generation in primary porcine cTAL cells grown in culture (7,20). cAMP is known to elicit elevation in $[Ca^{2+}]_i$ which may be involved with intracellular signaling (18). Accordingly, we tested the effect of cAMP on $[Ca^{2+}]_i$ in the porcine cTAL cells. Fig.11 illustrates a representative experiment which shows that 8-BrcAMP induces an increase in $[Ca^{2+}]_i$ (basal, 83 ± 3 to stimulated 427 ± 48 nM, n=3). In all of the cells studied, the increase in $[Ca^{2+}]_i$ with 8-BrcAMP returned to basal levels within 60-120 sec following initiation. The rapid return to basal levels suggests that the second phase, in which Ca^{2+} entry is normally observed, is absent, i.e. cAMP releases intracellular Ca^{2+} but does not activate Ca^{2+} entry. 8-BrcAMP-induced Ca^{2+} transients were not affected by either addition of nifedipine ($[Ca^{2+}]_i$ changes: 86 ± 4 to 390 ± 30 nM, n=4) or the removal of external Ca^{2+} ($[Ca^{2+}]_i$ changes: 84 ± 6 to 517 ± 142 nM, n=4) (Fig.11). Mn^{2+} did not significantly quench fluorescence during 8-BrcAMP administration (Fig.12) and thapsigargin completely inhibited the cAMP-induced Ca^{2+} signal ($[Ca^{2+}]_i$ changes: 81 ± 1 to 87 ± 4 nM, n=4) (Fig.13).

We next determined the effect of cAMP on hormone-mediated Ca^{2+} signalling. We postulated that pretreatment with cAMP would deplete intracellular Ca^{2+} stores and diminish or abolish the PTH- and AVP-mediated $[Ca^{2+}]_i$ transients. cTAL cells were pretreated with 8-BrcAMP for 30 min prior to the addition of maximal concentration of PTH or AVP (Fig.14A, Fig.14B). Pretreatment of cTAL cells with 8-BrcAMP abolished the PTH-mediated response ($[Ca^{2+}]_i$ changes: 87 ± 1 to 94 ± 8 nM, n=5) and diminished the AVP-mediated response ($[Ca^{2+}]_i$ changes: 87 ± 2 to 300 ± 86 nM, n=3). As PTH and AVP induce

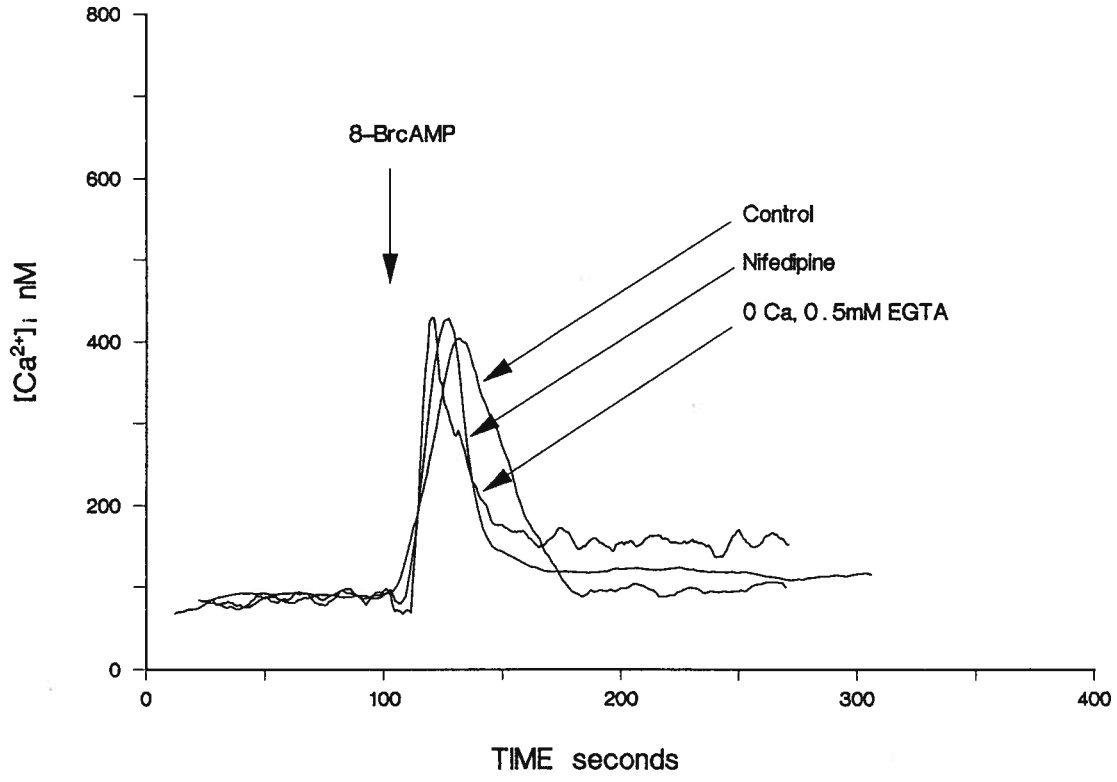

Fig.11. Cyclic adenosine monophosphate (cAMP) induces Ca^{2+} transients in porcine cTAL cells. Where indicated 10^{-4} M 8-bromo-adenosine-3',5'-cyclic monophosphate (8-BrcAMP) was added to cell bath solution. A representative Ca^{2+} transient is shown, as well as the effect on 8-BrcAMP-induced Ca^{2+} transients of 10 μM nifedipine prior to 8-BrcAMP application and the removal of external Ca^{2+} and addition of 0.5 mM EGTA. Fluorescence tracings are representative of 3-5 cells of each manipulation.

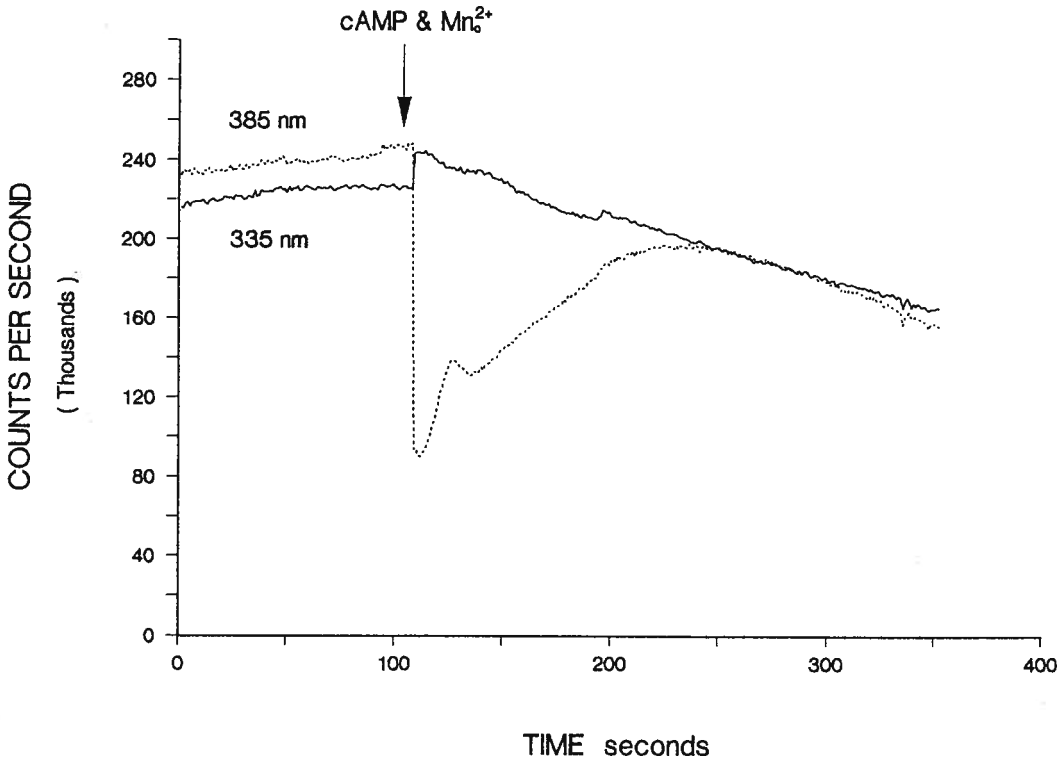

Fig.12. The effect of Mn^{2+} on fluorescence emission. 0.5 mM $MnCl_2$ was added to external buffer solution with 10^{-4} M 8-BrcAMP. The fluorescence emission was recorded at 335 nm and 385 nm excitation wavelengths (representative of 3 separate experiments).

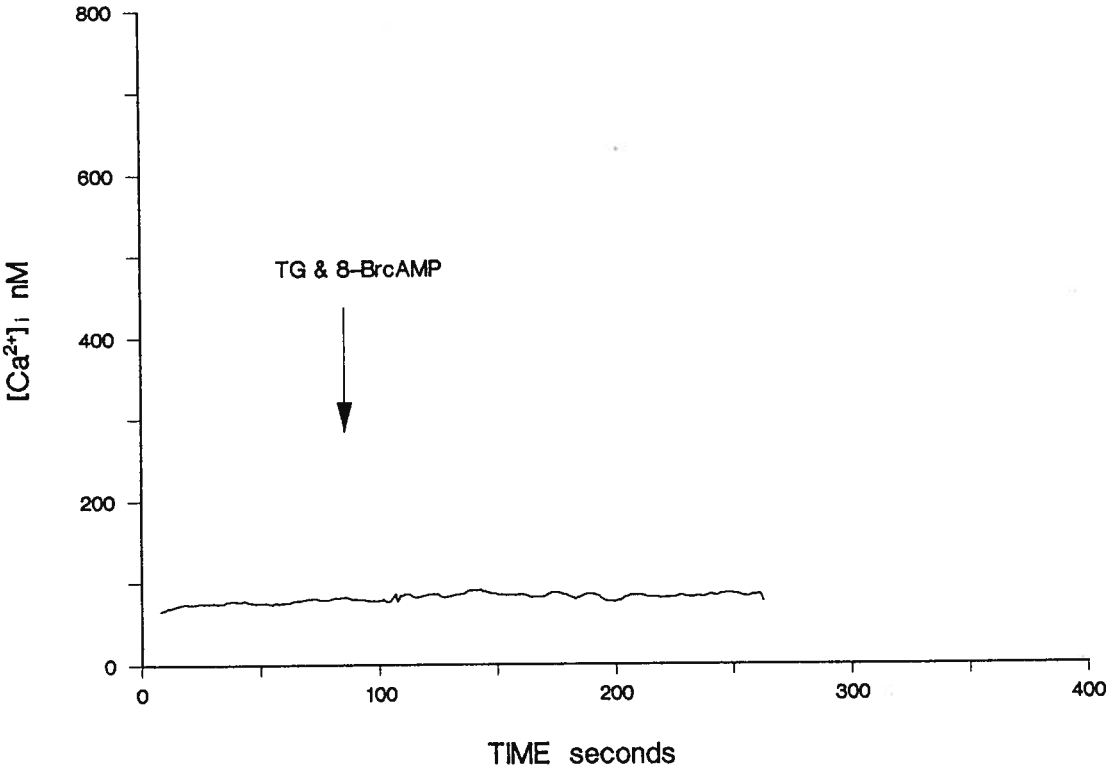

Fig.13. The effect of pretreatment of thapsigargin on the effect of 8-BrcAMP. Thapsigargin (TG, 1.5 μM) was added 30 min prior to the application of 10^{-4} M 8-BrcAMP. This tracing is representative of 3 individual cells.

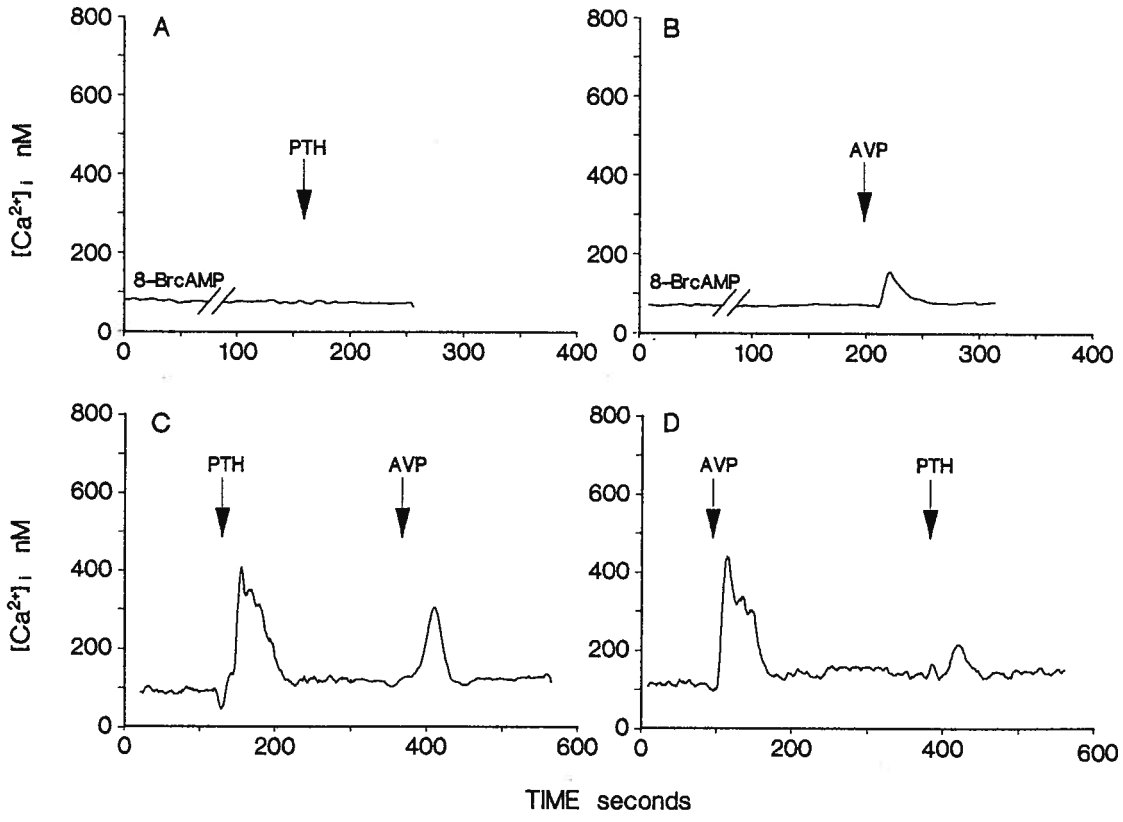

Fig.14. Effect of cAMP-induced depletion of intracellular Ca^{2+} stores on agonist-induced Ca^{2+} transients. cTAL cells were pretreated with 8-BrcAMP (10^{-4} M) for 30 min prior to addition of **A.** PTH (10^{-7} M), or **B.** AVP (10^{-7} M). **C.** Illustration of the results following pretreatment of cTAL cells with PTH (10^{-7} M) followed 20 min later by an AVP (10^{-7} M) challenge. **D.** The effect of pretreating cTAL cells with 10^{-7} M AVP followed by the addition of 10^{-7} M PTH where indicated. Traces are representative of 3-5 cells for each experimental manoeuvre.

receptor-mediated cAMP generation in cTAL cells (7), we tested the effect of PTH and AVP pretreatment on the ability of these agonists to induce changes in $[Ca^{2+}]_i$ (Fig.14C, Fig.14D). Pretreatment of cells with maximal concentrations of PTH for 5～20 min prior to addition of AVP diminished the AVP response ($[Ca^{2+}]_i$ changes: 88±4 nM prior to AVP and 319±39 nM post-AVP treatment, n=5, $P<0.05$, compared with control-stimulated levels). Pretreatment with AVP for 5～20 min prior to the addition of PTH inhibited the PTH-induced $[Ca^{2+}]_i$ response ($[Ca^{2+}]_i$ changes: 85±4 to 127±28 nM, n=5, $P<0.01$). These studies suggest that receptor-mediated generation of cAMP depletes intracellular Ca^{2+} stores resulting in a refractory cell, which does not respond to a subsequent application of hormone. Furthermore, these data suggest that PTH and AVP access similar intracellular Ca^{2+} stores probably through cAMP mediation. Hormone stimulation of adenylate cyclase and cAMP generation diminishes intracellular Ca^{2+} pools in the presence of enhanced Ca^{2+} entry from extracellular sources. Further studies are warranted to define the specific intracellular Ca^{2+} stores and mechanisms whereby these two hormones access these stores.

III.4. The effect of protein kinase C on hormone-mediated Ca^{2+} transients

Hormone-receptor coupling generates IP_3 and DAG which activate PKC, and cAMP which activates protein kinase A (PKA) (18,20). Accordingly, it was considered essential to determine the interaction of these two signaling pathways for each of the prototypic hormones, PTH and AVP. Activation of protein kinase C with phorbol esters did not initiate any changes in basal $[Ca^{2+}]_i$ in cTAL cells (data not shown). However, pretreatment of cTAL cells with the phorbol ester, 12-O-tetradecanoyl-phorbol 13--acetate (TPA), led to an inhibition of PTH-induced rise in $[Ca^{2+}]_i$ (85±3 to 85±3 nM, n=5). Similar pre-treatment

abolished AVP-induced and cAMP-induced increases in $[Ca^{2+}]_i$ respectively (Fig.15). To determine whether the inhibition with TPA was related in turn to protein kinase C activation, we treated cTAL cells for a prolonged period with phorbol esters to down-regulate this enzyme and then challenged the cells with agonists (40). If protein kinase C activation inhibited hormone-dependent Ca^{2+} transient, then in the absence of this enzyme, PTH and AVP would be effective. Following treatment of cells for 16 hours with TPA, we applied maximal concentrations of PTH (10^{-7} M), AVP (10^{-7} M) and cAMP (10^{-4} M). In down-regulated cells, PTH resulted in an increase in $[Ca^{2+}]_i$ from 91 ± 6 nM to 111 ± 11 nM, n=4 (Fig.15A) and AVP, 81 ± 2 nM to 206 ± 15 nM, n=5 (Fig.15B) and cAMP, 95 ± 8 nM to 239 ± 50 nM, n=3 (Fig.15C).

These data indicate a partial return of agonist-mediated responses following down-regulation of PKC activity with prolonged phorbol ester treatment. These results further support the notion that PKC interacts in a specific way with agonist-mediated changes in Ca^{2+} signaling which may play a physiological role in modulating receptor-mediated responses.

III.5. ANP-induced Ca^{2+} transients

Cortical thick ascending limb plays an important role in salt reabsorption within the nephron. Electrolyte transport within the cTAL cells is sensitively controlled by many regulatory hormones (11,19,20,41). There is some controversy as to whether ANP is one of these regulatory hormones. ANP acts through receptors to cause vasodilation, an increase in urinary flow and sodium excretion, and a reduction in blood volume (42,43,44). The principal renal actions of ANP are localized in the glomerulus and collecting tubule (42,43)

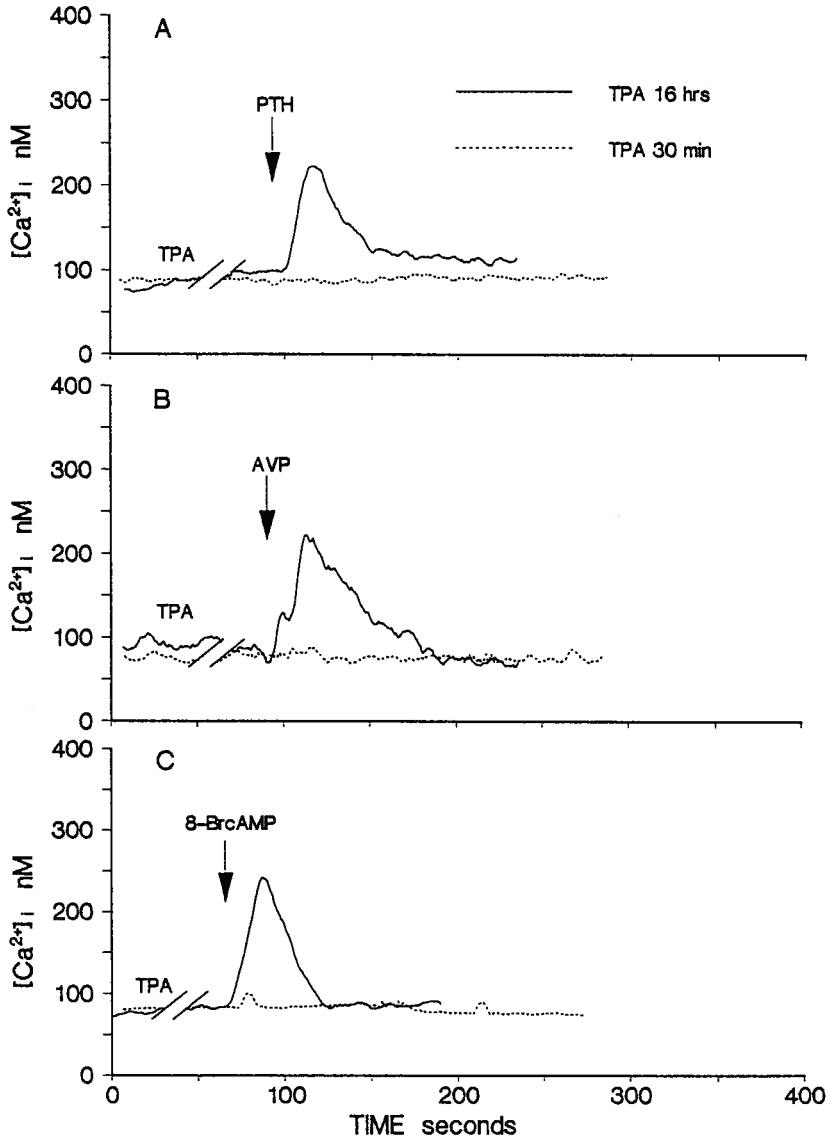

Fig.15. Effect of protein kinase C activation on agonist-induced Ca^{2+} transients in cTAL cells. Where indicated, cTAL cells were pretreated with 12-O-tetradecanoylphorbol 13-acetate (TPA, 10^{-7} M) for 30 min prior to experimentation. **A.** PTH (10^{-7} M); **B.** AVP (10^{-7} M); or **C.** 8-BrcAMP (10^{-4} M) were added where indicated. Fluorescence tracings are representative of 3 ~ 5 cells for each experiment. In a separate series of experiments the effect of prolonged phorbol ester treatment on agonist-induced Ca^{2+} transients in cTAL cells were determined. Where indicated, cTAL cells were treated with TPA, 10^{-7} M, for 16 hrs to down-regulate protein kinase C activity. Ca^{2+} transients were determined with microfluorometry following: **A.** PTH (10^{-7} M); **B.** AVP (10^{-7} M); and **C.** 8-BrcAMP (10^{-4} M) treatment. Fluorescent tracings are representative of 3-5 cells.

but some reports suggest that ANP may have other actions within the kidney (44,45). First is the observation that ANP administration results in an increase in urinary magnesium excretion in addition to sodium excretion (43). As magnesium is reabsorbed principally in the thick ascending limb, it would suggest an action for ANP at this site (41). Another possible role for ANP is related to Cl transport. Bailly *et al* (46) have provided direct evidence for cGMP action on chloride transport in the thick ascending limb. However, as ANP probably does not stimulate cGMP in rat or rabbit thick ascending limb segments, the link between ANP and Cl-transport is tenuous (47,48). Thus, there is some controversy concerning the presence of ANP receptors, the intracellular signals generated, and the function of ANP in the cTAL on the loop of Henle.

The natriuretic peptide family includes the 28-amino acid peptide, called atrial natriuretic peptide, ANP, which is the major circulatory form of atrial peptide (49) and two analogues, C-type natriuretic peptide (CNP) and brain natriuretic peptide (BNP). CNP is the most abundant natriuretic peptide in the brain and is not present in peripheral tissues (50,51). BNP is found in high concentrations in the heart (52). ANP and BNP are thought to recognize a common ANP_A receptor that possesses guanylyl cyclase activity (53). CNP recognizes a different receptor subtype called ANP_B that is structurally distinct from the ANP_A receptor, but also possesses a guanylyl cyclase domain (54). The ANP_C receptor binds ANP, CNP, and BNP, and is not coupled to guanylyl cyclase (45,55). This receptor was originally proposed to only function in clearing its ligands from the extracellular fluid, since it did not mediate the known renal functions of the natriuretic peptides (56). However, ANP_C may also mediate biological effects such as inhibition of the adenylyl cyclase system

(44,45,57).

Various ANP analogues were used to elicit changes in $[Ca^{2+}]_i$ in isolated porcine cTAL cells (Fig.2). Addition of vehicle alone to the perfusion solution did not alter $[Ca^{2+}]_i$. These data suggest the presence of ANP receptors in porcine cTAL cells. The effect of ANP on the change in $[Ca^{2+}]_i$ was dose dependent with a half-maximal response in the order of $5x10^{-8}$ M ANP concentration (Fig.16).

The profile of the Ca^{2+} transient suggested that it may be composed of intracellular Ca^{2+} release as well as entry across the plasma membrane (Fig.2). The following studies demonstrate that ANP-induced Ca^{2+} transients include intracellular Ca^{2+} release , likely from endoplasmic reticulum, and entry of extracellular Ca^{2+} into the cell through activation of Ca^{2+} channels. First, we performed studies in the absence of external Ca^{2+}. Fig.17 summarizes these results. Removal of Ca^{2+}_o and the addition of 0.5 mM EGTA to the bathing solution mitigated the rise in $[Ca^{2+}]_i$ ($[Ca^{2+}]_i$ changes: 80 ± 6 to 345 ± 120 nM, $n=3, P<0.05$ compared with control Ca^{2+} transients) which was induced by 10^{-7} M ANP. Second, we used nifedipine, a Ca^{2+} channel blocker, to determine the role of Ca^{2+} channels in the ANP-induced Ca^{2+} signaling (Fig.17). Addition of nifedipine, 10 μM, 30 min before the addition of 10^{-7} M ANP also diminished the $[Ca^{2+}]_i$ response ($[Ca^{2+}]_i$ changes: 91 ± 3 to 167 ± 25 nM, $n=5, P<0.05$ compared with control Ca^{2+} transients). Finally, by using other divalent cations, such as Mn^{2+}, that interact with Ca^{2+}-sensitive fluorescent dyes, it is possible to determine the relative importance of Ca^{2+} release from intracellular stores and Ca^{2+} entry across the plasma membrane in the signaling system (38). In the presence of extracellular Mn^{2+}, agonist-induced intracellular Ca^{2+} release may cause an initial increase (from intracellular

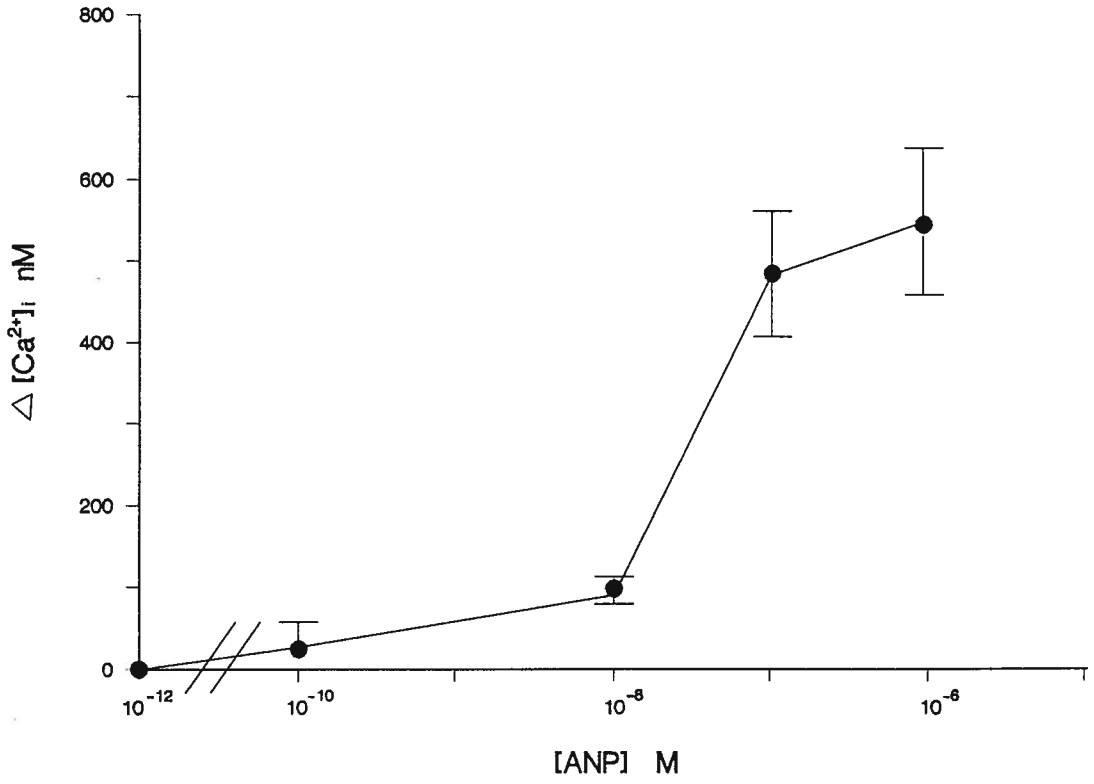

Fig.16. Dose-dependent initiation of Ca^{2+} transients with ANP in cTAL cells. $\Delta([Ca^{2+}]_i)$ is the change from basal-to-peak $[Ca^{2+}]_i$. Values are means ± SE for 3-5 cells.

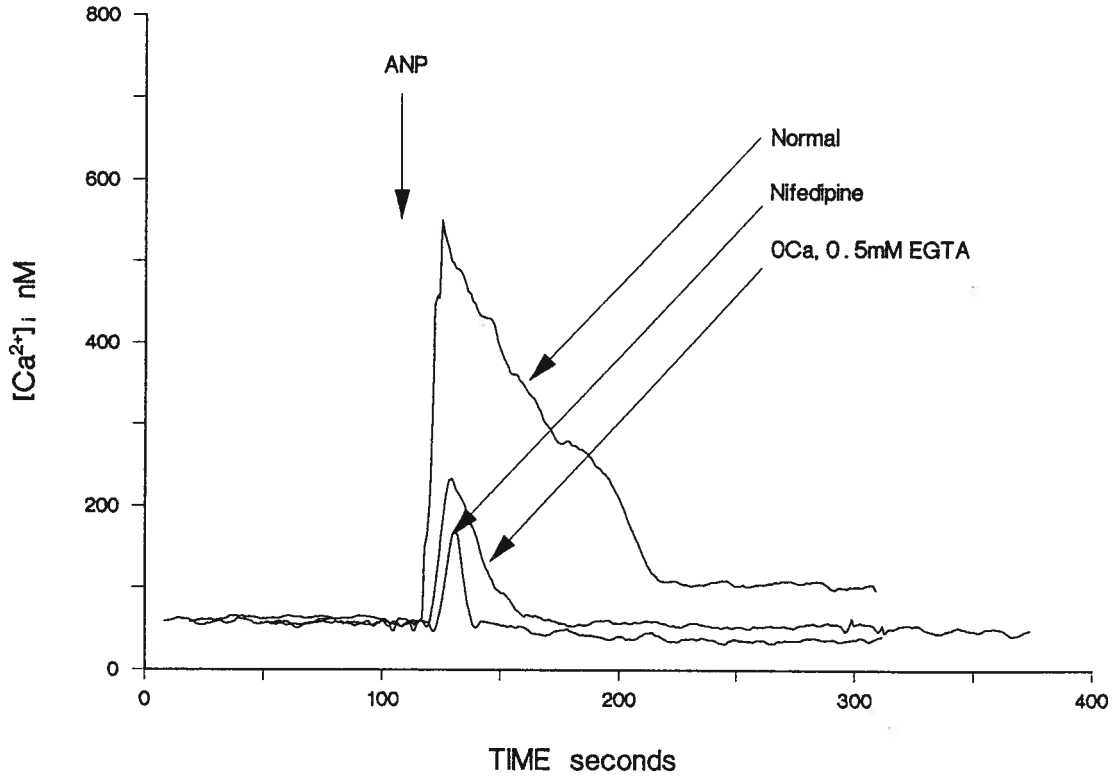

Fig.17. Characterization of ANP-induced Ca^{2+} transients in cTAL cells. A representative experiment (1 of 3) in which Ca^{2+} was removed from bath and 0.5 mM EGTA added 5 min before treatment with 10^{-7} M ANP; also shown is effect of 10 μM nifedipine applied to cell 30 min before application of 10^{-7} M ANP (representative of 5 cells from different preparations).

compartments) in fura-2 fluorescence that is followed by quench of fluorescence as Mn^{2+} crosses the plasma membrane into the cell. Fig.18 illustrates a representative experiment in which 10^{-7} M ANP lead to an initial increase in 335 nm and decrease in 385 nm fluorescence, which we interpret to be intracellular Ca^{2+} release followed by a quench of fluorescence in both channels due to Mn^{2+} entry. Note that the quench of fluorescence by Mn^{2+} entry continues even the $[Ca^{2+}]_i$ has returned to control levels, indicating that the Ca^{2+} channels are still activated when the Ca^{2+} signal has been terminated (Fig.18).

Next, thapsigargin was used to assess the source of ANP-induced Ca^{2+} release. 1.5 μM thapsigargin added to the buffer solution 30 min before the addition of 10^{-7} M ANP diminished the hormone-mediated increment in $[Ca^{2+}]_i$ ($[Ca^{2+}]_i$ changes: 88 ± 5 to 147 ± 37 nM, $n=6$, $P<0.05$ compared with control Ca^{2+} transients) (Fig.19). These data suggest that endoplasmic reticulum Ca^{2+} stores are important in ANP-mediated Ca^{2+} signaling.

One of the second messengers of ANP following binding to ANP_A receptors is cGMP. 8-Bromo-cGMP (8-BrcGMP), 10^{-4} M, does not alter $[Ca^{2+}]_i$ (90 ± 6 to 82 ± 5 nM, $n=4$) in porcine cTAL cells. Moreover, as shown in Fig.20, when the cTAL cells were pretreated with 8-BrcGMP, they became refractory to ANP (basal $[Ca^{2+}]_i$, 83 ± 5 nM, and following 10^{-7} M ANP, 88 ± 9 nM; $n=6$). These data indicate that ANP-induced Ca^{2+} changes may be inhibited by prior treatment with cGMP.

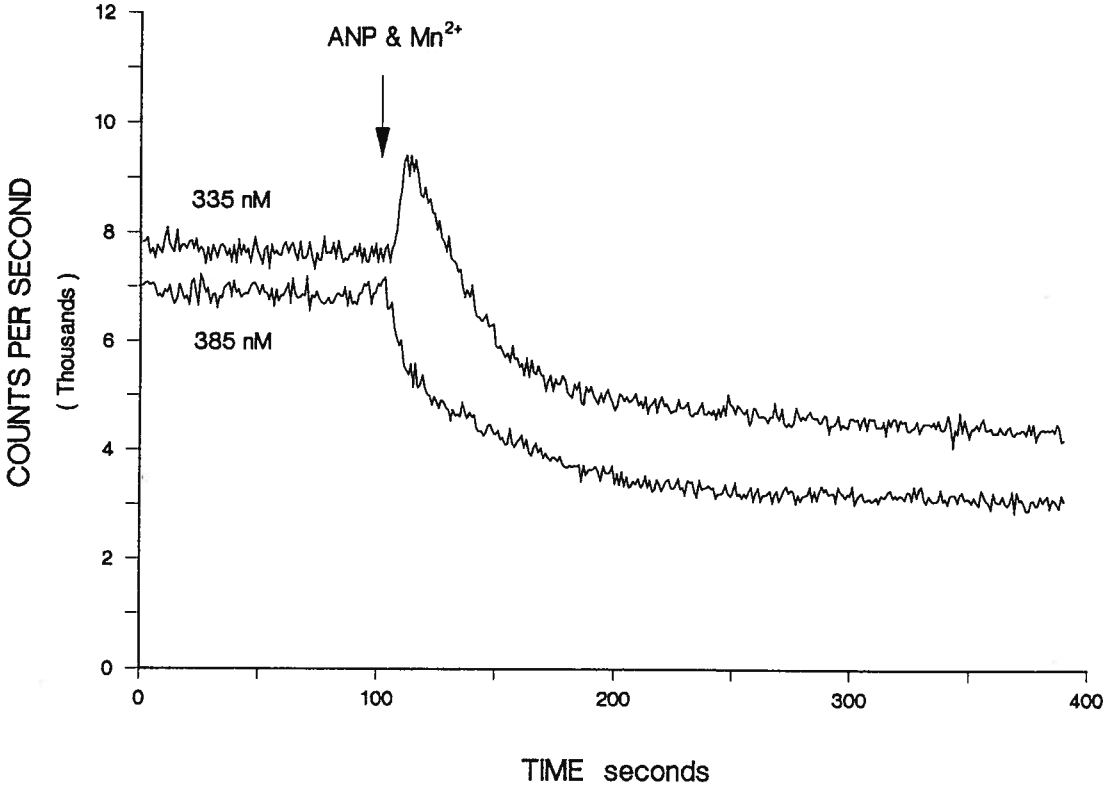

Fig.18. Changes in fluorescence emission at 335 nm and 385 nm excitation wavelengths with 0.5 mM $MnCl_2$ in external buffer solution. ANP (10^{-7} M) was added where indicated (representative of 3 separate experiments).

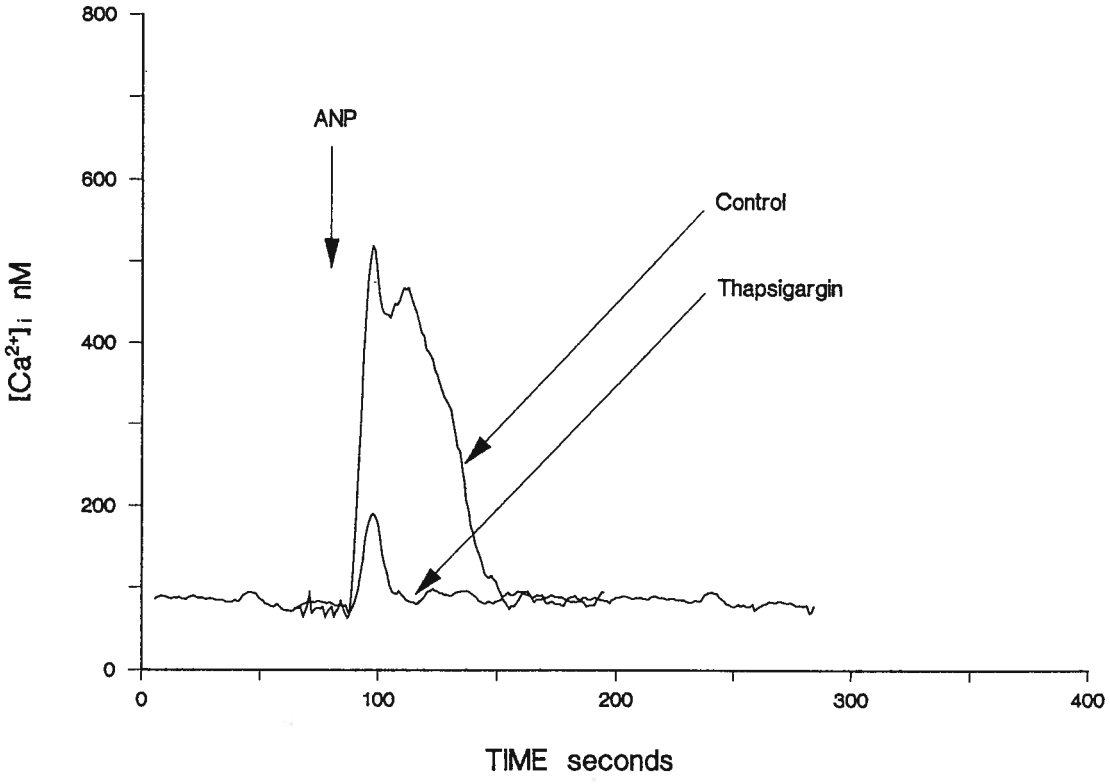

Fig.19. Effect of thapsigargin on ANP-induced Ca^{2+} transient. Thapsigargin (TG, 1.5 μM) was added 30 min before application of 10^{-7} M ANP (representative of 6 cells).

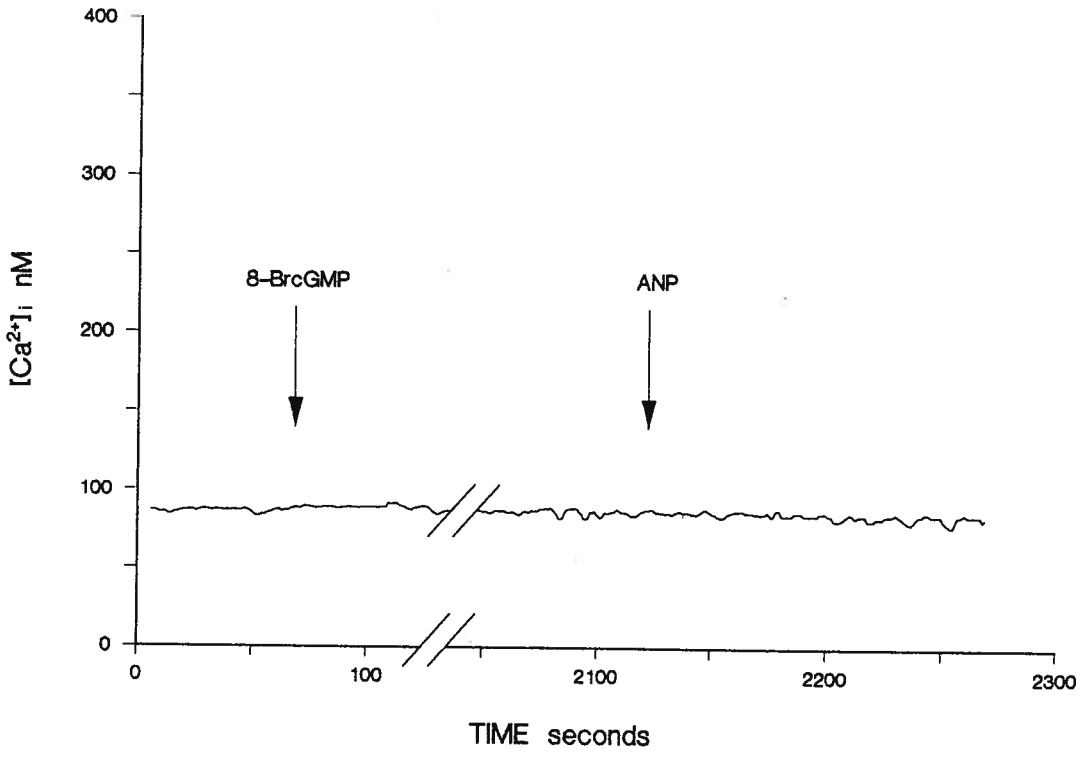

Fig.20. Effect of 8-BrcGMP pretreatment on ANP-mediated Ca^{2+} transients. Primary cTAL cells were pretreated with 8-BrcGMP (10^{-4} M) for 20-30 min before addition of ANP (10^{-7} M). Fluorescent tracing is representative of 6 cTAL cells.

IV. Discussion

Many hormones interact to orchestrate the regulation of salt transport in the cTAL of the loop of Henle (23,24,25,58,59). It is clear that many of these hormones act through receptor-activation of adenylate cyclase and the increase in cAMP (22,23). Morel and colleagues (18,19,60) have shown that the adenylate cyclase is sensitive to PTH, AVP, calcitonin, and glucagon in cTAL segments of rat and rabbit. These hormones also stimulate cAMP elevation in isolated porcine cTAL cells (7). An additional signaling pathway for these hormones involves receptor-mediated increase in $[Ca^{2+}]_i$ either through stimulation of membrane-bound phospholipase C and the formation of IP_3, or activation of receptor-operated Ca^{2+} channels (28,29). There is also growing evidence that inositol phosphates may have direct effects on Ca^{2+} channels within the plasma membrane (28). In turn, the intracellular Ca^{2+} transients may alter transport directly through modification of channel function or indirectly through activation of Ca^{2+}-dependent kinases (29,61,62). The present studies show that a number of hormones, including PTH, AVP, calcitonin, glucagon, bradykinin, angiotensin II, and ANP, initiate Ca^{2+} transients in isolated porcine cTAL cells (Fig.2). In order to understand the hormonal control of salt transport in the cTAL, it is important to know the sources and interaction of these Ca^{2+} signals.

IV.1. PTH- and AVP-induced Ca^{2+} transients

The present data indicate that Ca^{2+} transients induced by PTH and AVP are composed, in part, by intracellular Ca^{2+} release and, in part, by movement of Ca^{2+} into the cell across the plasma membrane. The evidence includes the mitigation of hormone-induced

Ca^{2+} transients by removal of external Ca^{2+}, and the inhibition of Ca^{2+} release by thapsigargin (Fig4, Fig.6, Fig.8, Fig.10). Interestingly, nifedipine inhibited the Ca^{2+} entry following PTH, but was not effective in the AVP-induced $[Ca^{2+}]_i$ elevation (Fig.4, Fig.8). The latter observation was also the conclusion of Nitschke *et al* (63) in perfused rabbit cTAL segments in which these investigators reported that AVP-induced Ca^{2+} transients were partly due to intracellular Ca^{2+} release and partly from Ca^{2+} influx. They were unable to block Ca^{2+} entry with nifedipine. These studies suggest that PTH and AVP lead to entry of Ca^{2+} into the cytosol by different mechanisms, such as nifedipine-insensitive calcium channels.

Our studies indicate that the secondary messenger, cAMP, may release intracellular Ca^{2+} which may be important in the receptor-mediated Ca^{2+} transient. This was not detected in the perfused rabbit cTAL segment (27). The reason for the difference in these findings is not apparent at the present time. The second messenger, cAMP, has been shown to release intracellular Ca^{2+} leading to the initiation of Ca^{2+} signals in many different cell types including renal epithelium (17,40,64,65,66). In the present studies, we consistently observed an increase in $[Ca^{2+}]_i$ with 8-BrcAMP (Fig.11). Interestingly, the increments in cytosolic Ca^{2+} appear to be from internal sources rather than entry through activation of Ca^{2+} channels. There is no evidence for the presence of cAMP-activated Ca^{2+} channels in this cell type (29,63). However, the present data do not rule them out as the PTH and AVP signals may be due, in part, to receptor-mediated or IP_3-mediated Ca^{2+} entry (28,29). The present data would suggest that cytosolic Ca^{2+} activity may be mediated by cAMP and/or IP_3 release of Ca^{2+} and Ca^{2+} entry across Ca^{2+} channels. Furthermore, our evidence suggest that cAMP elevates $[Ca^{2+}]_i$ through an IP_3-sensitive pool. Thapsigargin depletes Ca^{2+} from IP_3-sensitive

pool in a variety of cell types by specific inhibition of nonmitochondrial microsomal Ca^{2+}-ATPase activity without affecting inositol phosphate levels (67). Thapsigargin inhibited the cAMP-induced increase in $[Ca^{2+}]_i$ (Fig.13). Thapsigargin also inhibited the Ca^{2+} transients associated with PTH and AVP treatments. It is unknown if PTH or AVP release intracellular Ca^{2+}, possibly by an IP_3-dependent mechanism (40), directly or through the stimulation of cAMP.

Treatment of porcine cTAL cells with TPA resulted in diminished PTH-. AVP-, and cAMP-mediated Ca^{2+} signals (Fig.15). Other studies have reported that activation of protein kinase C with phorbol esters inhibits agonist-induced Ca^{2+} mobilization in many different cell types (68-72). The result obtained with phorbol ester treatment suggests that the inhibitory effect of hormonal induction of Ca^{2+} release from an internal store is, at least in part, mediated by protein kinase C which may provide a negative feedback control on receptor-mediated Ca^{2+} mobilization. Because phorbol esters also diminish the cAMP response, it is likely that protein kinase C activation inhibits internal Ca^{2+} release. Although these observations demonstrate that protein kinase C is responsible for the negative feedback on agonist-induced Ca^{2+} transients, it is not clear if this enzyme is also involved with receptor desensitization as has been shown for other cells (73,74).

PTH and AVP, as well as glucagon and calcitonin are thought to act on the same pool of adenylate cyclase (20). Elalouf and colleagues (73,74) have shown that administration of AVP to hormone-depleted rats rapidly desensitizes or down-regulates receptor density in the TAL. They also report that AVP desensitization is specific as glucagon and calcitonin were not affected by the prolonged presence of pharmacological

doses of AVP. The present studies, using Ca^{2+} signals, suggest that AVP desensitization in porcine cTAL cells may be non-specific with PTH as treatment with large amount of either AVP or PTH led to inhibition of both AVP- and PTH-mediated Ca^{2+} signals (Fig.14). Additionally, the present data suggest that cAMP and DAG, the second messengers, likely through protein kinase A and protein kinase C activation, may mediate desensitization. Further studies are required to determine if these second messengers cause desensitization through diminished receptor density or inhibition of intracellular Ca^{2+} release.

Based on our experimental results, we propose the following mechanisms whereby PTH and AVP induce Ca^{2+} signals in cTAL cells. PTH and AVP act on their respective receptors to activate a receptor-coupled G-protein. The G-protein transduces the signal to phospholipase C and results in generation of IP_3 and DAG. IP_3 liberates Ca^{2+} from the IP_3-sensitive Ca^{2+} store, which by some unknown mechanism activates Ca^{2+} influx through Ca^{2+} channels in order to refill the Ca^{2+} store (31). PTH and AVP, through IP_3 access the same intracellular Ca^{2+} pool to elevate $[Ca^{2+}]_i$. The elevated $[Ca^{2+}]_i$ together with DAG, activates protein kinase C to reduce the elevated $[Ca^{2+}]_i$ and limit hormonal action. Activation of protein kinase C may also play a role in desensitization or down-regulation of specific receptors (75). This system is also regulated by cAMP. Again, through hormone-receptor mediation, adenylate cyclase is activated and increases cAMP generation which in turn releases intracellular Ca^{2+} and depletes Ca^{2+} stores. Since TPA also inhibits cAMP-induced Ca^{2+} release, it is likely that cAMP works on the same signal cascade leading to the IP_3 receptor of the endoplasmic reticulum, thus initiating Ca^{2+} release or re-uptake. The IP_3-dependent and cAMP-dependent Ca^{2+} pools would appear to be the same in these cells.

However, cAMP does not increase Ca^{2+} entry as do the receptor agonists, PTH and AVP; it is likely that IP_3 somehow leads to the increase in Ca^{2+} influx, probably through IP_3-mediated responses, whereas cAMP only works on intracellular Ca^{2+} release.

IV.2. ANP-induced Ca^{2+} transients

Atrial natriuretic peptide is involved in the endocrine regulation of fluid and electrolyte balance. It links the heart and other organs involved in the control of cardiovascular function and body water homeostasis through specific receptors on the target organs (76). Three distinct receptors have been identified for ANP-derived agonists. The receptor ANP_A binds ANP and BNP, leading to the stimulation of guanylyl cyclase and cGMP generation (53). The second receptor, ANP_B, responds to CNP, again resulting in an increase in cGMP (54). Finally, ANP and CNP bind the ANP_C receptor, which is not associated with an increase in cGMP (45). This receptor is thought to function as a clearance receptor (56). The evidence for this involves receptor binding of ANP and rapid internalization into the cell where the ligand is hydrolysed and the receptor is recycled back to the membrane (56). This receptor is responsible for the rapid clearance rate of ANP and its analogues (56). The evidence provided here suggests that porcine cTAL cells possess these ANP_C receptors, since ANP, CNP, and C-ANP-(4-23) elicit Ca^{2+} signals (Fig.2). Our studies would support the hypothesis that the ANP receptors in cTAL cells are clearance receptors that are not directly associated with cGMP stimulation. In earlier studies, Butlen *et al* (77) failed to detect ^{131}I-labeled ANP binding in the loop, and Chabardès *et al* (47) failed to show an increase in cell cGMP with ANP in rat and rabbit thick ascending limb

segments. These observations are consonant with those of Nonoguchi *et al* (48) using microdissected thick ascending segments from rats. However, another study from the same laboratory localized mRNA to guanylyl cyclase-coupled ANP receptor in ascending segments using reverse transcription and polymerase chain reaction (78). These workers concluded that specific mRNAs encoding ANP receptors are broadly expressed along the nephron, raising the possibility that multiple sites of ANP action are present (78). Further studies are warranted to define receptor-mediated interaction of salt reabsorption within the loop of Henle.

Similar to PTH and AVP, atrial natriuretic peptides (ANP, CNP, and C-ANP-(4-23)) induce receptor-mediated Ca^{2+} transients in porcine cTAL cells (Fig.2). The ANP-induced Ca^{2+} signals are due, in part, to intracellular Ca^{2+} release, likely from endoplasmic reticulum, and in part, to influx of Ca^{2+} into the cytosol across the plasma membrane (Fig.17, Fig.18, Fig.19). As cGMP does not alter $[Ca^{2+}]_i$ in these cells, it is probable that the Ca^{2+} signals involve receptor-mediated IP_3 generation leading to Ca^{2+} release from intracellular stores. Hirate *et al* (79) reported that ANP binding to ANP_C receptors may lead to phosphoinositide hydrolysis, which would inferentially lead to IP_3-mediated Ca^{2+} release and diacylglycerol activation of protein kinase C. Studies are needed to determine whether ANP mediates IP_3 release in epithelial cells. The above observations are consonant with the earlier findings of Isales *et al* (80) in adrenal glomerulosa cells. These workers reported that a truncated ANP analogue, ANP-(7-23), which is specific for the ANP_C receptor, increased cytosolic Ca^{2+} in adrenal glomerulosa cells through a cGMP-independent mechanism. They speculated that this increase in Ca^{2+}, which was inhibited by nitrendipine, was through activation of Ca^{2+}

channels by the ANP_C receptor (80).

The present studies demonstrate the presence of ANP-responsive receptors, likely clearance receptors, in the porcine cTAL that initiate Ca^{2+} signals. The function of these Ca^{2+} signals is not apparent at this time, but they may be involved with initiating receptor-mediated endocytosis. A similar function has been postulated for low-density lipoprotein (LDL) receptor-mediated Ca^{2+} signals in MDCK epithelial cells, vascular smooth muscle cells, and cardiomyocytes (81-83). LDL receptor binding rapidly initiates Ca^{2+} transients, membrane endocytosis, and ligand-receptor internalization (81,82,83). Further studies are required to test this hypothesis. Other cell functions may be altered with ANP in these cells (44,45,84). It is not clear whether the ANP_C receptor has biological functions in addition to its role in peptide clearance (45,79). A number of studies have indicated that ANP through the ANP_C receptor may inhibit cAMP increments either through enhanced cyclic nucleotide hydrolysis or inhibition of adenylate cyclase (45,57,84,85). These data have lead Levin (45) to speculate that the clearance receptor, ANP_C, may modulate the actions of receptor-modulated increases in the second messengers, cGMP and cAMP. In addition, ANP inhibits the mobilization of intracellular Ca^{2+} most likely through the guanylate cyclase receptor, either ANP_A or ANP_B (45,86). Accordingly, the two ANP receptor subtypes appear to interact to modify hormone signal transduction pathways. The functional responses of ANP in the loop of Henle are unknown. Administration of pharmacological amounts of ANP results in an increase in urinary magnesium excretion (43). Magnesium is principally reabsorbed in the cTAL, and urinary magnesium excretion has been used as marker for loop function (7,41); accordingly, it is inferred that ANP may alter salt transport in this segment.

However, other studies have shown little effect of ANP on salt transport in the loop (42,43,87,88). More recently, Bailly *et al* (46) have shown that cGMP diminishes chloride transport in perfused mouse cTAL. Further studies are required to determine the role, if any, of ANP within the loop of Henle.

Our experiments showed that pretreatment with cGMP abolished the ANP-induced Ca^{2+} transients (Fig.20). Kato and coworkers (89,90) reported that cGMP selectively down-regulates the clearance receptor, ANP_C, in cultured pulmonary artery endothelial cells. These workers concluded that cGMP regulates the circulating levels of ANP by controlling the density of clearance receptors of vascular endothelial cells. Other studies have further established that ANP_C receptor expression on endothelial cells can be down-regulated by activation of the guanylyl cyclase receptor resulting from ANP-mediated cGMP generation (91). Although it is clear from the present data that pretreatment of cTAL cells with cGMP inhibits ANP-mediated Ca^{2+} response, it is not known if this involves down-regulation of the ANP_C receptors or direct inhibition of intracellular Ca^{2+} release. Further studies are required to determine at which site along the receptor-mediated signal transduction pathway that cGMP acts to mitigate the ANP-induced Ca^{2+} signals in cTAL cells.

In summary, we show that the atrial natriuretic peptides, ANP, CNP, and the analogue, C-ANP-(4-23), elicit Ca^{2+} signals in porcine cTAL cells likely through receptor-mediated responses. The Ca^{2+} transients are composed of intracellular Ca^{2+} release followed by Ca^{2+} entry across the plasma membrane. Finally. ANP-mediated Ca^{2+} transients are modulated by cGMP, which may play a regulatory role in these signals. The role of the ANP-induced Ca^{2+} signals may have significant physiological actions within this segment.

CHAPTER 2. Na^+/Ca^{2+} EXCHANGE IN cTAL CELLS

I. Background

Cells composing the cortical segment of the thick ascending limb of Henle's loop possess a large number of peptide hormone receptors, many of which induce large intracellular Ca^{2+} transients which may be involved with receptor-mediated signal transduction processes (92). In order for intracellular Ca^{2+} to play a role in signal transduction mechanisms it is necessary to have regulated processes which maintain intracellular Ca^{2+} concentrations at submicromolar levels. Na^+/Ca^{2+} exchange across the plasma membrane is an important determinant on intracellular Ca^{2+} levels. The primary role of Na^+/Ca^{2+} exchange is Ca^{2+} extrusion. The net direction of the Ca^{2+} movement mediated by this exchanger depends on the Na^+ electrochemical gradient, the Ca^{2+} electrochemical gradient, and the stoichiometry. Net efflux of Ca^{2+} is accomplished using the energy of the Na^+ gradient set up by the ATP-dependent Na^+ pump. The Na^+/Ca^{2+} exchangers are important Ca^{2+} transporting proteins present in many different species and cell types (93). The Na^+/Ca^{2+} exchanger is a high capacity, low Ca^{2+} affinity carrier which transports large quantities of Ca^{2+} at high intracellular Ca^{2+} levels such as occurs following agonist-stimulated increase in $[Ca^{2+}]_i$ (92).

The Na^+/Ca^{2+} exchanger was first cloned from canine heart (94) and subsequently from other species and tissues (95-100). Two kinds of Na^+/Ca^{2+} exchangers have been identified so far, the cardiac type with stoichiometry of 3 Na^+ to 1 Ca^{2+} and the rod outer segment (ROS) type with coupling ratio of 4 Na^+ to 1 Ca^{2+} + 1 K^+. Both types of the exchanger have similar structure but totally different amino acid composition and potential

amino-linked glycosylation sites (101). The exchanger cDNA encodes a protein with 970 amino acids. Hydropathy analysis has indicated that the exchanger fits into the general class of ion transporters, which contain 11 or 12 transmembrane segments and a relatively large hydrophilic domain. The mature exchanger has 11 potential transmembrane segments, with a 520-residue hydrophilic domain between membrane-spanning segments 5 and 6.

Recent cloning studies by Kofuji *et al* (102) and Lee *et al* (103) showed that the sodium-calcium exchanger is encoded by a single gene. Different isoforms, differing in the carboxyl end of intracellular loop 5-6, are generated by alternative splicing of exons in a tissue-specific manner. Fig.21 shows the location of alternatively spliced site. The unusual intron-exon arrangement of the sodium-calcium exchanger gene encoding this area of the intracellular loop potentially leads to as many as 32 isoforms. Splice variation at this site could provide a basis for differences in tissue-specific expression (103). Restriction enzyme analysis and sequencing data have revealed seven major isoforms specific for different species and tissues (103). Two distinct isoforms have been identified in the rabbit kidney, NACA2 (99) and NACA3 (104); and two in the rat kidney, NACA3 (103,104) and NACA7 (103). These transcripts are principally been found in the distal tubule (100). No evidence to date, either functional or molecular, has been given for Na^+/Ca^{2+} exchange in thick ascending limb cells (12,100). To explain this contradiction, Reilly *et al* (12) proposed following possibilities: 1) the absence of expression of the Na^+/Ca^{2+} exchanger in these segments; 2) the expression of the exchanger in levels below the threshold of the detection; or 3) the exchanger in these segments is represented by a different isoform.

Remarkably little is known about physiological modulation of Na^+/Ca^{2+} exchange,

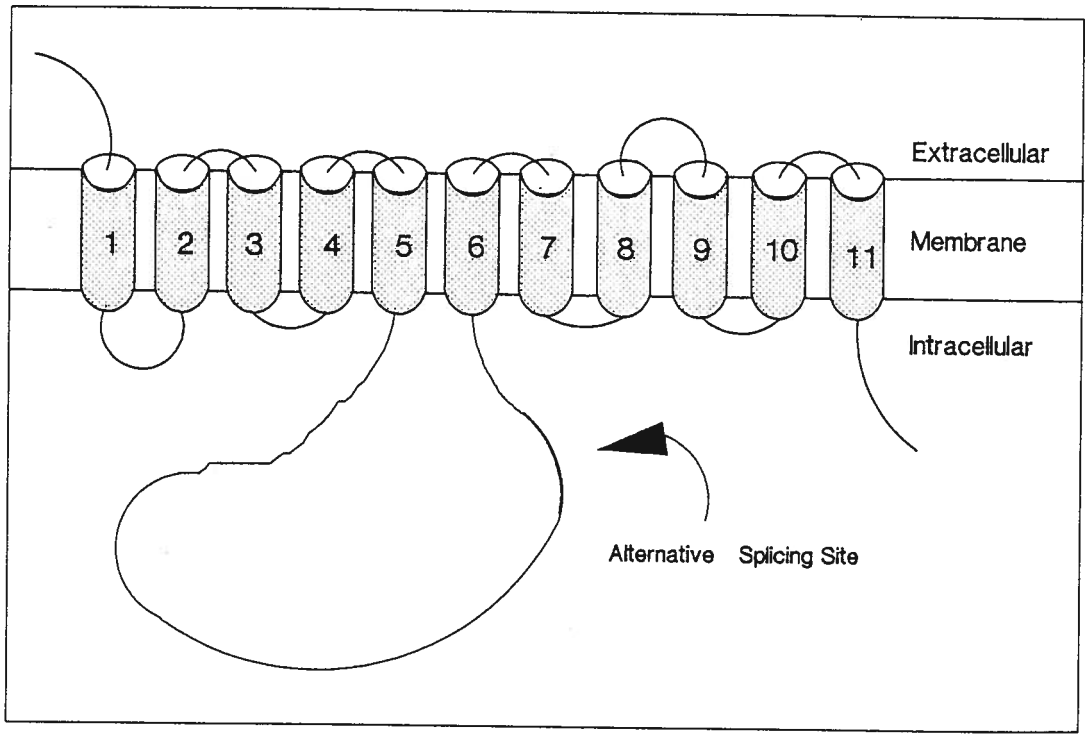

Fig.21. A model of cardiac type Na^+/Ca^{2+} exchanger. The exchanger is composed of 11 transmembrane segments and a intracellular loop. The location of the alternative splicing site is indicated. [Abstracted from Philipson *et al* (101) with slight modification]

except as a result of changes of cytosolic Ca^{2+} and Na^{+} concentrations (105). The kinetics and stoichiometry of Na^{+}/Ca^{2+} exchange have been well studied but its regulation has received less attention (93,105,106). Some studies have shown that Na^{+}/Ca^{2+} exchange may be regulated in renal cells by various factors, such as parathyroid hormone and vitamin D (107-109) which increase Ca^{2+} transport, and by phorbol esters which have been reputed to decrease exchange activity (110). The mechanisms underlying these effects are not understood.

The specific aims of the present study include: 1) functional demonstration of Na^{+}/Ca^{2+} exchange in isolated cTAL cells; 2) determination of the modulating effects of phosphorylation on Na^{+}/Ca^{2+} exchange activity; and finally 3) the molecular identification of Na^{+}/Ca^{2+} exchanger.

II. Materials and Methods

II.1. Materials

Taq DNA polymerase, SP6 RNA polymerase, restriction enzymes (Eco RI, Eco RV, and Taq I) and dsDNA Cycle Sequencing System were purchased from GIBCO/BRL. Original TA Cloning Kit was from Invitrogen (San Diego, CA). UTP-α-^{32}P and ATP-γ-^{32}P were obtained from ICN Pharmaceuticals Inc. (Irvine, CA). All other chemicals were those given in Chapter 1.

II.2. Methods

The isolation of cTAL cells from porcine kidneys and the determination of cytosolic free Ca^{2+} were performed by the same methods as described in Chapter 1. In all

experiments involving Ca^{2+} analysis, single traces are shown but similar results were obtained in at least five separate experiments from independent cell preparations.

II.2.1. Cytoplasmic Na^+ measurements

Cytosolic free Na^+ concentration, $[Na^+]_i$, was determined with SBFI/AM (Molecular Probes Inc) according to previously described techniques (111). cTAL cells were loaded with SBFI by adding equal volumes 10 μM (final concentration) SBFI/AM dissolved in dimethyl sulfoxide (DMSO) and the nonionic detergent Pluronic F-127 (20% wt/vol in DMSO). The cells were incubated for 60 min at 23°C and subsequently washed 3x with buffer to remove extracellular dye. Fluorescence was measured using a spectrofluorometer at alternately excited wavelengths of 345 and 385 nm and emission intensities recorded at 505 nm were calculated. All measurements were performed at room temperature. Calibration of SBFI fluorescence in terms of $[Na^+]_i$ was performed by addition of known extracellular Na^+ concentrations made up in Na^+-HEPES/K^+-HEPES buffer. The 345-to-385 nm intensity ratio was determined before and 3 min after the addition of the Na^+ ionophore gramicidin D (1 μM, final concentration). The changes in fluorescence ratio were then plotted as a function of Na^+ concentration. As in a previous report, a linear relationship was observed that was then used to calibrate the individual experimental ratios (111).

II.2.2. Isolation of total RNA from kidney tissues

Modified TRIzol technique was used to isolate total RNA from tissues (112,113). About 0.1 gm of tissue was obtained and frozen in liquid nitrogen. Frozen tissue was ground in a mortar and pestle under liquid nitrogen. Ground tissue was transferred into a 1.5 ml tube. 1 ml of TRIzol solution was added into the tube to lyse the cells. Lysed tissue was

incubated at room temperature for 5 min. To extract RNA, 0.2 ml of chloroform was added into the tube and it was then mixed by vortexing for 1 min prior to centrifugation at 14,000 xg for 15 min at 4°C. The aqueous phase was collected into a fresh tube and an equal volume of isopropanol was added. The mixture was incubated at room temperature for 1 hour. The RNA was obtained by centrifugation, 14,000 xg for 15 min at 4°C. The RNA pellet was then washed with 1 ml of 75% ethanol and dissolved in 40 μl of formamide.

II.2.3. Preparation of riboprobe

The NCE.F1 clone in the pcDNAII vector was from Dr. Jonathan Lytton (Harvard Medical School). The cDNA of this clone was derived from rat kidney transcripts (103). To make a probe, the NCE.F1 containing plasmid was transformed into host cells for the purpose of obtaining large quantities of plasmid DNA.

II.2.3.1. Fresh competent *E.coli* prepared using the calcium chloride method. A single colony of XLI Blue bacteria was inoculated into a 25 ml LB broth medium culture with tetracycline. The culture was incubated for 2.5-4 hours at 37°C with vigorous shaking (225 rpm) until OD_{600} was about 0.4. The culture was chilled to 0°C by placing the tubes on ice for 10 min. The cells were then harvested by centrifugation at 3000 rpm for 10 min at 4°C. Pellets were resuspended in half the original volume of ice-cold 0.1 M $CaCl_2$, and then incubated on ice for 15 min. After centrifugation at 3,000 rpm for 10 min at 4°C, the pellets were resuspended in 1/12.5 of the original volume of ice-cold 0.1 M $CaCl_2$. Competent cells were stored at -70°C following addition of glycerol/DMSO (50/50) to 15% final concentration (V/V).

II.2.3.2. Transformation. 10 ng of pcDNAII.RtKcNCE1.F1 was added to 0.2 ml of

competent cells and held on ice for 30 min. Cells were then heat-shocked at 42°C. Following addition of LB and 1 hour incubation at 37°C, bacteria were plated on LB plates (0.15% agar) with 60 μg/ml ampicillin and 50 μg/ml tetracycline and incubated overnight at 37°C.

II.2.3.3. Isolation of plasmid DNA from transformed *E.coli.* Plasmid Midi Kit (QIAGEN) was used to isolate pcDNAII.RtKcNCE1.F1 plasmid. This method is based on a modified alkaline lysis procedure. Purified plasmid DNA was quantitated by spectrophotometer. To confirm the identity of the plasmid, restriction enzyme analysis was then performed.

II.2.3.4. Preparation of riboprobe from pcDNAII.RtKcNCE1.F1. Prior to synthesis of the riboprobe, pcDNAII.RtKcNCE1.F1 was digested with Not 1 for 30 min at 37°C and then washed with phenol/chloroform. 1 μg of Not 1 digested plasmid and DNA-dependent RNA polymerase SP6 were used for RNA synthesis in the presence of 0.4 mM ATP, 0.4 mM CTP, 0.4 mM GTP, 0.01 mM UTP, and UTP-α-^{32}P. The riboprobe was purified using 1 ml G50 resin column. Columns were spun at 2000 rpm for 3 min. The column was washed once with 100 μl of TE (pH 7.5) and then loaded with 100 μl of labelling mixture. ^{32}P labelled probe was eluted into an eppendorf by centrifugation.

II.2.4. Northern blotting and hybridization.

II.2.4.1. Northern blotting. RNA samples were loaded into 1% agarose-formaldehyde (0.4 M) gel. To prepare sample for loading, 20 μg RNA was mixed with 5 μl 5X formaldehyde gel-running buffer and 1 μl EtBr (1 mg/ml), and then added to 3.5 μl formaldehyde and 10 μl formamide. The mixture was incubated at 65°C waterbath for 15

min. RNA samples were loaded after the gel was pre-run for 5 min at 100 V. The gel was run at 100 V for 10 min and then 40 V for 6-8 hours. Running buffer was replaced during the middle of the run.

Downward alkaline-transfer setup was prepared according to the method described by Chomczynski (114), with a minor modification. The bottom base was formed by a 4-5 cm-high stack of paper towels. The towels were sequentially covered with five sheets of blotting paper (Whatman), hybridization membrane (Nytran), followed by the agarose gel. The membrane was 2-3 mm larger than the gel. The gel was covered with three sheets of blotting paper (of the same size as the gel) and two sheets of blotting paper forming a connection (bridge) across the gel stack and two trays containing the transfer solution (composition: 3 M NaCl, 2 mM sarkosyl and 8 mM NaOH, pH 11.40-11.45). After the transfer the membrane was incubated in neutralization buffer (0.2 M NaH_2PO_4, pH 6.7-6.8) for 10 min and then fixed by UV cross-linking.

II.2.4.2. Hybridization. The membrane was pre-hybridized for 1 hr at 42°C. The components of pre-hybridization solution were: 8 ml of deionized formamide, 4 ml of 20% SDS, and 4 ml of 2 M NaH_2PO_4 in 4 mM EDTA (pH 7.2), the total volume was 16 ml with 1 mg/ml BSA and 100 μg/ml denatured salmon sperm DNA. Hybridization was made by adding riboprobe and incubated overnight at 42°C in the hybridization oven. After hybridization the membrane was washed six times at 55°C with 2x SSPE/0.3% SDS 2x 20 min, 1x SSPE/0.5% SDS 2x 20 min, and 0.3x SSPE/1% SDS 2x 20 min respectively. The Nytran membrane was exposed a X-ray film for 10 hr at -70°C.

II.2.5. Identification of Na^+/Ca^{2+} exchanger isoform with PCR technique.

II.2.5.1. cDNA synthesis. Total RNA extracted from cTAL and inner cortex tissue using TRIzol method as described above was utilized as starting material. Both random hexamer (20 ng/μl) and oligo dT (20 ng/μl) were used as primers for cDNA synthesis in the presence of $\sim$1 μg RNA, NTP (1 mM), DTT (10 mM), Reverse Transcriptase (4 U/μl), and RNasin (0.5 U/μl).

II.2.5.2. PCR primer design. Based on the sequence of NCE.F1 and a comparison between different species, including rat (96,98,103), rabbit (102), dog (94), bovine (95) and human (104), the most conserved regions flanking the alternatively spliced site were used in primer design. The sequence of sense primer selected was CTCGAA(G)TTCCAGAAT (C)GATGAAAT (nt 2207-2229 of NCE.F1) (103); the antisense primer was CTCTTGAATT CG(A)TAA(G)AAT(C)TCTTC (nt 2533-2555).

II.2.5.3. Polymerase chain reaction (PCR). The composition (final concentration in 50 μl volume) of the reaction was: 2.5 mM $MgCl_2$, 0.4 mM dNTP, 1 mM sense primer, 1 mM antisense primer, and 1.5 unit of Taq DNA polymerase. cDNA template was also included. pcDNAII.RtKcNCE1.F1 DNA was used as a positive control. Distilled water and the reaction buffer of cDNA synthesis were used as negative controls. The first 3 cycles were 94°C 2 min, 44°C 1.5 min and 72°C 2 min, and the next 35 cycles were taken at 94°C 1 min, 44°C 50 sec and 72°C 1 min. PCR products were analyzed by agarose gel electrophoresis.

II.2.5.4. Southern blotting and hybridization. To prepare cDNA probe, the amplified PCR product from the positive control was isolated and purified with GENECLEAN Kit (BIO 101). Random primer method was used to construct probes. In

a screw-cap vial, dH_2O was added to 20-100 ng of probe DNA to obtain a final volume of 9 μl. The sample was boiled for 5 min. The following were then added: 2.0 μl 10X Klenow buffer, 2.0 μl 10X ATG (2.5 mM), 1.0 μl random hexamer (100 pmol/μl), 1.0 μl Klenow, and 5.0 μl ^{32}P-dCTP, and incubated at 37°C for 50 min. A G50 column was used for probe purification. The probe was boiled before use in the hybridization reaction.

PCR products were separated on 1% agarose gel and transferred onto Nytran membrane using downward alkaline blotting technique. The membrane was hybridized with cDNA probe as the same way as in the northern hybridization.

II.2.5.5. Sequencing PCR product. dsDNA Cycle Sequencing System was used to sequence PCR product. Cycle sequencing permits direct sequencing of dsDNA. dsDNA is introduced into a set of dideoxy sequencing reactions, and is then subjected to thermal cycling. The first 20 cycles consist of a denaturation step at 95°C for 30 sec, an annealing step at 52°C for 30 sec, and an extension/termination step at 70°C for 60 sec. The next 10 cycles contained only two steps; denaturation at 95°C for 30 sec and extension/termination at 70°C for 60 sec. The sequencing reactions were analyzed on 6% acrylamide sequencing gel.

III. Results

III.1. Demonstration of Na^+/Ca^{2+} exchange in porcine cTAL cells

III.1.1. Effect of external Na^+ removal on $[Ca^{2+}]_i$ in ouabain-treated cTAL cells. Basal $[Ca^{2+}]_i$ is maintained in the range of 74-102 nM with a mean concentration of 86 ± 3 nM, n = 183, in normal cTAL cells. The abrupt removal of external Na^+ by replacement

of NaCl in the bathing solution with equivalent amounts of either choline Cl or NMDG (N-methyl-D-glucamine) Cl did not alter basal $[Ca^{2+}]_i$ in normal cells (Fig.22). When cTAL cells were pretreated with ouabain, 10^{-3} M, for 60 min followed by rapid replacement of external Na^+ in the bathing solution with either NMDG or choline, a marked increase in $[Ca^{2+}]_i$ was observed in the presence of external Ca^{2+} (Fig.22). During incubation with ouabain, mean basal $[Ca^{2+}]_i$ was 86 $\pm$ 2 nM, n = 22, which was similar to control cells over the period of experimentation. The increment in $[Ca^{2+}]_i$ was dependent on the presence of external Ca^{2+} as no changes were observed in ouabain-treated cells in Ca^{2+}-free solutions (Fig.22). Following removal of external Na^+ in ouabain-treated cells the mean increase in $[Ca^{2+}]_i$ was 1023 $\pm$ 74 nM, n = 22. In the absence of external Ca^{2+}, the $[Ca^{2+}]_i$ remained at basal levels, 82$\pm$3 vs 85$\pm$9 nM, n=5, during the period of external Na^+ removal in ouabain-treated cells (Fig.22). We interpret these changes to indicate that the removal of external Na^+ allows internal Na^+ to move out coupled to external Ca^{2+} moving from the bath into the cytosol. These studies suggest that there is a sodium-dependent Ca^{2+} entry into cTAL cells which was observed only in ouabain-treated cells, i.e. those cells which we infer have elevated $[Na^+]_i$.

In the absence of external Na^+ but presence of external Ca^{2+}, $[Ca^{2+}]_i$ increased transiently in ouabain-treated cells (Fig.22). $[Ca^{2+}]_i$ returned to near basal levels despite the absence of external Na^+. These results suggest the presence of Na^+-independent mechanisms of Ca^{2+} fluxes, either by cytosolic Ca^{2+} sequestration or by Ca^{2+} extrusion across the plasma membrane. This removal may involve Ca^{2+}-ATPases, therefore to determine the role of the Ca^{2+}-ATPase pumps in this phenomenon we treated the cTAL cells with vanadate, a general P-type ATPase inhibitor. Vanadate is not a specific inhibitor but proved

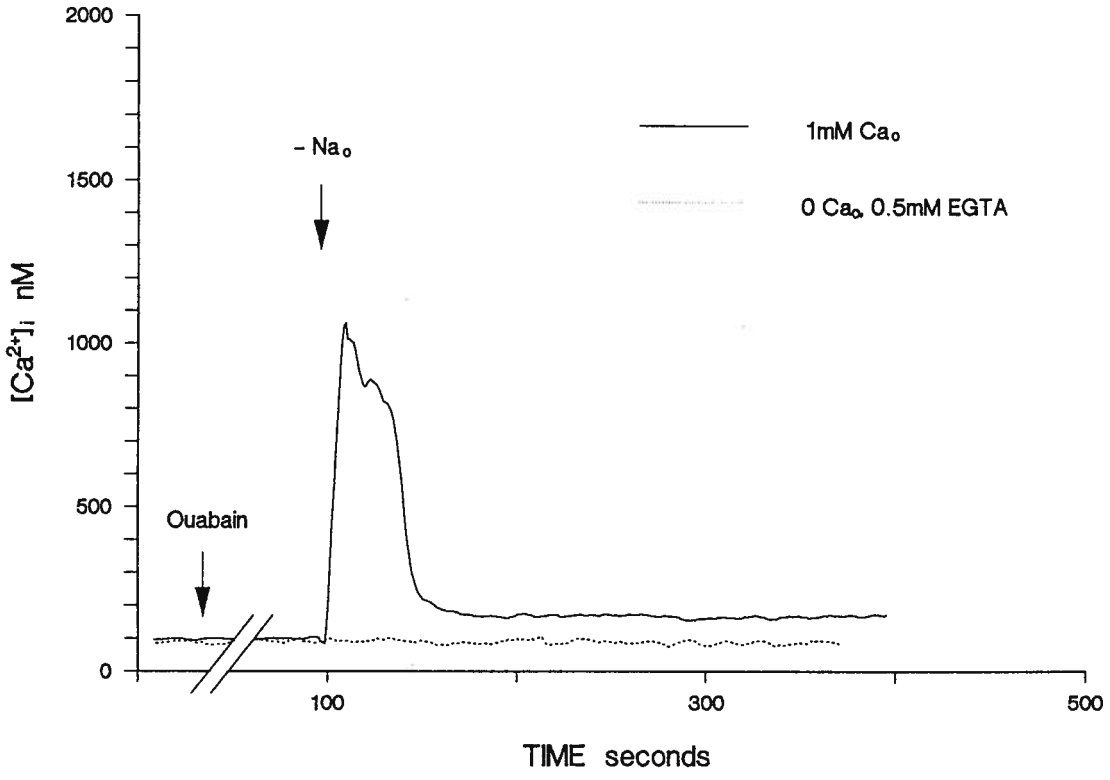

Fig.22. Effects of external Na^+ removal on $[Ca^+]_i$ in ouabain-treated cTAL cells. cTAL cells were pretreated for 60 min with ouabain, 10^{-3} M, in normal buffer solution containing (in mM): NaCl 145, KCl 4.0, Na_2HPO_4 0.8, KH_2PO_4 0.2, $CaCl_2$ 1.0, $MgCl_2$ 0.6, glucose 10, and HEPES-Tris 20, pH 7.4. For the sodium-free solution the composition was the same but sodium was replaced by NMDG-Cl 145 mM or choline Cl 145 mM (results were the same with either substitution). In the experiments indicated, $CaCl_2$ was deleted from the bathing solution and 0.5 mM EGTA was added to the bathing solution to provide a calcium-free solution. These fluorescent tracings are representative of 5 (0 mM Ca_o) and 22 (1 mM Ca_o) different experiments.

to be useful in isolating Na^+-dependent effects in the porcine cTAL cells. Fig.23 illustrates a representative experiment. Vanadate added with the Na^+-free solutions markedly attenuated the rate of decrease in $[Ca^{2+}]_i$ so that $[Ca^{2+}]_i$ levels (607±90 nM, n=5) were sustained for 60-180 sec. Fig.23 also showed that if 50 mM NaCl was added to the cTAL cells during this sustained period of elevated $[Ca^{2+}]_i$, the cytosolic $[Ca^{2+}]$ rapidly returned to basal levels, 86±9 nM, n=5. Note that with the addition of external Na^+, the $[Ca^{2+}]_i$ fell to basal levels whereas it did not in the absence of external sodium. These studies suggest that both a vanadate-sensitive sodium-independent Ca^{2+} pump, probably Ca^{2+}-ATPase, and a sodium-dependent process are important in maintaining $[Ca^{2+}]_i$ levels in cultured cTAL cells.

Addition of external Na^+ to vanadate-treated cells consistently resulted in a rapid fall in cytosolic Ca^{2+}. Addition of another monovalent cation, Li^+, during the sustained phase was without effect on $[Ca^{2+}]_i$ (data not shown). The removal of intracellular Ca^{2+} was selective and dependent on external Na^+; likely by Na^+/Ca^{2+} exchange.

III.1.2. Effect of the putative inhibitors on Na^+/Ca^{2+} exchange. A number of putative inhibitors were employed to determine if $[Ca^{2+}]_i$ changes were due to influx or efflux across the plasma membrane. First, we applied inorganic inhibitors, $LaCl_3$ and $MgCl_2$, at the time of removal of external Na^+ to determine the effects on the increase in $[Ca^{2+}]_i$; i.e. the movement of Ca^{2+} into the cell in exchange for Na^+ moving out of the cell, and with the readdition of external Na^+ to assess their effects on Ca^{2+} efflux (Fig.24). La^{3+} and Mg^{2+} mitigated the increase in $[Ca^{2+}]_i$ following external Na^+ removal, 810 ± 148 nM, n = 4, and 592 ± 157 nM, n = 4, versus control maximal levels of 1023 ± 72 nM, n = 22. La^{3+} and Mg^{2+} also inhibited the movement of Ca^{2+} out of the cell when external Na^+ was readded to

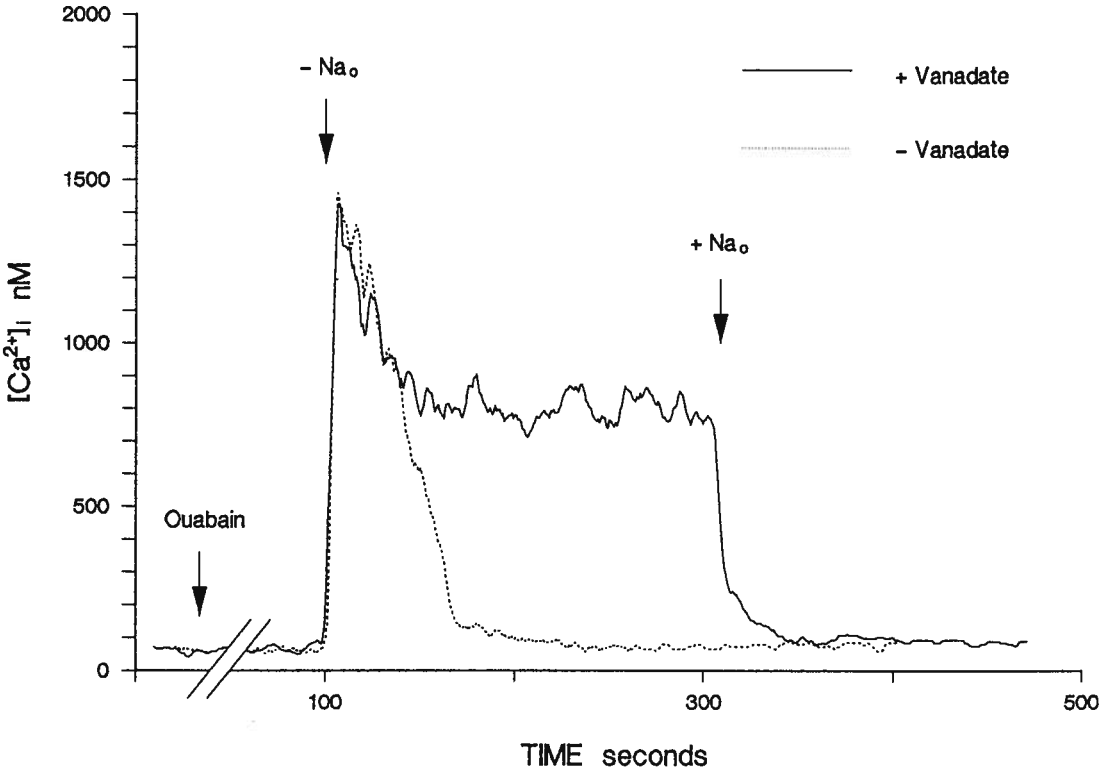

Fig.23. Effect of vanadate on Na^+ removal-induced $[Ca^{2+}]_i$ changes in ouabain-treated cTAL cells. Ouabain-treated cTAL cells were exposed to sodium-free solutions with and without the presence of vanadate, 1 mM. Where indicated sodium-containing buffer was added, containing (in mM): NaCl 50, NMDG-Cl 95, KCl 4.0, Na_2HPO_4 0.8, KH_2PO_4 0.2, $CaCl_2$ 1.0, $MgCl_2$ 0.6, glucose 10, and HEPES-Tris 20, pH 7.4. Fluorescence tracing is representative of 25 separate experiments.

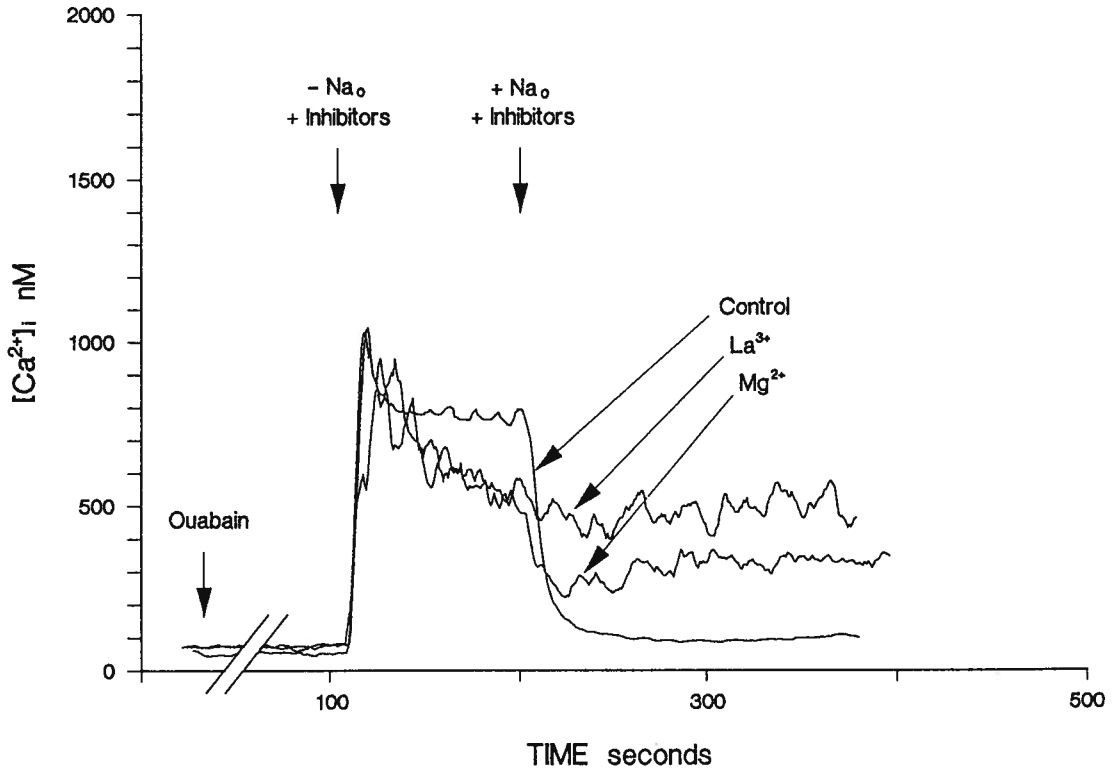

Fig.24. Effect of inorganic inhibitors on Na^+-dependent change in $[Ca^{2+}]_i$ in ouabain-treated cTAL cells. cTAL cells were pretreated with ouabain, 10^{-3} M, and Na^+_o was removed as given in legend to Fig.22. $LaCl_3$, 5.0 mM or $MgCl_2$, 5.0 mM, was added to the sodium-free buffer solution and with addition of buffer solution containing 50 mM NaCl. Vanadate, 10^{-3} M, was present in the Na^+-free solutions. Figures are representative of 4 different cells for each inhibitor.

the bathing solution (Fig.24). We did not attempt to quantitate the rate of Ca^{2+} influx and efflux as the changes in $[Ca^{2+}]_i$ are likely composed of different transport and sequestration processes. Nevertheless, the qualitative data suggested that the increment in $[Ca^{2+}]_i$ with external Na^+ removal and subsequent decrease in $[Ca^{2+}]_i$ following readdition of external Na^+ resulted from Ca^{2+} moving across the plasma membrane, likely through Na^+/Ca^{2+} exchange.

Next, we tested the effect of organic inhibitors, amiloride and its analogue bepridil which are thought to inhibit Na^+/Ca^{2+} exchange in addition to other sodium-dependent transport processes (115). In this case, the cTAL cells were pretreated with these agents for 10 min prior to removal of external Na^+. The Ca^{2+} influx on removal of external Na^+, and Ca^{2+} efflux following readdition of external Na^+ were significantly inhibited by the presence of amiloride and bepridil (Fig.25).

III.2. Transmembrane depolarization induces Na^+-dependent Ca^{2+} influx

III.2.1. The effect of transmembrane depolarization on $[Ca^{2+}]_i$ in ouabain-treated cTAL cells. The changes of $[Ca^{2+}]_i$ resulting from the removal of external Na^+ in ouabain-treated cells are likely due to Na^+/Ca^{2+} exchange functioning in reverse, i.e. Na^+ moving out coupled with Ca^{2+} moving into the cell. In all cells studied to date, the coupling has been reported to be $3Na^+$ for $1Ca^{2+}$ resulting in a stoichiometrical imbalance in electrical charge (116). Accordingly, depolarization (as with replacement of external Na^+ with K^+ in the presence of a large outside-to inside Ca^{2+} gradient) would be expected to drive Ca^{2+} in and Na^+ out via the exchanger. This approach has been used by others (117-120) to investigate Na^+/Ca^{2+} exchange. In the present study the membrane potential was altered by the substitution of

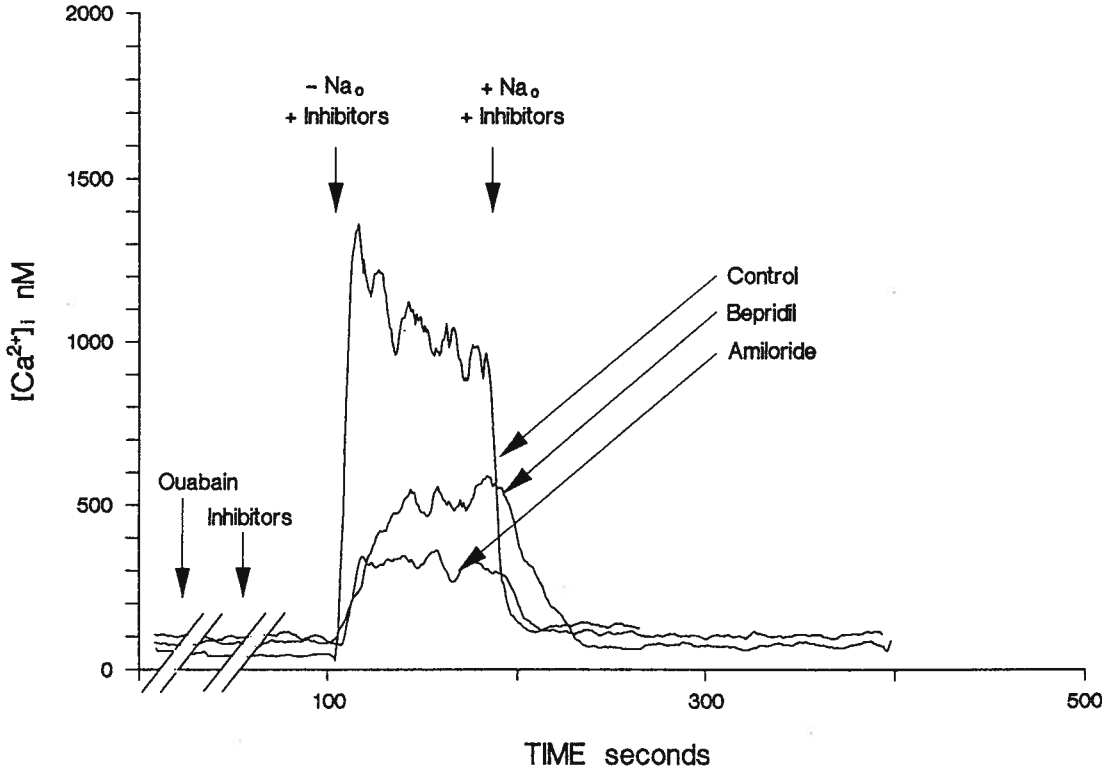

Fig.25. Effect of organic inhibitors on Na^+-dependent change in $[Ca^{2+}]_i$ in ouabain-treated cTAL cells. cTAL cells were pretreated with ouabain, 10^{-3} M, and Na^+_o was removed as given in legend to Fig.22. Bepridil, 0.25 mM, or amiloride, 1.0 mM was added 10 min prior to and with the sodium-free buffer solutions as indicated. Vanadate, 10^{-3} M, was present in the Na^+-free solutions. Figures are representative of 4 different cells for each inhibitors.

50 mM KCl in the external buffer solution in lieu of 50 mM NaCl. Depolarization with high KCl solutions did not have any effect on basal $[Ca^{2+}]_i$ in normal cTAL cells (Fig.26). However, membrane depolarization of ouabain-treated cells (10^{-3} M ouabain for 60 min) resulted in a rapid increase in $[Ca^{2+}]_i$ which was dependent on the concentration of Ca^{2+} in the external buffer solution (Fig.26). In the absence of external Ca^{2+} (and presence of 1.0 mM EGTA) there was no detectable change in $[Ca^{2+}]_i$, whereas the presence of 0.5-to-2.0 mM external Ca^{2+} resulted in graded increases in $[Ca^{2+}]_i$ dependent on the Ca^{2+} concentration in the buffer solution (Fig.27). We interpret these findings to indicate that a decrease in transmembrane voltage induces internal Na^+ to move out of the cell coupled to external Ca^{2+} moving into the cell. The increments in $[Ca^{2+}]_i$ following a change in transmembrane voltage occurred in the presence of external Na^+ suggesting that the putative Na^+/Ca^{2+} exchange is electrogenic.

III.2.2. The effects of inhibitors on voltage-stimulated Na^+/Ca^{2+} exchange. The next series of studies examined the effect of inorganic and organic inhibitors on voltage-stimulated Ca^{2+} influx. First, we tested the effects of a number of multivalent cations. The inhibitor was added with the KCl depolarization solution. La^{3+} and Mg^{2+} significantly inhibited the increase in $[Ca^{2+}]_i$ following depolarization, $63 \pm 6\%$ and $60 \pm 6\%$ of control respectively, n=3-6 (Fig.28). Fig.29 illustrates the effects of the organic inhibitors, amiloride and bepridil, on voltage-dependent increase in $[Ca^{2+}]_i$. Amiloride inhibited the increase in $[Ca^{2+}]_i$ to $29 \pm 8\%$, n = 3, of control and bepridil $8 \pm 4\%$, n = 5, of control values. Unlike the inorganic inhibitors, both drugs were added into the bathing solution 10 min prior to depolarization.

The data from these functional studies support the notion that there is coupling of Na^+

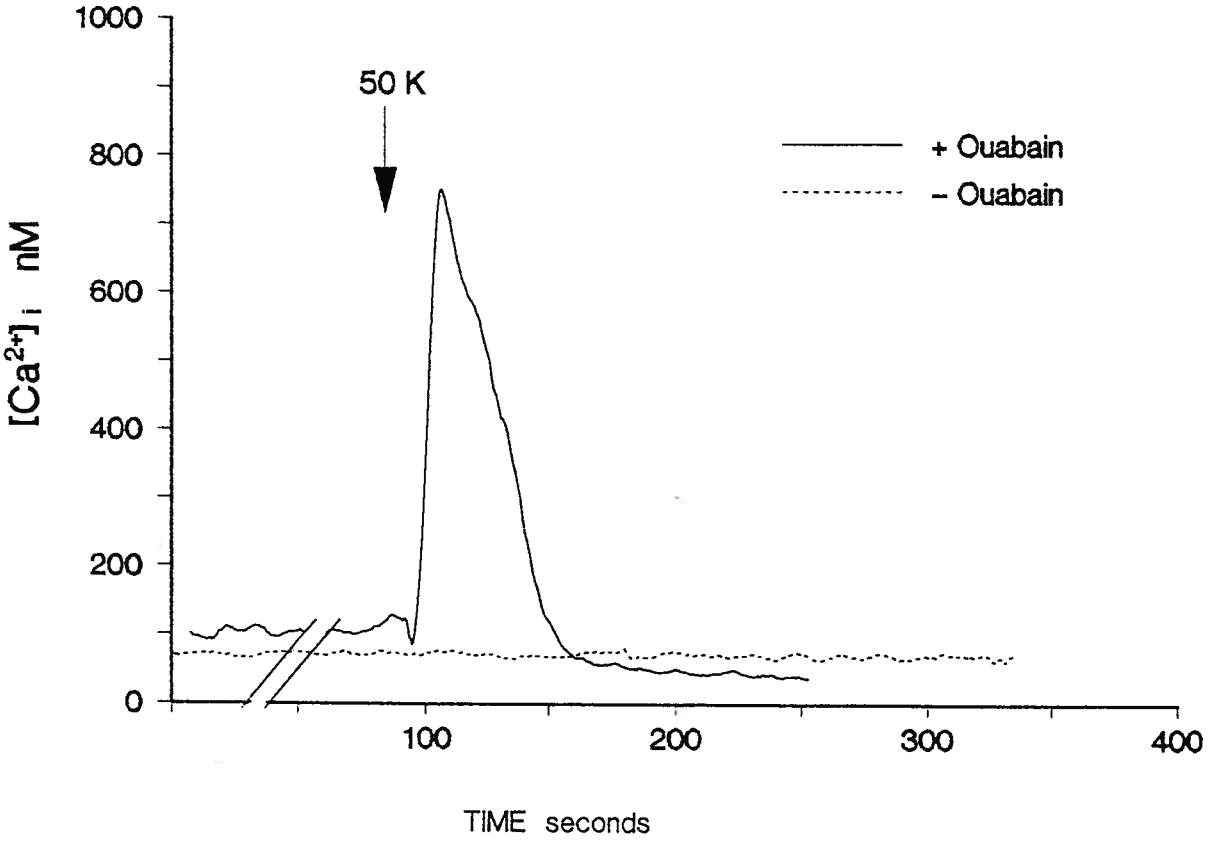

Fig.26. Effect of transmembrane voltage on sodium-dependent Ca^{2+} influx. Cultured cTAL cells were pretreated with and without ouabain, 10^{-3} M, for 60 min prior to experimentation. The normal buffer solution contained (in mM): NaCl 145, KCl 4.0, Na_2HPO_4 0.8, KH_2PO_4 0.2, $CaCl_2$ 1.0, $MgCl_2$ 0.6, glucose 10, and HEPES-Tris 20, pH 7.4. The depolarization solution contained (in mM): NaCl 95, KCl 50, Na_2HPO_4 0.8, KH_2PO_4 0.2, $CaCl_2$ 1.0, $MgCl_2$ 0.6, glucose 10, and HEPES-Tris 20, pH 7.4. 1.0 mM $CaCl_2$ was added to depolarization solution. Fluorescent tracings are representative of 5 different cTAL cells.

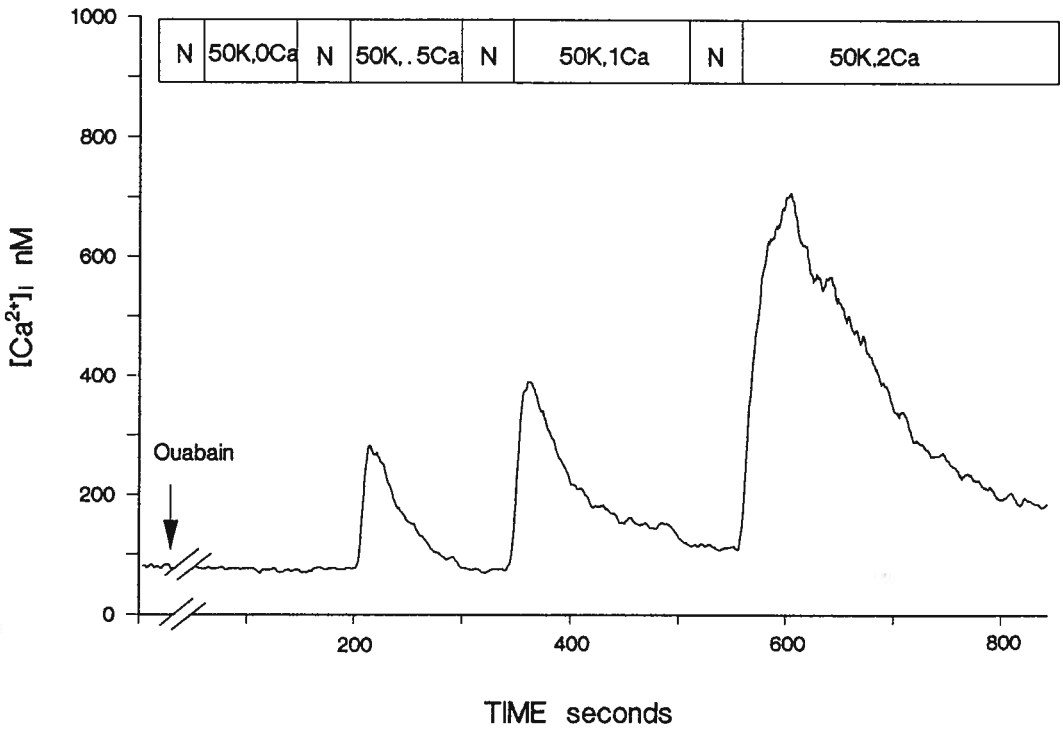

Fig.27. Dose-dependent response of depolarization-induced change in $[Ca^{2+}]_i$. cTAL cells were pretreated with ouabain, 10^{-3} M, for 60 min prior to experimentation. The composition of normal buffer solution (N) and depolarization solution (50K) was same as given in Fig.26. Various amounts of $CaCl_2$ (0, 0.5, 1.0 and 2.0 mM) were added as indicated. Fluorescent tracing is representative of 5 different cTAL cells.

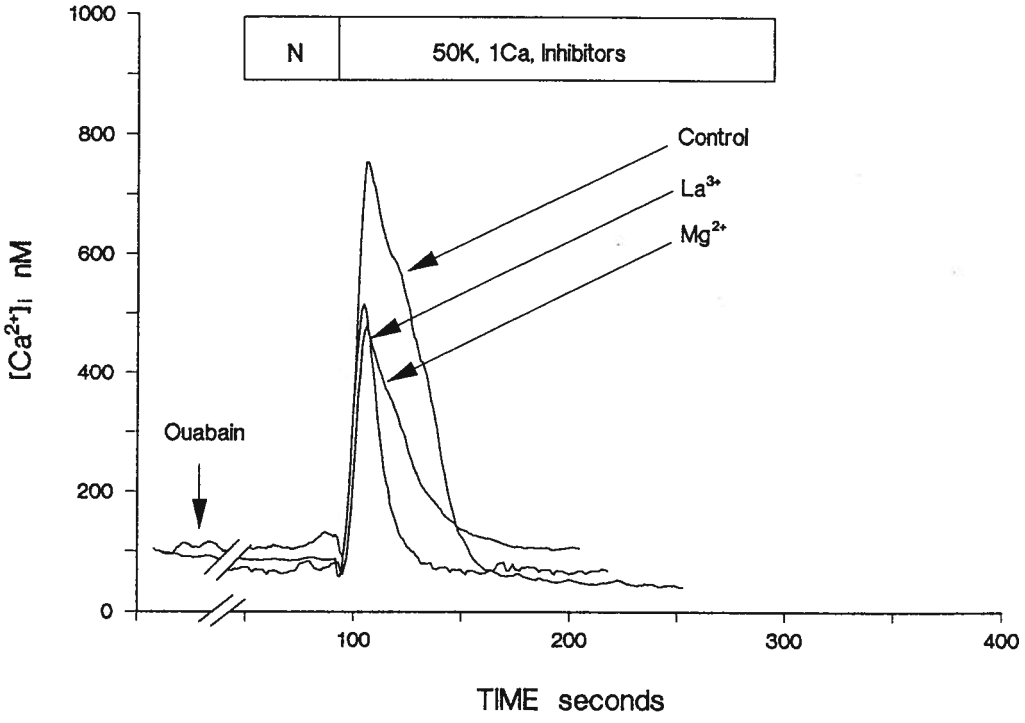

Fig.28. Effect of inorganic inhibitors on voltage-dependent Ca^{2+} influx in ouabain-treated cTAL cells. Cultured cTAL cells were pretreated with ouabain, 10^{-3} M, for 60 min prior to experimentation. The composition of normal buffer solution (N) was the same as indicated in Fig.26. The depolarization solution contained $LaCl_3$, 5.0 mM, or $MgCl_2$, 5.0 mM. Fluorescent tracings are representative of 3-6 different cells.

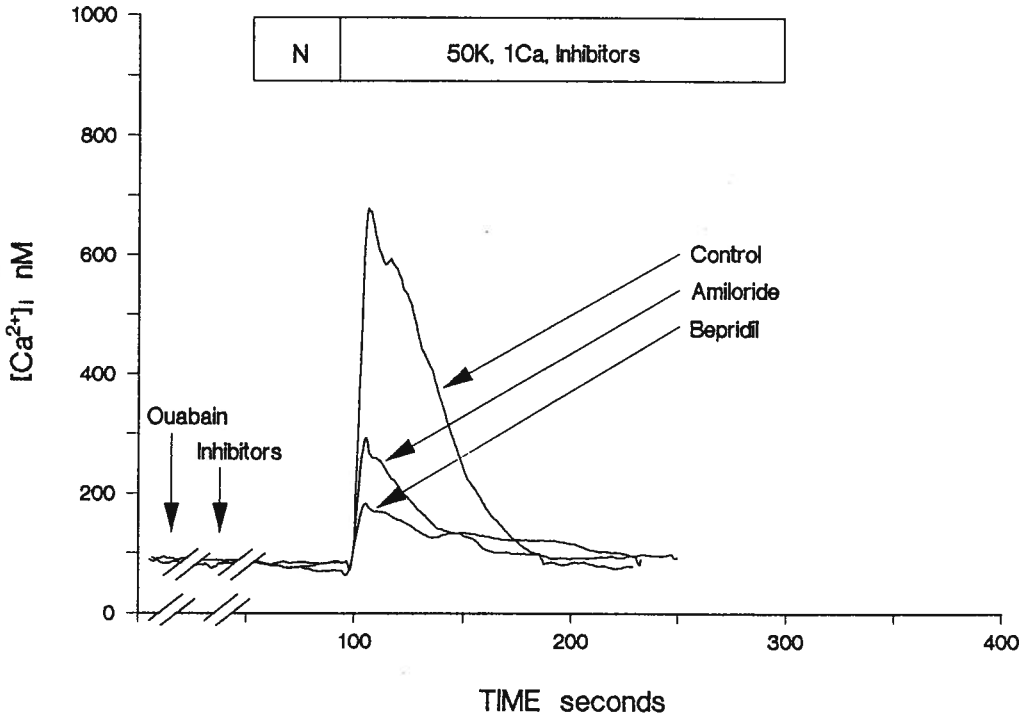

Fig.29. Effect of organic inhibitors on voltage-dependent Ca^{2+} influx in ouabain-treated cTAL cells. cTAL cells were pretreated with ouabain, 10^{-3} M, for 60 min prior to experimentation. The composition of normal buffer solution (N) was the same as indicated in Fig.26. Amiloride, 10^{-3} M, or bepridil, 25 μM, were added 10 min prior to depolarization. Fluorescent tracings are representative of 3-6 different cTAL cells.

for Ca^{2+} in the plasma membrane of cTAL cells which is reversible and dependent on the transmembrane sodium concentration and voltage gradients.

III.2.3. Dependence of Na^+/Ca^{2+} exchange on intracellular $[Na^+]$. The observation that changes in $[Ca^{2+}]_i$ with the removal of external Na^+ or the addition of KCl required pretreatment of cTAL cells with ouabain suggested that an elevation of intracellular sodium concentration ($[Na^+]_i$) was necessary to demonstrate Na^+/Ca^{2+} exchange. To determine the association of Na^+/Ca^{2+} exchange with $[Na^+]_i$, we varied the $[Na^+]_i$ by treating cells with ouabain in the presence of variable external Na^+ concentrations (Fig.30). $[Na^+]_i$ was determined by fluorescence with SBFI and calibrated as previously reported (111). Basal $[Na^+]_i$, 10 ± 2 mM, in normal cells and increased with time following treatment with ouabain. The increase in $[Na^+]_i$ was dependent on the Na^+ concentration in the bathing solution. $[Na^+]_i$ increased 2.5 fold over 60 min of ouabain treatment with normal bathing solutions containing 145 mM NaCl whereas there was little rise in $[Na^+]_i$ when external Na^+ removed from the bath. Using this approach we were able to reproducibly alter the $[Na^+]_i$ in cTAL cells.

With this method, we varied $[Na^+]_i$ and determined the changes in $[Ca^{2+}]_i$ following KCl depolarization at various $[Na^+]_i$. The changes in $[Ca^{2+}]_i$, $\Delta([Ca^{2+}]_i)$, was associated with basal $[Na^+]_i$ levels in a sigmoidal fashion, with a maximal change at $[Na^+]_i$ of 22 mM and a half-maximal $\Delta([Ca^{2+}]_i)$ at about 16 mM $[Na^+]_i$ (Fig.31). The changes in $[Ca^{2+}]_i$ with $[Na^+]_i$ are in keeping with a model of an imbalance of Na^+_i-Ca^{2+}_o coupling.

III.2.4. Modulation of Na^+/Ca^{2+} exchange by calmidazolium and okadaic acid. Our studies provide evidence for a Na^+/Ca^{2+} exchange located on the plasma membrane which

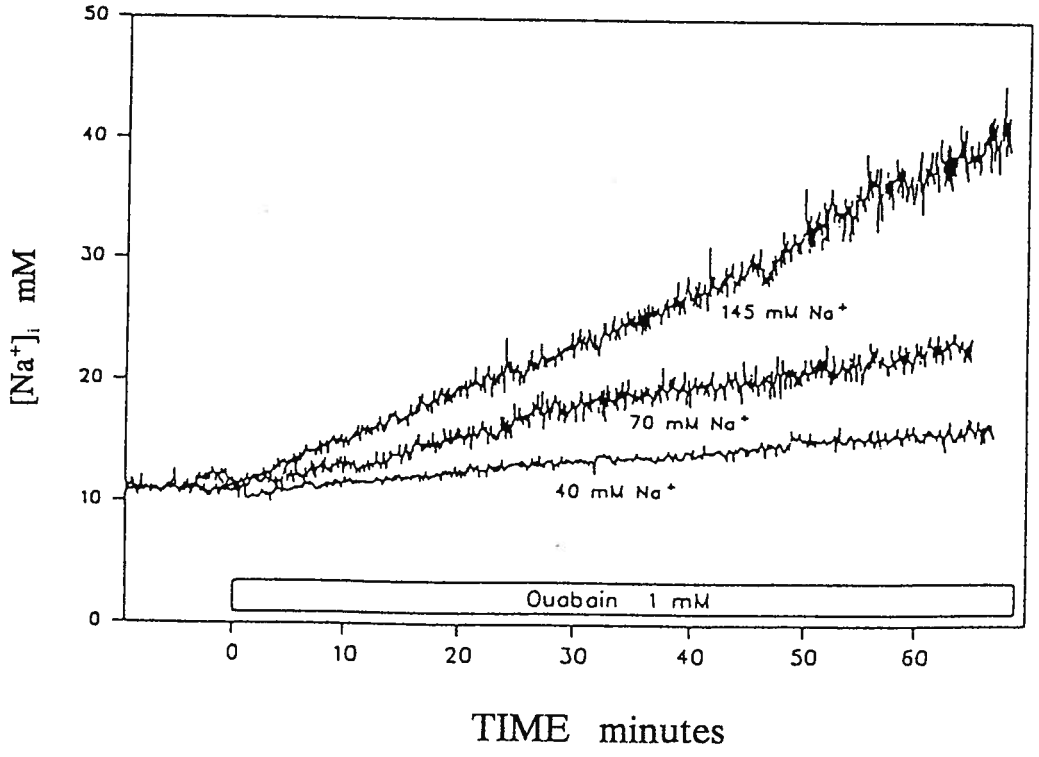

Fig.30. Changes of intracellular $[Na^+]$ in ouabain-treated cTAL cells. Subconfluent cTAL cells were treated with ouabain, 10^{-3} M, for the time periods indicated in the presence of buffer solutions (as given in legend to Fig.25) but with variable $[Na^+]_o$. NaCl was replaced with equivalent amounts of NMDG-Cl to attain the indicated $[Na^+]_o$. Illustrated tracings are the means of 3 different determinations for each external sodium concentration in the buffer solution.

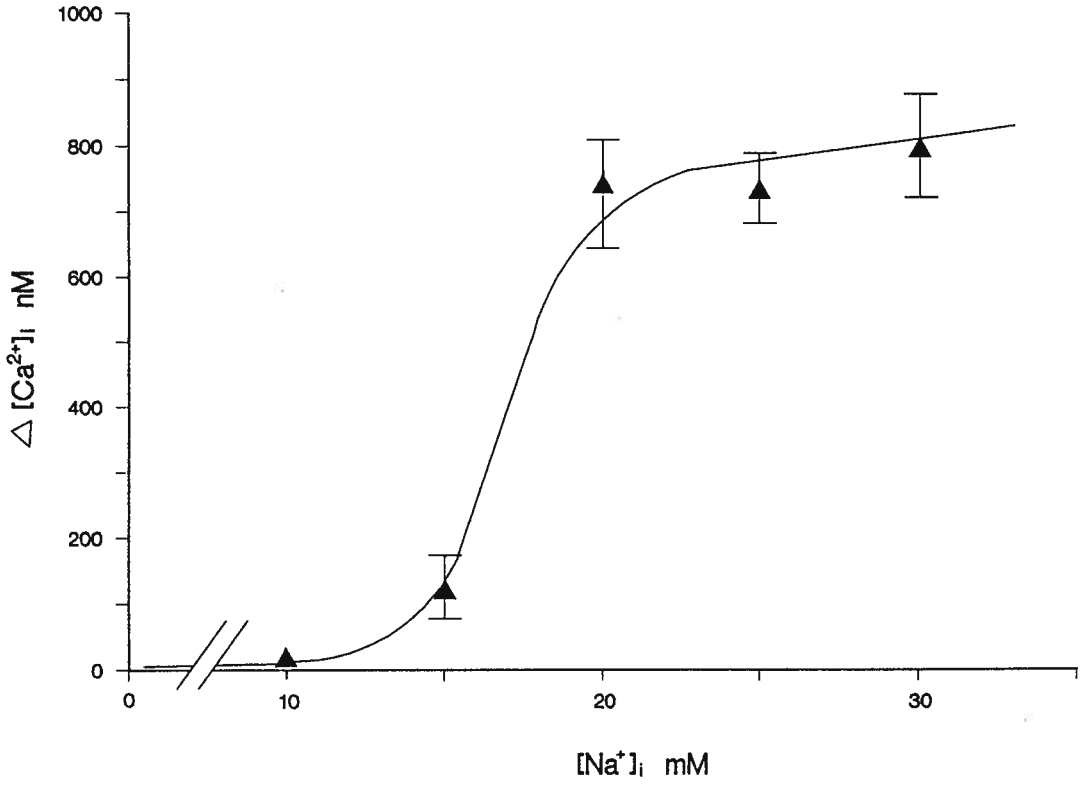

Fig.31. Association of $[Ca^{2+}]_i$ with $[Na^+]_i$ following depolarization. cTAL cells were treated with ouabain, 10^{-3} M, for variable times and with variable amounts of Na^+_o to produce the given $[Na^+]_i$. Depolarization was performed as given in Fig.26 and the changes in $[Ca^{2+}]_i$, $\Delta([Ca^{2+}]_i)$, were plotted as a function of $[Na^+]_i$. The depolarization solution contained (in mM): NaCl 95, KCl 50, Na_2HPO_4 0.2, $CaCl_2$ 1.0, $MgCl_2$ 0.6, glucose 10, and HEPES-Tris 20, pH 7.4.

is demonstrable either through alteration in transmembrane Na^+ gradient or by decrease in membrane voltage, but only in cells with elevated $[Na^+]_i$. In order for this exchange to be physiologically meaningful, it should be regulated in the range of normal external and internal Na^+ and Ca^{2+} concentrations. In the next series of experiments, we provide data to indicate that the Na^+/Ca^{2+} exchange activity is altered through Ca^{2+}-calmodulin complex likely through phosphorylation events.

First, we treated cTAL cells with the compound R24571, a calmodulin inhibitor (calmidazolium, Sigma). Compound R24571 did not alter levels in normal or ouabain-treated cells over the duration of the study. We next determined the effect of compound R24571 on the control of $[Ca^{2+}]_i$ following KCl depolarization (Fig.32). The maximal change in $[Ca^{2+}]_i$ from basal levels, $\Delta([Ca^{2+}]_i)$, following KCl depolarization were determined at various $[Na^+]_i$. The association of $\Delta([Ca^{2+}]_i)$ with $[Na^+]_i$ following depolarization was shifted to the right of normal maximal Ca^{2+} changes, occurring at about 25 mM and half-maximal concentration at 20 mM $[Na^+]_i$ (Fig.31). The maximal $\Delta([Ca^{2+}]_i)$ was similar in both control and compound R24571-treated cells, however, it required greater increments in $[Na^+]_i$ in the treated cells. The shift of the $\Delta([Ca^{2+}]_i)$ vs $[Na^+]_i$ curve to the right following depolarization suggested that the inhibitor R24571 decreased the affinity of the Na^+/Ca^{2+} exchange for $[Na^+]_i$ with little effect on the maximal transport rate. Thus, these data suggest that Ca^{2+}-calmodulin complex may activate the Na^+/Ca^{2+} exchange process by increasing Na^+ affinity leading to exchange within the normal $[Na^+]_i$ of the cTAL cells. To test this postulate, we used okadaic acid, an inhibitor of types 1 and 2a protein phosphatases, to test whether phosphorylation may be involved in controlling exchange activity. Pretreatment of cTAL

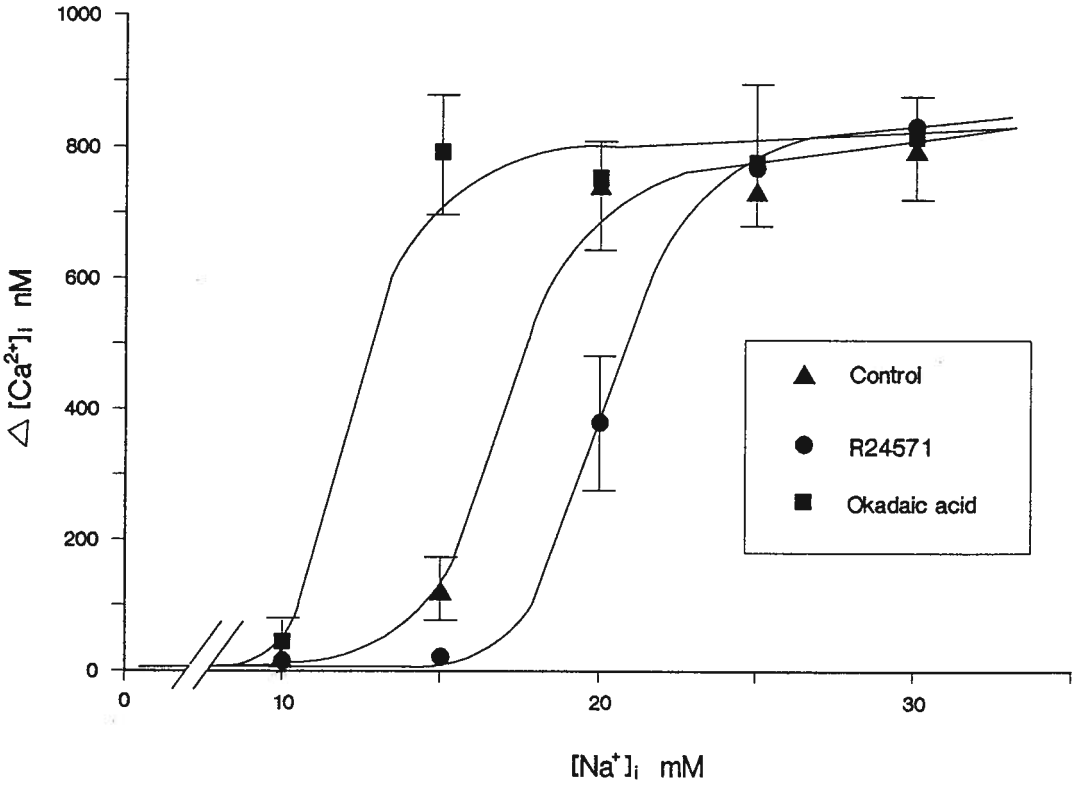

Fig.32. Alteration of Na^+/Ca^{2+} exchange with compound R24571 and okadaic acid. cTAL cells were pretreated with ouabain, 10^{-3} M, and variable $[Na^+]_o$ to produce the given $[Na^+]_i$. cTAL cells were pretreated with R24571 (10^{-4} M), a calmodulin inhibitor, or okadaic acid (10^{-6} M), a phosphatase enzyme inhibitor, for 10 min prior to depolarization with 50 mM KCl (as given in legend to Fig.26. $\Delta([Ca^{2+}]_i)$ was determined in the presence of depolarization solution at various $[Na^+]_i$ as given in legend to Fig.30. Values represent mean $\pm$ SE with n = 3-6 experiments (cells) at each $[Na^+]_i$.

cells with okadaic acid did not have any effect on basal $[Ca^{2+}]_i$ in ouabain-treated cTAL cells. Depolarization of okadaic acid-treated cells resulted in a shift of the $\Delta([Ca^{2+}]_i)$ vs $[Na^+]_i$ curve to the left again without notable change in maximal transport rates (Fig.32). On inspection of the relationship of $\Delta([Ca^{2+}]_i)$ with $[Na^+]_i$ it appeared that changes in $[Ca^{2+}]_i$ occurred at near basal $[Na^+]_i$ concentrations of 8-12 mM following depolarization. If this were the case, then treatment of cTAL cells with ouabain and rise in $[Na^+]_i$ would not be necessary to elicit a voltage-dependent increase in $\Delta([Ca^{2+}]_i)$ in the presence of okadaic acid. Accordingly, we performed studies on normal cTAL cells which were not treated with ouabain but pretreated with the phosphatase inhibitor. Okadaic acid resulted in similar increase in $[Ca^{2+}]_i$ in normal cells as with those treated with ouabain but possessing comparable $[Na^+]_i$ (Fig.33). We conclude from these studies that phosphorylation may increase Na^+/Ca^{2+} exchange activity at physiological $[Na^+]_i$.

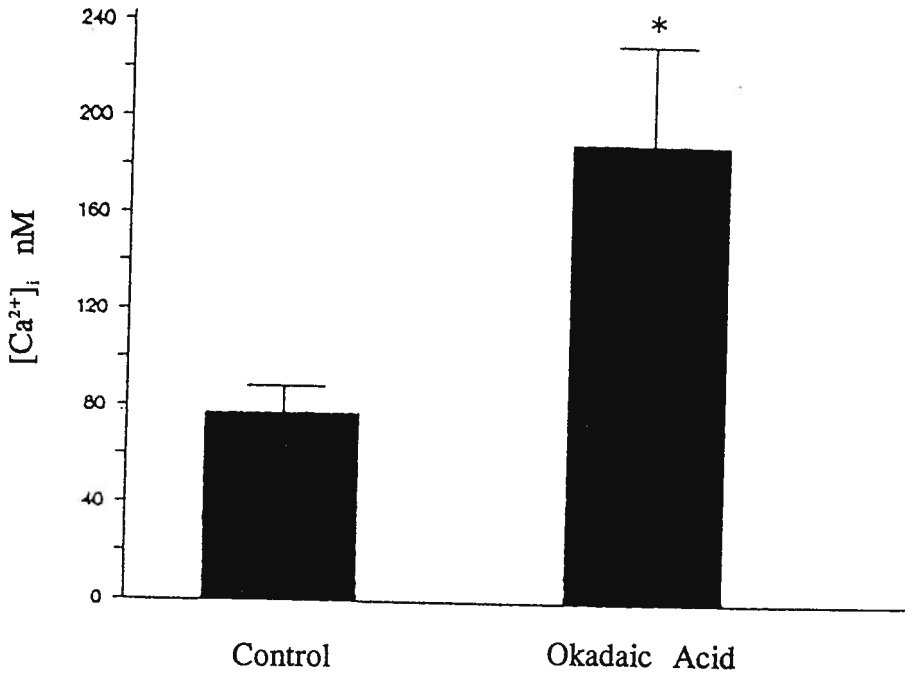

Fig.33. Sodium-dependent increase in $[Ca^{2+}]_i$ in okadaic acid-treated cTAL cells. Porcine cTAL cells were not pretreated with ouabain but treated with okadaic acid, 10^{-6} M, prior to depolarization. The increase in $[Ca^{2+}]_i$ was determined with fluorescence according to methods given in legend to Fig.26. Values are mean $\pm$ SE for 5 cells.

III.3. Identification of Na^+/Ca^{2+} exchanger by molecular biology techniques

III.3.1. The distribution of Na^+/Ca^{2+} exchanger in porcine tissues. Total RNA was extracted from various porcine organs including brain, heart, liver, muscle, and kidney. Kidney samples were taken from four different parts, outer cortex, inner cortex, outer medulla and inner medulla.

For northern blotting, a riboprobe was made from the NCE.F1 cDNA clone contained within pcDNAII.RtKcNCE1.F1 plasmid. As shown in Fig.34, Na^+/Ca^{2+} exchanger transcripts were recognized by NCE.F1 riboprobe in northern hybridization. 7.5-Kb hybridizing transcripts were seen in all tested kidney tissues, including outer cortex, inner cortex, outer medulla and inner medulla. Hybridizing transcripts were also seen in heart and muscle. On this total RNA blot, no transcripts were detected in brain and liver.

III.3.2. Identification of Na^+/Ca^{2+} exchanger in isolated cTAL cells. To demonstrate the presence of Na^+/Ca^{2+} exchanger in cTAL cells, subconfluent cTAL cells were collected from glass cover slips. These cells were of the same age as the cells used in the functional assays. Total RNA was extracted from cTAL cells and used for cDNA synthesis. This cDNA was used as a template with primers designed from NCE.F1 clone in a PCR reaction. As shown in Fig.35, one prominent band ($\sim$290 bp) was obtained from cTAL cell cDNA. This PCR product was smaller than the comparable sequence within NCE.F1 ($\sim$350 bp). Southern blot analysis (Fig.36) also suggested that the amplified cDNA from cTAL cells was a fragment of Na^+/Ca^{2+} exchanger gene which differed from the NCE.F1 cDNA. There were a number of amplified fragments seen in inner cortex tissue cDNA, but only one fragment ($\sim$290 bp) hybridized to the NCE.F1 probe (Fig.35, Fig.36).

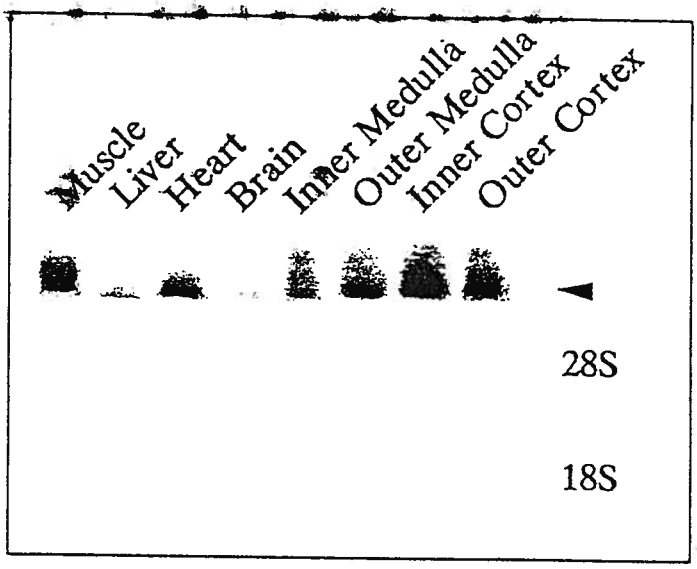

Fig.34. Northern blot analysis of Na^+/Ca^{2+} exchanger. 20 μg of total RNA from each of the indicated tissues was run on 1% agarose-formaldehyde gels as detailed in the text. The total RNA was hybridized to UTP-α-^{32}P labelled riboprobe from NCE F1. The locations of 28S and 18S are indicated. Arrow points the location of 7.5 Kb.

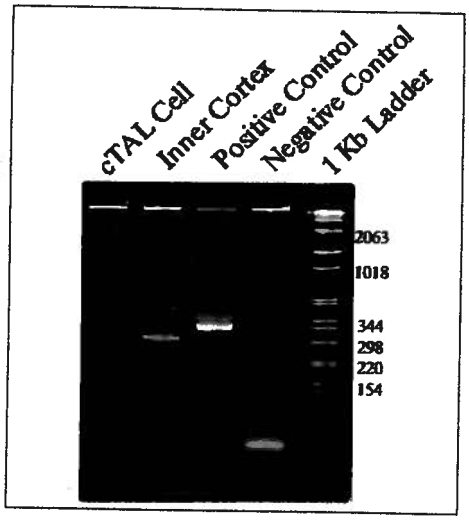

Fig.35. PCR amplification of the variable region of the exchanger mRNA from inner cortex and cTAL cells. cDNAs synthesized from total RNA extracted from inner cortex and isolated cTAL cells were used as templates for PCR amplification. The NCE.F1 clone and the reaction buffer for cDNA synthesis were employed as positive and negative controls, respectively. The PCR products were separated by acrylamide gel (7%) and stained with ethidium bromide.

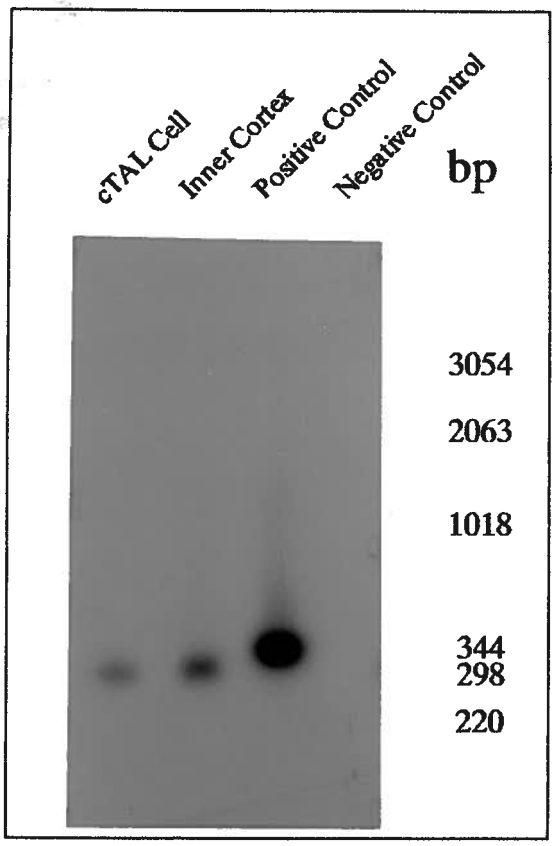

Fig.36. Southern blot analysis of PCR products from inner cortical tissue and isolated cTAL cells. PCR products from inner cortex and cTAL cells were separated by 1% agarose gel and transferred onto Nytran membrane. The membrane was hybridized with ^{32}P labelled cDNA probe made from PCR product of positive controls. The molecular size markers are indicated.

Fig.37 shows the nucleotide sequence of the PCR product obtained from cTAL cell cDNA. Based on the genomic DNA sequence data of Kofuji *et al* (102), this sequence lacked the A,C,E,Fexons but contained exon B and exon D in the alternative splicing region of the cytoplasmic segment of the exchanger. The sequence obtained was the same as that of the NACA3 isoform reported by Lee and colleagues (103). Although there were a number of nucleotide differences between porcine cDNA and those of the rat and rabbit, the encoded amino acid sequences are identical except for n.t.1210 which encodes a serine instead of a threonine (Fig.37).

Fig.37. Nucleotide sequence of PCR product from cTAL cells. All available sequences of Na^+/Ca^{2+} exchanger isoforms expressed in the kidney were compared. The sequence of NACA3 (pig) is the sequence of the PCR product from cTAL cell of porcine in this study. The sequence data of NACA7 (rat) and NACA3 (rat) are from Lee *et al* (103); NACA2 (rabbit) from Reilly *et al* (99). Exons B,C,D,and F are indicated based on Kofuji *et al* (102). Dashes (-) indicate that no nucleic acid was present (i.e., there is a deletion).

IV. Discussion

Porcine cTAL cells possess a large number of peptide hormone receptors which stimulate intracellular Ca^{2+} release and extracellular entry (92). The present studies show that control of $[Ca^{2+}]_i$ is, in part, through Ca^{2+} extrusion via a Na^+/Ca^{2+} exchange process. The latter can move Ca^{2+} out of the cytosol across the plasma membrane in exchange for entry of Na^+. The evidence indicates that the Na^+/Ca^{2+} exchange is reversible so that Ca^{2+} can move into or out of the cytosol across the plasma membrane, the direction depending on the transmembrane Na^+ chemical and voltage gradients (121).

IV.1. Functional demonstration of Na^+/Ca^{2+} exchange

The evidence for a functional and reversible Na^+/Ca^{2+} exchange system in porcine cTAL cells is persuasive. The removal of external Na^+ or depolarization of the plasma membrane in ouabain-treated cTAL cells results in marked increase in $[Ca^{2+}]_i$ which is dependent on the presence of external Ca^{2+} (Fig.22, Fig.26). This is interpreted as a favourable electrochemical gradient for Na^+ such that cytosolic Na^+ moves out coupled to entry of external Ca^{2+}. The entry may be inhibited by multivalent cations such as La^{3+} and Mg^{2+} (Fig.24, Fig.28). Agents like amiloride and bepridil which are known to inhibit Na^+/Ca^{2+} exchange in other cells are also effective (Fig.25, Fig.29) (115). Although amiloride and bepridil are not specific inhibitors of Na^+/Ca^{2+} exchange, their actions are supportive of the observations with the inorganic blockers. The Na^+/Ca^{2+} exchange is specific for Na^+ as Li^+ is unable to drive the exchanger in the forward direction (93,117). The apparent characteristics of the Na^+/Ca^{2+} exchanger in porcine cTAL cells are similar to those reported for many other cell-types, i.e. it is altered by the transmembrane voltage suggesting an

electrogenic process (93,106). However, it is of interest that in order to demonstrate the exchange in unstimulated cTAL cells, the intracellular [Na^+] must be elevated above basal levels. Elevation of intracellular Na^+ is also required to demonstrate Na^+/Ca^{2+} exchange in intact cells isolated from rat collecting tubules (122), but not rat proximal tubules (123,124), nor rabbit connecting tubules (125). To our knowledge, only one other study has looked at this exchange in thick ascending limb cells. Nitschke *et al* were unable to detect changes in $[Ca^{2+}]_i$ following removal of bath external Na^+ in perfused rabbit cTAL segments (126). However, these investigators did not pretreat the perfused segments with ouabain and thus probably did not elevate intracellular [Na^+] prior to experimentation. Our data indicate that Na^+/Ca^{2+} exchange is present in porcine cTAL cells.

IV.2. The effect of phosphorylation on Na^+/Ca^{2+} exchange activity

Although the Na^+/Ca^{2+} exchanger appears to be widespread, little is known about the regulation of this transport. Intracellular ligands may regulate activity of the exchanger (such as Ca^{2+}, Mg^{2+}, or H^+). The levels of cytosolic ATP appear to modulate Na^+/Ca^{2+} exchange in squid axons, barnacle muscles, erythrocytes, and cardiac cells (106,121). There is also physiological and biochemical evidence that Na^+/Ca^{2+} exchange is regulated by receptor-mediated mechanisms. First, parathyroid hormone and cAMP have been reported to increase exchange in basolateral membranes isolated from renal cortex (108,109) and the distal tubule (108). These recent studies are confirmatory of earlier ones by Hanai *et al* (108). Scoble, Hruska, and coworkers demonstrated a Na^+/Ca^{2+} exchange in basolateral membrane vesicles, probably proximal in origin, from dog cortical tissue (109). PTH, but not cAMP, increases exchange activity in these studies. The discrepancy in these reports

from rabbit and dog remains to be explained. Calcitonin also increases Na^+/Ca^{2+} exchange in membrane vesicles isolated from the rabbit distal tubule, but vitamin D, which increases calcium reabsorption in the distal nephron does not have any effect on Na^+/Ca^{2+} exchange (127). Other factors have been reported to increase Na^+/Ca^{2+} exchange in various cell types. Recently, Zhu *et al* have shown that angiotensin I increases Na^+/Ca^{2+} exchange in vascular smooth muscle perhaps through alteration in $[Na^+]_i$ or phosphorylation (128). The second messenger, cGMP, has also been reported to stimulate Na^+/Ca^{2+} exchange in vascular smooth muscle cells (129). By contrast, phorbol esters, perhaps through activation of protein kinase C, decrease Na^+/Ca^{2+} exchange in human mesangial cells (130) and cotransport in rabbit collecting tubules (110). However, others have shown that phorbol esters increase Na^+/Ca^{2+} exchange activity in aortic smooth muscle cells (120). Finally, biochemical evidence supports the notion that Na^+/Ca^{2+} exchange may be regulated. Caroni and Carafoli reported that kinase-mediated phosphorylation activates Na^+/Ca^{2+} exchange in cardiac plasma membranes (131). This activation was dependent on Ca^{2+}, inhibited by anticalmodulin agents and was not affected by cAMP. The present studies indicate that phosphorylation may be involved, either directly to the exchange protein or indirectly through some other steps in regulation.

Our results with the calmodulin-inhibitor, R24571, or the phosphatase-inhibitor, okadaic acid, suggest that Na^+ interaction with the Na^+/Ca^{2+} exchanger may be altered by phosphorylation events. Pretreatment of cTAL cells with calmodulin-inhibitor shifted the Na^+-dependence curve to the right to a higher half-maximal $[Na^+]_i$ whereas the phosphatase inhibitor shifted it to a lower half-maximal $[Na^+]_i$ (Fig.32). Indeed, the latter resulted in

activation of exchange in normal Na^+_i concentrations so that elevation of $[Ca^{2+}]_i$ could be observed in normal cTAL cells in the absence of ouabain and elevation of $[Na^+]_i$ (Fig.33). We postulate that the acute elevation of $[Ca^{2+}]_i$, for instance by receptor-mediated mechanisms, results in the formation of Ca^{2+}-calmodulin coupling which in turn stimulates the Na^+/Ca^{2+} exchanger at normal $[Na^+]_i$. This would mitigate the increase in $[Ca^{2+}]_i$ and return it to normal levels. Our studies with okadaic acid indicate that Ca^{2+}-calmodulin acts through phosphorylation events possibly by stimulation of Ca^{2+}-calmodulin kinases. Ca^{2+}-calmodulin may also modulate the Na^+/Ca^{2+} exchange protein through allosteric effects. It is unlikely that these phosphorylative actions directly involve the exchanger as deletion of almost all of the intracellular loop had little effect on exchange activity (93). How these observations fit into our understanding of physiological controls remains unknown.

IV.3. Identification of Na^+/Ca^{2+} exchanger transcripts in cTAL cell RNA

The results of many different studies have suggested that a Na^+/Ca^{2+} exchanger may operate in proximal (93,123,124) and distal convoluted tubules (122,132), connecting tubules (125,133), and collecting tubules (122). There is some controversy as to the segmental location of Na^+/Ca^{2+} exchanger. Ramachadran and Brunette have reported that Na^+/Ca^{2+} exchanger is located in the distal tubule (convoluted connecting tubule) and not in the proximal tubule (132). More recently, cDNA and antibody probes have been used to determine the presence of Na^+/Ca^{2+} exchanger transcripts and protein expression, respectively, along the nephron (12). With the exception of ref. 134, these studies have failed to detect the presence of exchanger transcripts in cells other than the distal tubule and connecting tubule (99,100,133). The distribution of the Na^+/Ca^{2+} exchanger, by

immunolocalization, was confined to basolateral membranes of connecting tubules, with little or no exchanger being found in other parts of the nephron (12,133). It should be noted that the Na^+/Ca^{2+} exchanger is a high capacity system, thus it is possible that only small amounts of the protein are sufficient to account for the present functional results.

The Na^+/Ca^{2+} exchanger is composed of five amino-terminal membrane-spanning segments, a large intracellular loop, and a carboxy-terminal region containing six additional membrane-spanning segments. There appears to be a high degree of similarity (greater than 90%) at the amino acid level among the homologs of various species studied so far: dog (94), rat (100), cow (95), rabbit (104), and human (104). The differences among the various Na^+/Ca^{2+} exchanger clones appear in the coding sequence for the carboxyl end of the large putative intracellular loop. Alternative splicing within this sequence region could potentially result in 32 different mRNAs, and therefore in the production of as many isoforms of the expressed Na^+/Ca^{2+} exchanger protein perhaps having different functions (102).

The cytoplasmic domain of the Na^+/Ca^{2+} exchanger is encoded by combinations of exons designated A, B, C, D, E, and F. Cardiac tissue contains the exons ACDEF, the brain contains ADF or AD, skeletal muscle BDF, and kidney and intestine BDF and BD exons (102,103). Two splice variants have been found in the rat kidney (NACA3, with exons BD, and NACA7, exons BDF) (103); and two in the rabbit kidney (NACA2, exons BCD, and NACA3, exons BD) (102,104). The NACA3 isoform appears to be the most abundant in the kidney and principally localized in the connecting segment of the distal tubule (100). Although there is some controversy as to whether Na^+/Ca^{2+} exchanger is present in proximal tubules, no reports have been given to date for exchanger in the thick ascending limb

(12,122). The fluorescent studies described herein suggest that Na^+/Ca^{2+} exchange occurs in porcine cTAL cells. In this regard, RNA isolated from cTAL tissue and isolated cells confirmed the presence of exchanger expression and also demonstrated the alternative splicing variant present in porcine cTAL cells.

Northern hybridization of total RNA from porcine kidney, brain, liver, heart and skeletal muscle and Southern hybridization of the PCR product from porcine single cTAL cells were used to determine the presence of these Na^+/Ca^{2+} exchanger transcripts. The size of the transcript of kidney and heart is about 7.5 Kb (Fig.34), which is consistent with the observation of Lee *et al* (103) and Komuro *et al* (104). The failure to detect the transcripts in brain and liver indicates the possibility that different isoforms of Na^+/Ca^{2+} exchanger may exist in these organs which is in keeping with the notions of Kofuji *et al* (102) and Lee *et al* (103). Further studies are required to show that this is another isoform of the Na^+/Ca^{2+} exchanger.

Several cDNA fragments from inner cortex tissue were amplified by PCR, but only one clear PCR product ($\sim$290 bp) was found in the cTAL reaction (Fig.35). Southern blot analysis exhibited that only the 290 bp product is a part of Na^+/Ca^{2+} exchanger (Fig.36). Since the primers used in PCR were designed from the regions flanking the alternative splicing site, 350 bp cDNA was obtained from NCE.F1 positive control which was composed of three exons, B, D, and F. 290 bp PCR products from inner cortex and cTAL cells are shorter than the positive control, suggesting that less than three exons are involved in this region. Sequencing of the 290 bp PCR product revealed that the alternative splicing segment of the Na^+/Ca^{2+} exchanger in the cTAL cells is composed of exons B and D

(Fig.37). This isoform conforms to NACA3 which is the major Na^+/Ca^{2+} exchanger found in rat and rabbit kidneys (102,103).

In summary, we have demonstrated functional Na^+/Ca^{2+} exchange in single cTAL cells through microspectrophotometry. The exchange activity is sensitive to some inorganic and organic inhibitors. The present data also suggests that this exchange may be altered through changes including calmodulin-dependent and okadaic acid-inhibitable phosphatases. Further, we have shown through biochemical approaches that the Na^+/Ca^{2+} exchanger message is expressed in the cTAL cells and that this is the same isoform as that reported for distal connecting tubules. Under normal conditions, transepithelial calcium reabsorption is thought to be passive and through the paracellular pathway in the cTAL (135,136) but active and transcellular in the distal tubule (97). It is thus of interest to note that the isoform of the Na^+/Ca^{2+} exchanger reported here in porcine cTAL cells is the same isoform identified in rat connecting tubule cells (100). It would appear that the same isoform may perform different functions; maintenance of $[Ca^{2+}]_i$ in cTAL cells and calcium reabsorption in distal connecting cells. The functional cell-specific differences have yet to be explained.

GENERAL CONCLUSIONS

The present studies show that a number of peptide hormones elicit Ca^{2+} signals in porcine cTAL cells likely through receptor-mediated responses. The Ca^{2+} transients elicited by the prototypical hormones, PTH, AVP, and ANP, are composed of intracellular release followed by Ca^{2+} entry across the plasma membrane. These signals are likely due to IP_3-mediated Ca^{2+} release from the endoplasmic reticulum. PTH- and AVP-mediated Ca^{2+}

Ca^{2+} transients are modulated by cAMP and protein kinase C activation, which may play a role in regulating the responses to these hormones. ANP-mediated Ca^{2+} transients are modulated by cGMP, which may play a regulatory role in these signals. Accordingly, the signaling pathways interact in a complicated way to orchestrate hormonal controls in cTAL.

Na^+/Ca^{2+} exchange was functionally demonstrated by both removal of external Na^+ and voltage depolarization in ouabain-treated cTAL cells. The activity of this exchange may be altered through changes including calmodulin-dependent and okadaic acid-inhibitable phosphatases. The presence of a Na^+/Ca^{2+} exchanger was confirmed with northern hybridization techniques. Total RNA from inner cortex was probed using a riboprobe made from NCE.F1 clone. A gene transcript which encodes a portion of the intracellular loop of the renal Na^+/Ca^{2+} exchanger was amplified from cortical tissue and cTAL cells by PCR using primers flanking the alternative splicing site. Southern hybridization and DNA sequencing demonstrated the isoform contained exons B and D characteristic of one isoform of the renal Na^+/Ca^{2+} exchanger in cTAL cells of the porcine kidney. Under physiological conditions, it is likely that Na^+/Ca^{2+} exchange plays an important role in $[Ca^{2+}]_i$ control and thus hormonal regulation of electrolyte reabsorption within the cTAL cells of the loop of Henle in the kidney.

REFERENCES

1. Costanzo L.S., and Windhager E.E.: Renal regulation of calcium balance. In: Seldin D.W. and Giebisch G., ed. The Kidney: Physiology and Pathophysiology, Second Edition, Raven Press Ltd., New York, PP2375-2393, 1992.

2. Lee C.O., Taylor A., and Windhager E.E.: Cytosolic calcium ion activity in epithelial cells of Necturus kidney. Nature 287:859-861, 1980.

3. Ullrich K.J., Rumrich G., and Kloss S.: Active Ca^{2+} reabsorption in the proximal tubule of the rat kidney. Dependence on sodium- and buffer transport. Pflügers Archiv. 364:223-228, 1976.

4. Rouse D., Ng R.C., and Suki W.N.: Calcium transport in the pars recta and thin descending limb of Henle of the rabbit, perfused in vitro. J. Clin. Invest. 65:37-42, 1980.

5. Pennica D., Kohr W.J., Kuang W.J., Glaister D., Aggarwal B.B., Chen E.Y., and Goeddel D.V.: Identification of human uromodulin as the Tamm-Horsfall urinary glycoprotein. Science 236:83-88, 1988.

6. De Rouffignac C., and Quamme G.A.: Renal magnesium handling and its hormonal control. Physiol. Rev. 74:305-322, 1994.

7. Dai L.J., and Quamme G.A.: Intracellular Mg^{2+} and magnesium depletion in isolated renal thick ascending limb cells. J. Clin. Invest. 88:1255-1264, 1991.

8. Good D.W., Knepper M.A., and Burg M.B.: Ammonia and bicarbonate transport by thick ascending limb of rat kidney. Am. J. Physiol. 247:F35-F44, 1984.

9. Bourdeau J.E., and Burg M.B.: Effect of PTH on calcium transport across the cortical thick ascending limb of Henle's loop. Am. J. Physiol. 239:F121-F126, 1980.

10. Suki W.N., and Rouse D.: Hormonal regulation of calcium transport in thick ascending limb renal tubules. Am. J. Physiol. 241:F171-F174, 1981.

11. Shimizu T., Yoshitomi K., Nakamura M., and Imai M.: Effects of PTH, calcitonin, and cAMP on calcium transport in rabbit distal nephron segments. Am. J. Physiol. 259:F408-F414, 1990.

12. Rouffignac C. de, Di Stefano A., Wittner M., Roinel N., and Elalouf J.M.: Consequences of differential effects of ADH and other peptide hormones on thick ascending limbs of mammalian kidney. Am. J. Physiol. 260:R1023-R1035, 1991.

13. Reilly R.F., Shugrue C.A., Lattanzi D., and Biemesderfer D.: Immunolocalization of the Na^+/Ca^{2+} exchanger in rabbit kidney. Am. J. Physiol. 265:F327-F332, 1993.

14. Bronner F.: Renal calcium transport: mechanisms and regulation---an overview. Am. J. Physiol. 257:F707-F711, 1989.

15. Carafoli E.: The calcium pump of the plasma membrane. J. Biol. Chem. 267:2115-2118, 1992.

16. Blaustein M., DiPolo R., and Reeves J.P.: Sodium-calcium exchange. Proceedings of the second international conference. Ann. N. Y. Acad. Sci. 639:1-671, 1991.

17. Pozzan T., Rizzuto R., Volpe P., and Melsolesi J.: Molecular and cellular physiology of intracellular calcium stores. Physiol. Rev. 74:595-636, 1994.

18. Mauger J.-P. and Claret M.: Mobilization of intracellular calcium by glucagon and cyclic AMP analogues in isolated rat hepatocytes. FEBS Let. 195:106-110, 1986.

19. Morel F.: Sites of hormone action in the mammalian nephron. Am. J. Physiol. 240:F159-F164, 1981.

20. Morel F., Chabardès D., Imbert-Teboul M., Le Bouffant F., Hus-Citharel A., and Montégut M.: Multiple hormonal control of adenylatecyclase in distal segments of the rat kidney. Kidney Int. 21:S55-S62, 1982.

21. Davis T.N.: What's new with calcium? Cell 71:557-564, 1992.

22. Artalejo C.R., Adams M.E., and Fox A.P.: Three types of Ca^{2+} channel trigger secretion with different efficacies in chromaffin cells. Nature 367:72-76, 1994.

23. Greger R.: Ion transport mechanisms in thick ascending limb of Henle's loop of mammalian nephron. Physiol. Rev. 65:760-797, 1985.

24. Herbert S.C., and Andreoli T.E.: Control of NaCl transport in the thick ascending limb. Am. J. Physiol. 246:F745-F756, 1984.

25. Di Stefano A., Wittner M., Nitschke R., Braitsch R., Greger R., Bailly C., Amiel C., Roinel N, and de Rouffignac C.: Effects of parathyroid hormone and clacitonin on Na^+, Cl^-, K^+, Mg^{2+} and Ca^{2+} transport in cortical and medullary thick ascending limbs of mouse kidney. Pflügers Arch. 417:161-167, 1990.

26. Wittner M., Di Stefano A., Mandon B., Roinel N., and de Rouffignac C.: Stimulation of NaCl reabsorption by antidiuretic hormone in the cortical thick ascending limb of Henle's loop of the mouse. Pflügers Arch. 419:212-214, 1991.

27. Rouffignac C. de, Elalouf J.M., Roinel N., Bailly C., and Amiel C.: Similarity of the effects of antidiuretic hormone, parathyroid hormone, clacitonin, and glucagon on rat kidney. In: Robinson R.R. (ed) Nephrology. Springer, Berlin Heidelberg New York, pp 340-357, 1984

28. Berridge M.J.: Inositol triphosphate and calcium signalling. Nature 361:315-325, 1993.

29. Hallam T.J., and Rink T.J.: Receptor-mediated Ca^{2+} entry in diversity of function and mechanism. Trends Pharmacol. Sci. 10:8-10, 1989.

30. Kuno M., and Gardner P.: Ion channels activated by inositol 1,4,5-trisphosphate in plasma membrane of human T-lymphocytes. Nature 326:301-304, 1987.

31. Rosenthal W., Hescheler J., Trautwein W., and Schultz G.: Control of voltage-dependent Ca^{2+} channels by G protein-coupled receptors. FASEB J. 2:1784-1790, 1988.

32. Roe M.W., Lemasters J.J., and Herman B.: Assessment of fura-2 for measurement of cytosolic free calcium. Cell Calcium 11:63-73, 1990.

33. Tsien R.Y., Rink T.J. and Poenie M.: Measurement of cytosolic free Ca^{2+} in individual cells using fluorescent microscopy with dual excitation wavelengths. Cell Calcium 6:145-157, 1985.

34. Quamme G.A., and Dai L.J.: Presence of a novel influx pathway for Mg^{2+} in MDCK cells. Am. J. Physiol. 259:C521-C525, 1990.

35. Grynkiewicz G., Poenie M., and Tsien R.Y.: A new generation of Ca^{2+} indicators with greatly improved fluorescence properties. J. Biol. Chem. 260:3440-3450, 1985.

36. Malgaroli A., Milani D., Meldolesi J., and Pozzan T.: Fura-2 measurement of cytosolic free Ca^{2+} in monolayers and suspensions of various types of animal cells. J. Cell. Biol. 105:2145-2155, 1987.

37. Allen M.L., Nakao A., Sonnenburg W.K., Burnatowska-Hledin M., Spielman W.S., and Smith W.L.: Immunodissection of cortical and medullary thick ascending limb cells from rabbit kidney. Am. J. Physiol. 255:F704-F710, 1988.

38. Glennon M.C., Bird G.S.J., Kwan C.-Y., and Putney J.Jr: Actions of vasopressin and the Ca^{2+}-ATPase inhibitor, thapsigargin, on Ca^{2+} signalling in hepatocytes. J. Biol. Chem. 267:8230-8233, 1992.

39. Thastrup O., Cullen P.J., Drobak B., Hanley M.R., and Dawson A.P.: Thapsigargin, a tumor promoter, discharges intracellular Ca^{2+} stores by specific inhibition of the endoplasmic reticulum Ca^{2+}-ATPase. Proc. Natl. Acad. Sci. USA 87:2466-2470, 1990.

40. Hor V.J., Baum B.J., and Ambudkar I.S.: ß-Adrenergic receptor stimulation induces inositol trisphosphate production and Ca^{2+} mobilization in rat acinar cells. J. Biol. Chem. 263:12454-12460, 1988.

41. Rouffignac C. de, Elalouf J.M., and Roinel N.: Physiological control of the urinary concentrating mechanisms by peptide hormones. Kidney Int. 31:611-620, 1987.

42. Cogan M.G.: Renal effects of atrial natriuretic factor. Annu. Rev. Physiol. 52:1255-1264, 1991.

43. Gunning M.E., and Brenner B.M.: Natriuretic peptides and the kidney: current concepts. Kidney Int. 42:S127-S133, 1992.

44. Jamison R., Canaan-Kuhl S., and Pratt P.: The netriuretic peptide and their receptors. Am. J. Kidney Dis. 20:519-530, 1992.

45. Levin E.R.: Natriuretic peptide C-receptor more than a clearance receptor. Am. J. Physiol. 264:E483-E489, 1993.

46. Neant F., and Bailly C.: Luminal and intracellular cGMP inhibit the mTAL reabsorptive capacity through different pathways. Kidney Int. 44:741-746, 1993.

47. Chabardès D., Montegut M., Mistaoui M., Butlen D., and Morel F.: Atrial natriuretic peptide effects on cGMP and cAMP contents in microdissected glomeruli and segments of the rat and rabbit nephrons. Pflüegers Arch. 408:366-372, 1987.

48. Nonoguchi H., Knepper M.A., and Manganiello V.C.: Effects of atrial natriuretic factor on cyclic guanosine monophosphate and cyclic adenosine monophosphate accumulation in microdissected nephron segments from rats. J. Clin. Invest. 79:500-507, 1987.

49. Sudoh T., Kangawa K., Minamino N., and Matsuo H.: A new natriuretic peptide in porcine brain. Nature 332:78-81, 1988.

50. Furuya M., Takehisa M., Minamitake Y., Kitajima Y., Hayashi Y., Ohnuma N., Ishihara T., Minamino N., Kangawa K., and Matsuo H.: Novel natriuretic peptide, CNP, potently stimulates cyclic GMP production in rat cultured vascular smooth muscle cells. Biochem. Biophys. Res. Commun. 170:201-208, 1990.

51. Kojima M., Minamino N., Kangawa K., and Matsuo H.: C-type natriuretic peptide (CNP), a new member of natriuretic peptide family identified in porcine brain. Biochem. Biophys. Res. Commun. 168:863-868, 1990.

52. Suga S.-I., Nakao K., Mukoyama M., Arai H., Hosoda K., Ogawa Y., and Imura H.: Characterization of natriuretic peptide receptors in cultured cells. Hypertension Dallas

19:762-765, 1992.

53. Schulz S., Singh S., Bellet R.A., Singh G., Tubb D.J., Chin H., and Garbers D.L.: The primary structure of a plasma membrane guanylate cyclase demonstrates diversity within this new receptor family. Cell 58:1155-1162, 1989.

54. Koller K.J., Lowe D.G., Bennett G.L., Minamino N., Kangawa K., Matsuo H., and Goeddel D.V.: Selective activation of the B natriuretic peptide receptor by C-type natriuretic peptide (CNP). Science 252:120-123, 1991.

55. Almeida F.A., Suzuki M., Scarborough R.M., Lewicki J.A., and Maack T.: Clearance function of type C receptors of atrial natriuretic factor in rats. Am. J. Physiol. 256:R469-R475, 1989.

56. Maack T., Suzuki M., Almeida F.A., Nussenzveig D., Scarborough R.M., McEnroe G.A., and Lewicki J.A.: Physiological role of silent receptors of atrial natriuretic factor. Science 238:675-678, 1989.

57. Johnson B.G., Trachte G.J., and Drewett J.G.: Neuromodulatory effect of the atrial natriuretic factor clearance receptor binding peptide cANF(4-23)-NH_2 in rabbit isolated vasa deferentia. J. Pharmacol. Exp. Ther. 257:720-726, 1991.

58. Elalouf J.M., Sari D.C., and de Rouffignac C.: Additive effects of glucagon and vasopressin on renal Mg reabsorption and urine concentrating ability in the rat. Pflügers Arch. 407:S66-S71, 1986.

59. Elalouf J.M., Di Stefano A., and de Rouffignac C.: Sensitivities of rat kidney thick ascending limbs and collecting ducts to vasopressin (in vitro). Proc. Natl. Acad. Sci. USA 83:2276-2280, 1986.

60. Chabardès D., Imbert M., Clique A., Montégut M., and Morel F.: PTH sensitive adenyl cyclase activity in different segments of the rabbit nephron. Pflügers Arch. 354:229-239, 1975.

61. Kikawa U., and Nishizuka Y.: The role of protein kinase C in transmembrane signalling. Annu. Rev. Cell Biol. 2:149-178, 1986.

62. Uneyama H., Uneyama C., and Akaike N.: Intracellular mechanisms of cytoplasmic Ca^{2+} oscillation in rat megakaryocyte. J. Biol. Chem. 268:168-174, 1993.

63. Nitschke R., Fröbe U., and Greger R.: Antidiuretic hormone acts via V_1 receptors on intracellular calcium in the isolated perfused rabbit cortical ascending limb. Pflügers Arch. 417:622-632, 1991.

64. Bourdeau J.E., Eby B.K., and Hu J.: cAMP-stimulated rise of $[Ca^{2+}]_i$ in rabbit connecting tubules: role of peritubular calcium. Am. J. Physiol. 258:F751-F755, 1990.

65. Luini A., Lewis D., Guild S., Corda D., and Axelrod J.: Hormone secretagogues increase cytosolic calcium by increasing cAMP in corticotropin-secreting cells. Proc. Natl. Acad. Sci. USA 82: 8034-8038, 1985.

66. Schiebinger R.J., Braley L.M., Menachery A., and Williams G.H.: Calcium, a "third messenger" of cAMP-stimulated adrenal steroid secretion. Am. J. Physiol. 248:E89-E94, 1985.

67. Thastrup O., Cullen P.J., Drobak B., Hanley M.R., and Dawson A.P.: Thapsigargin, a tumor promoter, discharges intracellular Ca^{2+} stores by specific inhibition of the endoplasmic reticulum Ca^{2+}-ATPase. Proc. Natl. Acad. Sci. USA 87:2466-2470, 1990.

68. Ansah T.-A., Dho S., and Case R.M.: Calcium concentration and amylase secretion in guinea pig pancreatic acini: interactions between carbachol, cholecystokinin, octapeptide, and the phorbol ester, 12-O-tetradecanoylphorbol 13-acetate. Biochim. Biophys. Acta 889:326-333, 1986.

69. Bird G.St J.,Rossier M.F., Obie J.F., and Putney J.W.Jr: Sinusoidal oscillations in intracellular calcium requiring negative feedback by protein kinase C. J. Biol. Chem. 268:8425-8428, 1993.

70. Bruzzone R., Regazzi R., and Wollheim C.B.: Caerulin causes translocation of protein kinase C in rat acini without increasing cytosolic free Ca^{2+}. Am. J. Physiol. 255:G33-G39, 1988.

71. Willems P.H., Van Den Brock B.A., Van Os C.H., and De Pont J.J.: Inhibition of inositol 1,4,5-triphosphate-induced Ca^{2+} release in permeabilized pancreatic acinar cells by hormonal and phorbol eater pretreatment. J. Biol. Chem. 264:9762-9767, 1989.

72. Woods N.M.,Cuthbertson K.S.R.,and Cobbold P.T.S.:Phorbol ester-induced alterations of free calcium ion transients in single rat hepatocytes. Biochem. J. 246:619-623, 1987.

73. Dublineau I., Elalouf J.-M., Pradelles P., and de Rouffignac C.: Independent desensitization of rat renal thick ascending limbs and collecting ducts to ADH. Am. J. Physiol. 256:F656-F663, 1989.

74. Elalouf J.M., Chabane-Sari S., Roinel N., and de Rouffignac C.: Desensitization of rat renal thick ascending limb to vasopressin. Proc. Natl. Acad. Sci. USA 85:2407-2416, 1988.

75. Tan Y.P., and Marty A.: Protein kinase C-mediated desensitization of the muscarinic

response in rat lacrimal gland cells. J. Physiol. 433:357-371, 1991.

76.de Zeeuw D., Janssen W.M.T., and de Jong P.: Atrial natriuretic factor: Its (patho)-physiological significance in humans. Kidney Int. 41:1115-1133, 1992.

77.Butlen D., Mistaoui M., and Morel F.: Atrial natriuretic peptide receptor along the rat and rabbit nephrons: [^{125}I] alpha-rat atrial netriuretic peptide binding in microdissected glomeruli and tubules. Pflügers Arch. 408:356-365, 1987.

78.Terada Y., Moriyama T., Martin B.M., Knepper M.A., and Garcia-Perez A.: RT-PCR microlocalization of mRNA for guanylyl cyclase-coupled ANF receptor in rat kidney. Am. J. Physiol. F1080-F1087, 1991.

79.Hirata M., Chang C.-H., and Murad F.: Stimulating effects of atrial natriuretic factor on phosphoinositide hydrolysis in cultured bovine aortic amooth muscle cells. Biochem. Biophys. Acta 1010:346-351, 1989.

80.Isales C.M., Lewicki J.A., Nee J.J., and Barrett P.Q.: ANP-(7-23) stimulates a DHP-sensitive Ca^{2+} conductance and reduces cellular cAMP via a cGMP-independent mechanism. Am. J. Physiol. 263:C334-C342, 1992.

81.Li C.X., Stifani S., Schneider W.J., and Poznansky M.J.: Low density lipoprotein receptors in epithelial cell (Madin-Darby canine kidney) monolayers. Asymmetric distribution correlates with functional difference J. Biol. Chem. 266:9263-9270, 1991.

82.Liu K., and Pierce G.N.: The effects of low density lipoprotein on Ca transients in isolated rabbit cardiomyocytes. J. Biol. Chem. 268:3767-3775, 1993.

83.Sachinidis A., Locher R., Mengden T., and Vetter W.: Low-density lipoprotein elevates intracellular calcium and pH in vascular smooth muscle cells and fibroblasts without mediation of LDL receptor. Biochem. Biophys. Res. Commun. 67:353-359, 1990.

84.Anand-Srivastava M.B., Butkowska J., and Cantin M.: The presence of atrial natriuretic factor receptors of ANF-R_2 subtype in rat platelets. Coupling to the adenylyl cyclase/cyclic AMP signal-transduction. Biochem. J. 278:211-221, 1991.

85.Hu R.-M., Levin E.R., Pedram A., and Frank J.L.: Atrial natriuretic peptide inhibits the production and secretion of endothelin from cultured indothelial cells: mediation through the C receptor. J. Biol. Chem. 267:17384-17389, 1992.

86.Hassid A.: Atriopeptins decrease resting and hormone-elevated cytosolic Ca in cultured mesangial cells. Am. J. Physiol. 253:F1077-F1082, 1987.

87.Kondo Y., Imai M., Kangawa K., and Matsuo H.: Lack of direct action of alpha-human

atrial natriuretic polypeptide on the in vitro perfused segments of Henle's loop isolated from rabbit kidney. Pflügers Arch. 406:273-278, 1986.

88. Peterson L.N.,de Rouffignac C., Sonnenberg H., and Levine D.Z.: Thick ascending limb responses to dDAVP and atrial natriuretic factor in vivo. Am. J. Phsiol. 252:F374-F381, 1987.

89. Kato J., Lanier-Smith K.L., and Currie M.G.: Cyclic GMP downregulates atrial natriuretic peptide receptors on cultured cascular endothelial cells. J. Biol. Chem. 266:14681-14685, 1991.

90. Kato J., Oehlenschlager W.F., Newman W.H., and Currie M.G.: Inhibition of endothelial cell clearance atrial natriuretic peptide by cyclic GMP treatment. Biochem. Biophys. Res. Commun. 182:420-424, 1992.

91. Cahill P.A., Redmond E.M., and Keenan A.K.: Vascular atrial natriuretic factor receptor subtypes are not independently regulated by atrial peptides. J. Biol. Chem. 265:21896-21906, 1990.

92. Dai L.J., and Quamme G.A.: Hormone-mediated Ca^{2+} transients in isolated renal cortical thick ascending limb cells. Pflügers Arch. 427:1-8, 1994.

93. Gmaj P., Murer H., and Kinne R.: Calcium ion transport across plasma membranes isolated from rat kidney cortex. Biochem. J. 178:549-557, 1979.

94. Nicoll D.A., Longoni S., and Philipson K.D.: Molecular cloning and functional expression of the cardiac sarcolemmal Na^{+}-Ca^{2+} exchanger. Science 250:562-565, 1990.

95. Aceto J.F., Condrescu M., Kroupis C., Nelson H., Nelson N., Nicoll D., Philipson K.D., and Reeves J.: Cloning and expression of the bovine cardiac sodium-calcium exchanger. Arch. Biochem. Biophys. 298:553-560, 1992.

96. Furman I., Cook O., Kasir J., and Rahamimoff H.: Cloning of two isoforms of the rat brain Na^{+}-Ca^{2+} exchanger gene and their functional expression in HeLa cells. FEBS 319:105-109, 1993.

97. Kofuji P., Lederer W.J., and Schulze D.H.: Na/Ca exchanger isoforms expressed in kidney. Am. J. Physiol. 265:F598-F603, 1993.

98. Low W., Kasir J., and Rahamimoff H.: Cloning of the rat heart Na^{+}-Ca^{2+} exchanger and its functional expression in HeLa cells. FEBS 316:63-67, 1993.

99. Reilly R.F., and Shugrue C.A.: cDNA cloning of a renal Na^{+}-Ca^{2+} exchanger. Am. J.Physiol. 262:F1105-F1109, 1992.

100. Yu A.S.L., Hebert S.C., Lee S.-L., Brenner B.M., and Lytton J.: Identification and localization of renal Na^+-Ca^{2+} exchanger by polymerase chain reaction. Am. J. Physiol. 263:F680-F685, 1992.

101. Philipson K.D., and Nicoll D.A.: Molecular and kinetic aspects of sodium-calcium exchange. Int. Rev. Cytol. 137C:199-227, 1993.

102. Kofuji P., Lederer W.J., and Schulze D.H.: Mutually exclusive and cassette exons underlie alternatively apliced isoforms of the Na/Ca exchanger. J. Biol. Chem. 269:5145-5149, 1994.

103. Lee S.-L., Yu A.S.L., and Lytton J.: Tissue-specific expression of Na^+-Ca^{2+} exchanger isoforms. J. Biol. Chem. 269:14894-14852, 1994.

104. Komuro I., Wenninger K.E., Philipson K.D., and Izumo S.: Molecular cloning and characterization of the human cardiac Na^+/Ca^{2+} exchanger cDNA. Proc. Natl. Acad. Sci. USA 89:4769-4773, 1992.

105. Smith J.B., Zheng T., and Smith L.: Relationship between cytosolic free Ca^{2+} and Na^+/Ca^{2+} exchange in aortic smooth muscle cells. Am. J. Physiol. 256:C147-C154, 1989.

106. Rasgado-Flores H, Santiago E.M., and Blaustein M.P.: Kinetics and stoichiometry of coupled Na^+ efflux and Ca^{2+} influx (Na^+/Ca^{2+} exchange) in barnacle muscle cells. J. Gen. Physiol. 93:1219-1241, 1989.

107. Bouhtiauy I., Lejeunesse D., and Brunette M.G.: The mechanisms of parathyroid hormone action on calcium reabsorption by the distal tubule. Endocrinology 128:251-258, 1991.

108. Hanai H., Ishida M., Liang C.T., and Sacktor B.: Parathyroid hormone increases sodium/calcium exchange activity in renal cells and the blunting of the response in aging. J. Biol. Chem. 261:5419-5425, 1986.

109. Scoble J.E., Mills S., and Hruska K.A.: Calcium transport in canine renal basolateral membrane vesicles: effects of parathyroid hormone. J. Clin. Invest. 75:1096-1105, 1985.

110. Bindels R,J.M., Dempster J.A., Rumakers P.L.M., Willems P.H., and Van Os C.H.: Effect of protein kinase C activation and down-regulation on active calcium transport. Kidney Int. 43:295-300, 1993.

111. Quamme G.A.: Intracellular free Mg^{2+} and pH changes in cultured epithelial cells. Am. J. Physiol. 264:G383-G389, 1993.

112. Chomczynski P., and Sacchi N.: Single-step of RNA isolation by acid guanidinium triocyanate-phenol-chloroform extraction. Anal. Biochem. 162:156-159, 1987.

113. Chomczynski P.: A reagent for the single-step simultaneous isolation of RNA, DNA, and proteins from cell and tissue samples. BioTechniques 15:532-535, 1993.

114. Chomczynski P.: One-hour downward alkaline capillary transfer for blotting of DNA and RNA. Anal. Biochem. 201:134-139, 1992.

115. Smith J.B., Cragoe E.J., and Smith L.: Na^+/Ca^{2+} antiporter in cultured arterial smooth muscle cells. J. Biol. Chem. 262:11988-11994, 1987.

116. Crespo L.M., Grantham C.J., and Cannell M.B.: Kinetics, stoichiometry and role of the Na^+/Ca^{2+} exchange mechanism in isolated cardiac myocytes. Nature 345:618-621, 1990.

117. Blaustein M.P.: Effects of internal and external cations and of ATP on sidium-calcium and calcium-calcium exchange in squid axons. Biophys. J. 20:79-111, 1974.

118. Simchowitz L., and Cragoe E.J.Jr.: Na^+/Ca^{2+} exchange in human neutrophils. Am. J. Physiol. 254:C150-C164, 1988.

119. Tornquist K., and Tashjran A.H.Jr.: Dual actions of 1,25-dihydroxycholecalciferol on intracellular Ca^{2+} in GH_4C_1 cells: evidence for effects on voltage-operated Ca^{2+} channels and Na^+/Ca^{2+} exchange. Endocrinology 124:2765-2776, 1989.

120. Vigne P., Breittmayer J.-P., Duval D., Frelin C., and Lazdunski M.: The Na^+/Ca^{2+} antiporter in aortic smooth muscle cells. Characterization and demonstration of an activation by phorbol esters. J. Biol. Chem. 263:8078-8083, 1988.

121. DiPolo R., and Beauge L.: Characterization of the reverse Na/Ca exchange in squid axons and its modulation by Ca and ATP. J. Gen. Physiol. 90:505-525, 1987.

122. Tanigushi S., Marchetti J., and Morel F.: Na/Ca/ exchangers in collecting cells of rat kidney. A single tubule fura-2 study. Pflügers Arch. 415:191-197, 1989.

123. Dominguez J.H., Mann C., Rothrock J.K., and Bhati V.: Na^+-Ca^{2+} exchange and Ca^{2+} depletion in rat proximal tubules. Am. J. Physiol. 261:F328-F335, 1990.

124. Friedman P.A., Figueiredo J.F. Maack T., and Windhager E.E.: Sodium-calcium interactions in the renal proximal convoluted tubule of the rabbit. Am. J. Physiol. 240:F558-F568, 1981.

125. Bourdeau J.E., and Lau K.: Basolateral cell membrane Ca-Na exchange in single rabbit connecting tubules. Am. J. Physiol. 258:F1497-F1503, 1990.

126. Nitschke R., Frobe U., and Greger R.: Antidiuretic hormone acts via V_1 receptors on intracellular calcium in the isolated perfused rabbit cortical thick ascending limb. Pflügers Arch. 417:622-632, 1991.

127. Bouhtiauy I., Lejeunesse D., and Brunette M.G.: Effect of vitamin D depletion on calcium transport by the luminal and basolateral membranes of the proximal and distal nephrons. Endocrinology 132:115-120. 1993.

128. Zhu Z., Tepel M., Neusser M., and Zidek W.: Role of Na^+-Ca^{2+} exchange in agonist-induced changes in cytosolic Ca^{2+} in vascular smooth muscle cells. Am. J. Physiol. 266:C794-C799, 1994.

129. Furukawa K.-I., Ohshima N., Tawada-Iwata Y., and Shigekawa M.: Cyclic GMP stimulates Na^+/Ca^{2+} exchange in vascular smooth muscle in porcine cell lines. J. Biol. Chem. 266:12337-12341, 1991.

130. Mene P., Pugliese F., and Cinotti G.A.: Regulation of Na^+-Ca^{2+} exchange in cultured human mesangial cells. Am. J. Physiol. 261:F466-F473, 1991.

131. Caroni P., and Carafoli E.: The regulation of the Na^+-Ca^{2+} exchanger of heart sarcolemma. Eur. J. Biochem. 132:451-460, 1983.

132. Ramachandran C., and Brunette M.G.: The renal Na^+-Ca^{2+} exchange system is located exclusively in the distal tubule. Biochem. J. 257:259-264, 1989.

133. Bourdeau J.E., Taylor A.N., and Iacopino A.M.: Immunocytochemical localization of sodium-calcium exchanger in canine nephron. J. Am. Soc. Nephrol. 4:105-110, 1993.

134. Domingues J.H., Juhaszodu M., Kleibaeker S.B., Hale C.C., and Feister H.A.: Na^+-Ca^{2+} exchange of rat proximal tubule: gene expression and subcellular location. Am. J. Physiol. 263:F945-F950, 1992.

135. Friedman P.A.: Basal and hormone-activated calcium absorption in mouse renal thick ascending limbs. Am. J. Physiol. 254:F62-F70, 1988.

136. Wittner M., Mandon B., Roinel N., de Rouffignac C., and Di Stefano A.: Hormonal stimulation on Ca^{2+} and Mg^{2+} transport in the cortical thick ascending limb of Henle's loop of the mouse: evidence for a change in the paracellular pathway permeability. Pflügers Arch. 423:387-396, 1993.